

The Messenger



No. 143 – March 2011

Brasil to join ESO
The 2nd generation VLT instrument GRAVITY
Spectroscopy of planet-forming discs
Large Lyman-break galaxy survey



Adriaan Blaauw, 1914–2010

In the last issue of *The Messenger* (142, p. 51) only a brief obituary of Adriaan Blaauw, the second Director General of ESO, could be included at the time of going to press.

There follow three tributes to Adriaan Blaauw: by Tim de Zeeuw, current ESO Director General; by his long-term colleague at the Kapteyn Institute, Stuart

Pottasch; and by Raymond Wilson, who led the Optics Group during his tenure as Director General.

Tim de Zeeuw¹

¹ ESO

Professor Adriaan Blaauw, ESO's second Director General and one of the most influential astronomers of the twentieth century, passed away on 1 December 2010.

Adriaan Blaauw was born in Amsterdam, the Netherlands, on 12 April 1914. He studied astronomy at Leiden University, under de Sitter, Hertzsprung and Oort, and obtained his doctorate (cum laude) with van Rhijn at the Kapteyn Laboratory in Groningen in 1946. His PhD thesis was entitled "A study of the Scorpio–Centaurus Cluster". During his career, Blaauw became renowned for his ground-breaking studies of the properties of OB associations (groups of young, hot stars) which contain the fossil imprint of their star formation history. Perhaps his most famous work explained why some OB stars are found in isolation travelling at unusually high velocity: the so-called "run-away stars". Blaauw proposed in 1961 that these stars had originally been members of binary systems, and when one star in the binary experiences a supernova explosion, its companion suddenly ceases to feel the gravitational pull that keeps it in its orbit and hence it "runs away" at its orbital velocity.

In addition to his distinguished research career, Blaauw played a central role in the creation of ESO. In 1953, Baade and Oort proposed the idea of combining European resources to create an astronomical research organisation that could compete in the international arena. Blaauw had returned to Leiden in 1948,

but moved to Yerkes Observatory in 1953, becoming its associate director in 1956, and moved back to Groningen in 1957, where he was in a key position to contribute to transforming the idea of Baade and Oort into reality. He was Secretary of the ESO Committee (the proto-Council) from 1959 through 1963, a period which included the signing of the ESO Convention on 5 October 1962. Blaauw became ESO's Scientific Director in 1968. In this position he also provided the decisive push which led to the creation of *Astronomy and Astrophysics*, which successfully combined and replaced the various individual national journals for astronomy, and today is one of the leading astronomy research publications in the world. The article by Pottasch (1994) and the following tribute provide further details of Blaauw's creative leadership in the founding of the European astronomical journal.

Blaauw was Director General from 1970 through 1974. During this period several telescopes, including the ESO 0.5-metre and 1-metre Schmidt telescopes, began operating at ESO's first observatory site, La Silla, in Chile, and much work was done on the design and construction of the ESO 3.6-metre telescope, which had its first light in 1976. Blaauw decided that it was crucial for this project to move ESO's Headquarters and the Technical Department from Hamburg to Geneva, to benefit from the presence of the experienced CERN engineering group. He also oversaw the development of the Protocol for Privileges and Immunities that is critical for ESO's functioning. In May 1974 he launched *The Messenger* with the stated goal: "to promote the participation of ESO staff in what goes on in the organisation, especially at places of duty other than our own. Moreover,



Figure 1. Adriaan Blaauw in 1973 while Director General of ESO. From a photograph taken during a contract-signing ceremony for building works at La Silla.

The Messenger may serve to give the world outside some impression of what happens inside ESO." The continuing popularity of *The Messenger* is a testimony to Blaauw's foresight.

After stepping down as Director General of ESO, Blaauw returned to Leiden, where I had the privilege to be amongst his students. He continued to play a very important role in international astronomy. He was President of the International Astronomical Union from 1976 to 1979, during which period he used his considerable diplomatic skills to convince China to rejoin the IAU. From 1979 to 1982 he served on the ESO Council on behalf of the Netherlands. He retired from

his Leiden professorship in 1981 and moved back to Groningen, but stayed active in various areas. This included organising the historical archives of ESO and of the IAU — work which resulted in two books, *ESO's Early History* (Blaauw, 1991) and *History of the IAU* (Blaauw, 1994). He also served as Chairman of the Scientific Evaluation Committee for the European Space Agency satellite HIPPARCOS, advising on many aspects of its scientific programme. When the data became available in 1996, he was actively involved in the re-analysis of the young stellar groups that he had studied first during his PhD research.

Blaauw remained keenly interested in developments at ESO. After a discussion with him in late 2008, he drove himself to Garching and back in July 2009 in order to take another look at the historical documents in the library and to discuss

ESO's early history with some of us (see the photograph in *The Messenger*, 137, p. 6). During this visit he revealed his wish to visit Chile one more time if his health would allow this. It was a pleasure to organise this trip in February 2010. He met ESO "legends" Albert Bosker, Jan Doornenbal, Erich Schumann and Daniel Hofstadt and was driven to La Silla and Paranal by car to enjoy Chile's beautiful landscapes. He characteristically engaged young people at the telescopes and in Vitacura in interesting discussions and throughout the visit displayed a crystal-clear perspective on the development of ESO and on the exciting opportunities for the future programme (a photograph of this visit is shown in *The Messenger*, 139, p. 61). The characteristic sparkle in his eye was as bright as ever.

Blaauw won many academic distinctions, including membership of many academies

of science, honorary doctorates from the University of Besançon and from l'Observatoire de Paris and, like his predecessor as ESO Director General, Otto Heckman, the Bruce Medal of the Astronomical Society of the Pacific. He was well known for his warm personality, wisdom, humour, legendary patience, and the rare gift of being able to slow down when the pressure mounted. The personal account of his life, entitled "My Cruise Through the World of Astronomy", published in the 2004 *Annual Reviews of Astronomy and Astrophysics* (Blaauw, 2004), provides an accurate and inspiring picture of a truly remarkable person, who positively influenced the lives of many.

References

- Blaauw, A. 2004, *ARAA*, 42, 1
Pottasch, S. R. 1994, *The Messenger*, 76, 62

Stuart Pottasch¹

¹ Kapteyn Laboratorium, Groningen, the Netherlands

Adriaan has contributed to many fields of astronomy. In the long years we have known and worked with each other there are two aspects that may be less well known and that I would like to highlight.

First of all is the deep interest he took in the formation of the European journal *Astronomy and Astrophysics*. Adriaan took part in the initial discussions, which first began to take real shape in 1967 and especially in 1968. The discussions in 1967 took place in several European countries. At first they were independent of each other and took place because of a general feeling in Europe that existing European astronomical journals were not being read to the same extent as the American journals. In December 1967 a meeting took place in France which was attended by almost all French as-

tronomers of PhD level or higher, with the result that 75% of those present agreed that a new journal was desirable. Similar meetings took place at a somewhat higher level in other countries. At this point there was much enthusiasm to begin a new journal. This led to a meeting of European astronomers on 8 April 1968.

In spite of the enthusiasm for the European astronomical journal, there were rather difficult problems ahead. These problems were of a practical nature and arose because the new journal was to be a combination of journals published in various European countries. The individual journals all had a rather different status. Some were owned by private publishers, some by astronomical organisations. The French journals were owned by the ministry in France, which could not contribute financially to a European journal without an official treaty between various countries. The timescale for such a treaty, essentially the creation of an international organisation, was expected to be long, and the discussions complicated.

This is where Adriaan, who was at that time Scientific Director of ESO, came in. He suggested, organised and implemented a legal status for the new journal. The basic idea was that ESO would make use of the fact that it was an official European organisation. Its administrative and legal services were made available to the journal through a formal agreement between ESO and the Board of Directors of the journal. This agreement was confirmed at the December 1968 ESO Council meeting, just before the first issue of the new journal *Astronomy and Astrophysics* appeared in January 1969. Individual countries could now contribute financially to the journal, but ESO itself would carry no financial responsibility for the journal. At the same time the Board would be entirely independent of any influence from the ESO side on its scientific policy.

But this did not end Adriaan's connection with the new journal. He accepted an invitation to become a member of the Board of Directors and was in fact elected chairman of that body. The

importance of this can be seen in the fact that the journal at the time was more turbulent than it is at present. Not only were there more disputes between individual scientists, there were also disputes between different countries, especially about the refereeing. Some of these disputes were brought to the Board

where Adriaan was able to reconcile the differences. He was chairman of the A&A Board for about ten years.

A second aspect of Adriaan's career that is worth highlighting can be stated more simply. He remained an active scientist for his whole life, and was able

to combine his scientific curiosity with various administrative responsibilities without letting the one cloud out the other. I think that he was able to do this because he approached science in an unhurried and patient way. Astronomy interested him; there was always time for it.

Raymond Wilson¹

¹ Rohrbach/Illm, Germany

It is an honour and a pleasure to write a tribute to Adriaan Blaauw, whom I consider to be an underrated Director General of ESO, above all through being in the long shadow thrown by his successor Lodewijk Woltjer.

I am unable to make any comments regarding his achievements in the astronomical field. I am only going to comment on my personal experience of his work as ESO Director General, above all at the time when I was engaged by him personally to create and head a new Optics Group on the technical side of ESO's activities. At this time, his office was still in Hamburg, where ESO was founded, above all, by Professor Otto Heckman, for the 3.6-metre telescope project. This project was intended to bring ESO up to the level of the American telescopes with, at that time, one of the larger telescopes built in the post-Palomar (5-metre) era.

I left the firm of Carl Zeiss to go to ESO in 1972, when Zeiss, at the time of a serious recession in German industry, started laying off staff, including those of my own Optical Design department, where I had conceived my idea of active optics. Professor Blaauw interviewed me over a good lunch in Geneva. He immediately offered me a senior position at ESO in Geneva, where, through his initiative, ESO had a small barrack-type

building on the CERN campus. The total staff in this fledgling technical division of ESO cannot have numbered more than ten or twelve.

A major contractual problem now emerged. I had clearly understood, from Blaauw's interview with me, that I would be the leader of a newly-founded Optics Group, dealing with all optical aspects of telescopes (at that time, mainly the 3.6-metre telescope) and instrumentation. However, in the technical group, led by Svend Laustsen, the responsibility for telescope optics was in the hands of a German astronomer, Alfred Behr, and for instrumentation optics in the hands of Anders Reiz, a Danish astronomer. My role in this existing structure appeared only to be that of a senior assistant to them, above all to Alfred Behr. This situation was unacceptable to me and not as I had understood the scope of the position I had accepted.

Blaauw normally only came to Geneva for one day a week. However, when I rang him up and explained the gravity of the situation and the inevitability of my leaving ESO immediately if he could not rectify it, he came at once and we discussed the matter over another good lunch. I emphasised my clear position on the matter and that I would try to return to Zeiss immediately, in spite of the bad situation there. Blaauw recognised that I was very serious and stated he would inform Laustsen at once that a new Optics Group would immediately be founded under my leadership. Without this bold and clear direction by Blaauw there

would have been no active optics at ESO and, consequently, no NTT, VLT or E-ELT project. The readers of this tribute will understand, I am sure, why I hold Adriaan Blaauw in such high esteem.

Finally, there was another aspect of his leadership which I greatly admired. Once settled in with my new Optics Group, things were going quite well for me and I was elected to be Staff Representative. In Blaauw's weekly one-day visits to Geneva, I was always the first person he visited. But he was not concerned about my technical function, which we had organised: he left that to Laustsen, who had, of course, accepted the new Optics Group, in which Behr's work was now integrated under my leadership. No, he visited me first as Staff Representative to ask if the staff were content or whether there were any problems where he should intervene. This proves again his absolutely fair and humane leadership!

Adriaan Blaauw was not only a great ESO Director General, he was also an admirable gentleman of impeccable integrity.

Brazil to Join ESO

Tim de Zeeuw¹

¹ ESO

On 29 December 2010, at a ceremony in Brasilia, the Brazilian Minister of Science and Technology, Sergio Machado Rezende and the ESO Director General, Tim de Zeeuw signed the formal accession agreement, paving the way for Brazil to become a Member State of the European Southern Observatory. Brazil will become the fifteenth Member State and the first from outside Europe. Since the agreement implies accession to an international convention, the agreement must

now be submitted to the Brazilian Parliament for ratification. The signing of the agreement followed its unanimous approval by the ESO Council during an extraordinary meeting, by teleconference, on 21 December 2010.

“Joining ESO will give new impetus to the development of science, technology and innovation in Brazil as part of the considerable efforts our government is making to keep the country advancing in these strategic areas,” said Minister Rezende.

“The membership of Brazil will give the vibrant Brazilian astronomical community full access to the most productive observatory in the world and open up opportu-

nities for Brazilian high-tech industry to contribute to the ESO programme, including the European Extremely Large Telescope project. It will also bring new resources and skills to the organisation at the right time for them to make a major contribution to this exciting project,” added Tim de Zeeuw.

The president of ESO’s governing body, the Council, Laurent Vigroux, concluded: “Astronomers in Brazil will benefit from collaborating with European colleagues, and naturally from having observing time at ESO’s world-class observatories at La Silla, Paranal and APEX at Chajnantor, as well as on ALMA, which ESO is constructing with its international partners.”

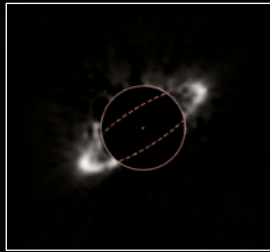
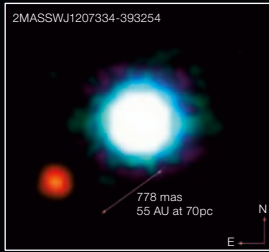
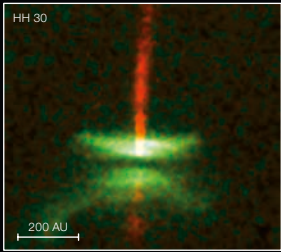


Figure 1. ESO Director General, Tim de Zeeuw, (right) in discussion with the Brazilian Minister of Science and Technology, Sergio Machado Rezende, during the accession ceremony in Brasilia on 29 December 2010.

Telescopes and Instrumentation



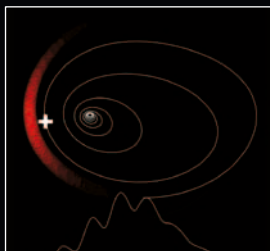
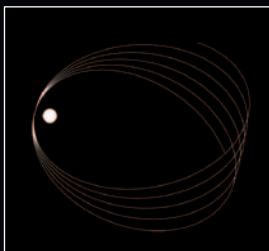
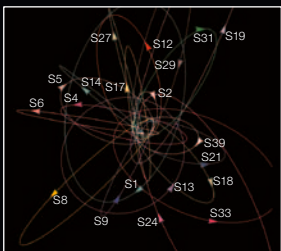
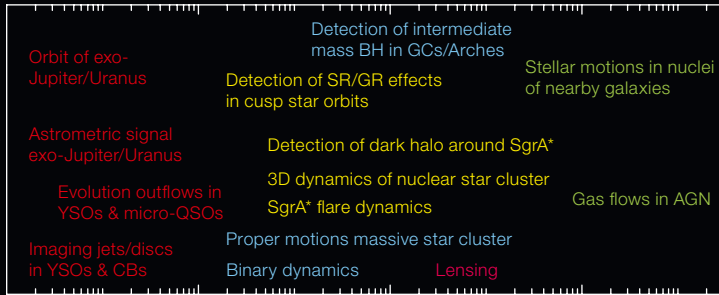
Fisheye image of the interior of the dome for VLT UT4 Yepun. See potw1049 for details.



Ten year large programme

Three year large programme

Single season campaign



Key experiments with GRAVITY are illustrated (see article by Eisenhauer et al. p. 16). Clockwise from top left are: jet/discs in a nearby star-forming region; planet-brown dwarf binary; dust disc with central gap; Arches star cluster; M31 star discs; NGC 1068 outflow/narrow line region; modelling of a Galactic Centre flare; radial precession of stellar orbits; S-star orbits; nuclear star cluster and radio emission in the Galactic Centre. In the central inset the horizontal axis denotes the maximum distance from Earth, the vertical axis the time span of the measurements.

HARPSpol – The New Polarimetric Mode for HARPS

Nikolai Piskunov¹
 Frans Snik²
 Andrey Dolgoplov³
 Oleg Kochukhov¹
 Michiel Rodenhuis²
 Jeff Valenti⁴
 Sandra Jeffers²
 Vitaly Makaganiuk¹
 Christopher Johns-Krull⁵
 Eric Stempels¹
 Christoph Keller²

¹ Department of Physics and Astronomy, Uppsala University, Sweden

² Sterrekundig Instituut Utrecht, Utrecht University, the Netherlands

³ Crimean Astrophysical Observatory, Crimea, Ukraine

⁴ STScI, Baltimore, USA

⁵ Rice University, Houston, USA

The HARPS spectrograph can now perform a full polarisation analysis of spectra. It has been equipped with a polarimetric unit, HARPSpol, which was jointly designed and produced by Uppsala, Utrecht and Rice Universities and by the STScI. Here we present the new instrument, demonstrate its polarisation capabilities and show the first scientific results.

Introduction

Spectropolarimetry is one of a very few direct ways of detecting and studying magnetic fields. Magnetic fields are presumed to play crucial roles in all kinds of objects and environments in space, stirring turbulence, transporting angular momentum, converting kinetic energy to radiation, controlling plasma motion, etc. Magnetic fields create polarisation in spectral lines through the Zeeman effect, and thus polarisation measurements allow us to measure the strength and the orientation of the field vector, providing important clues for understanding star formation, the origin of structures in stellar atmospheres and stellar activity. In fact, the origin and the evolution of magnetic fields remains one of the most important topics in modern astrophysics.

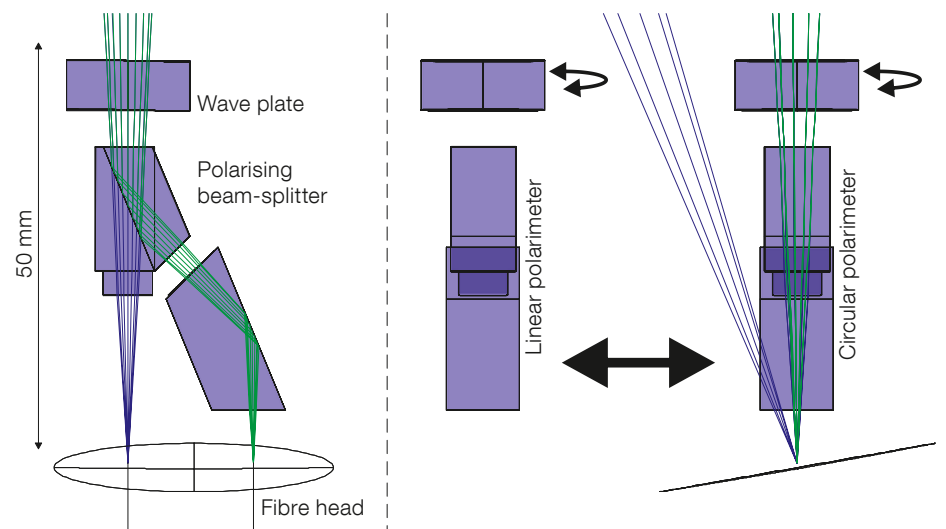
Spectral lines formed in the presence of a magnetic field generally exhibit circular

and linear polarisations across their profiles. For non-degenerate objects, the continuum is mostly unpolarised, which offers a reliable intrinsic calibration that is necessary for measuring very weak fields, but such measurements require a very stable spectropolarimetric instrument.

The HARPS spectrograph at ESO's 3.6-metre telescope at La Silla is one of the most successful spectroscopic astronomical instruments ever built (Mayor et al., 2003). The exceptional temporal and spatial stability of HARPS makes it an ideal instrument for spectropolarimetry. The new polarimeter takes full advantage of the two optical fibres to bring the collected light, split into two orthogonal polarisations, from the Cassegrain focus of the 3.6-metre telescope to the HARPS spectrograph. Analysing polarisations at the Cassegrain focus minimises the influence of instrumentation on the measurements. The new module, called HARPSpol, allows sensitive and accurate measurements of both circular and linear polarisations of stellar light as a function of wavelength, at high spectral resolution. In this article we give a short presentation of the polarimeter and show some results from the first year of operation.

HARPSpol – What's inside the box?

HARPSpol is installed inside the Cassegrain adapter, located directly below the primary mirror of the 3.6-metre telescope.



This sets very stringent limits on the dimensions of the polarimeter, because it needs to fit in between various mechanisms (calibration light feeds, calibration mirror and fibre cover) filling the adapter. The polarimeter consists of the enclosure hosting a precision horizontal slider. The slider holds two identical optical tables installed perpendicular to the sliding direction. Each optical table contains a full set of polarisation optics (Figure 1), separating the incoming light into two beams. Since the polarising beam-splitter position is fixed relative to the fibres, the polarisation of the incoming light needs to be converted to the frame of the beam-splitter. This is achieved by rotating wave plates in front of the beam-splitters: a half-wave plate for the linear polarimeter and a quarter-wave plate for the circular one. The relative intensity of the two beams at each wavelength carries the information about the polarisation of the light.

The polarising beam-splitters consist of a Foster prism (a modified Glan-Thompson polariser). The primary beam suffers from crystal astigmatism, which is corrected by a cylindrical lens. The secondary beam is deviated by 45°. Beam-channelling prisms align the optical axis and the focus of the secondary beam with the second HARPS fibre. The selected optical scheme solves two

Figure 1. Schematic of the HARPSpol optical design. Left: the view in the sliding direction. Right: side view of the two polarimeters.

difficulties: (1) it is highly achromatic, that is, the image of a star after projection through HARPSpol is essentially the same in the red and in the blue parts of the spectrum; and (2) slight errors in positioning of the slider do not affect the optical/polarisation performance. More information about the optical design of HARPSpol can be found in Snik et al. (2008, 2010).

The selected wave plates are super-achromatic. They consist of five layers of birefringent polymer. This makes the polarimeters suitable for the entire HARPS wavelength range (380–690 nm) without introducing (polarised) fringes. The simultaneous measurements in two polarisation directions, together with the polarisation modulation by the wave plates, renders the polarimetry with HARPSpol to first order insensitive to seeing and fibre/spectrograph throughput (Semel et al., 1993; Bagnulo et al., 2009).

Integration

Once installed at the Cassegrain adapter, HARPSpol was integrated with the HARPS instrument control electronics and software. When inserted into the optical path, HARPSpol shifts the focus of the telescope by approximately 2 mm, which is compensated for by moving the secondary mirror. Figure 2 shows HARPSpol installed inside the Cassegrain adapter. Spectropolarimetry is performed by selecting the corresponding template(s) in the observing software. Calibration and science templates are available for circular and linear polarimetry. The science

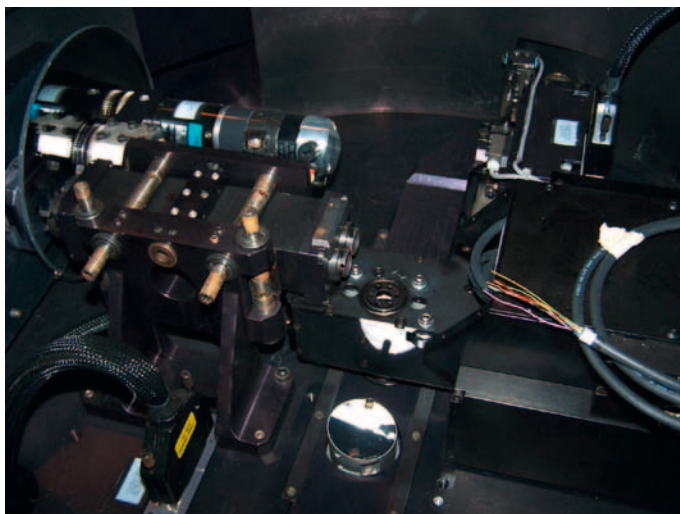


Figure 2. HARPSpol is shown during installation. The HARPSpol enclosure is on the right. The slider is in the linear polarisation position. The half-wave plate for the linear polarimeter is visible in the middle of the picture. The round mirror below the linear polarimeter is one of the HARPS fibre heads.

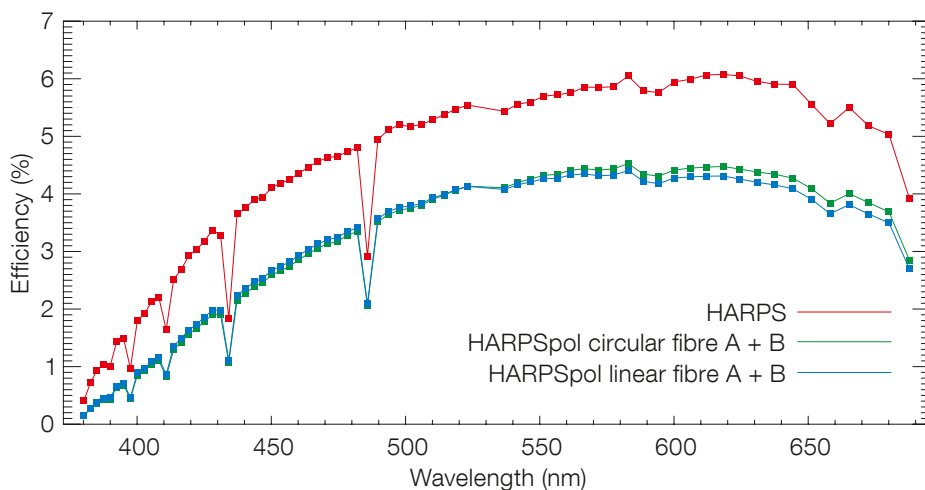


Figure 3. The total throughput from the telescope to the detector with and without HARPSpol is shown. The sharp drops are not real: they are due to hydrogen lines that are treated differently in spectrophotometry and spectropolarimetry.

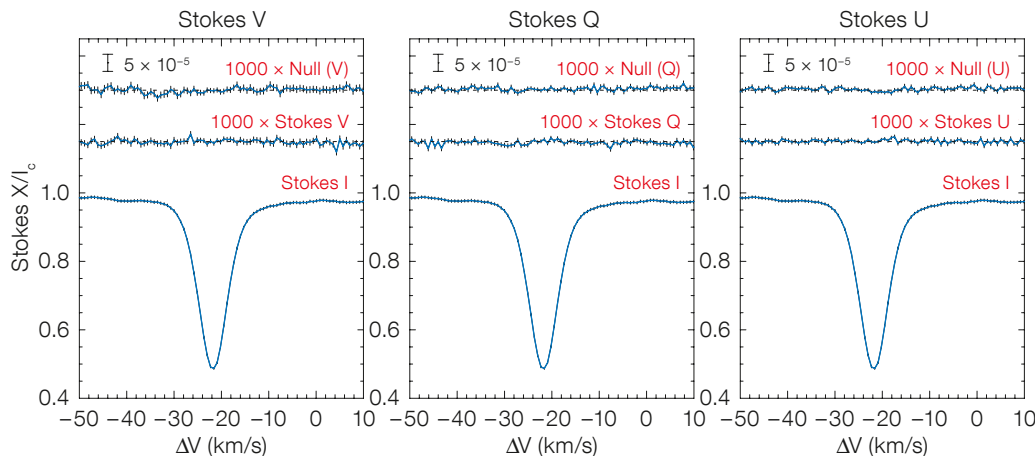


Figure 4. The combined average profile for intensity and polarisation (lower and middle plots) for α Cen A. Left panel shows circular polarisation measurements (Stokes parameter V). Middle and right panels are for linear polarisations. The null profile is shown uppermost.

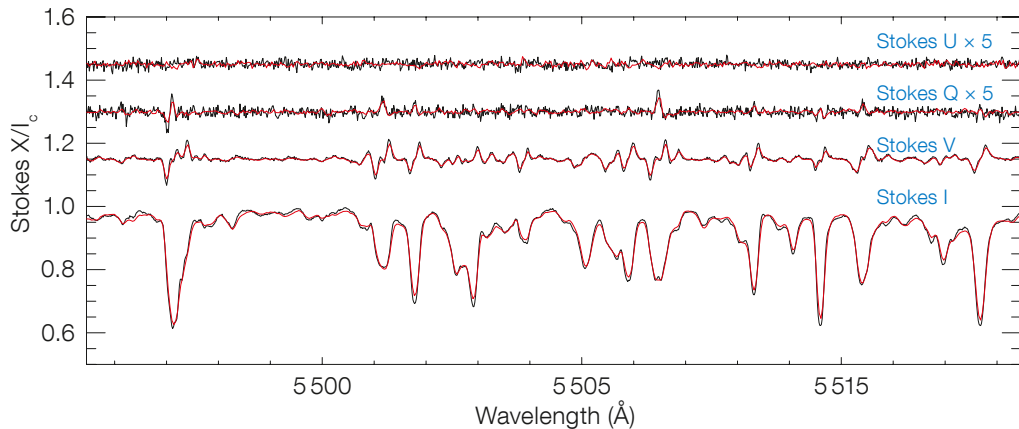


Figure 5. Comparison of the Stokes spectra of a standard magnetic star γ Equ taken at the CFHT with the ESPADONS spectropolarimeter (red line) and with HARPSpol (black line) is shown. The ESPADONS spectra were taken as part of CFHT's calibration and engineering plan, and were retrieved from the Canadian Astronomy Data Centre. The visible differences are mostly due to the higher resolving power of HARPS.

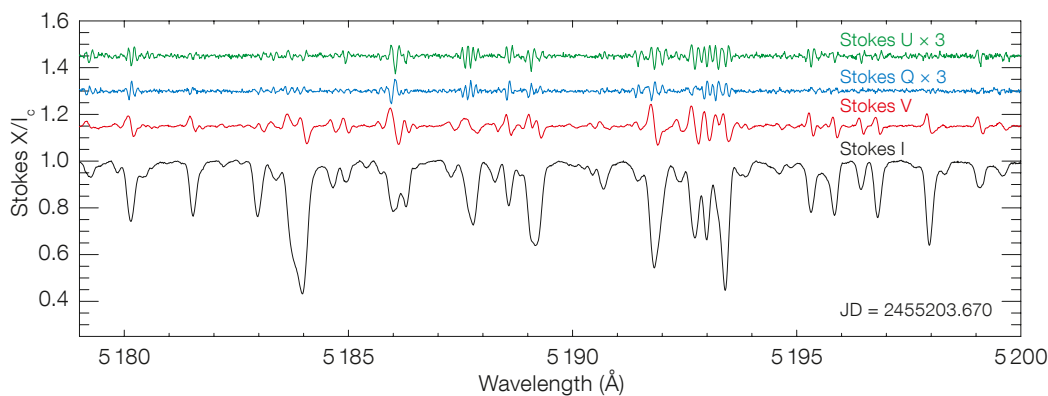


Figure 6. One of the HARPS polarisation spectra of a CP star, HD 24712, is shown. Both circular and linear polarisations are detected for practically every spectral line.

template allows multiple exposures to be taken in the selected mode (circular or linear) for a sequence of wave-plate angles. The full complement of polarisation characteristics can be registered in six or twelve exposures, with the latter offering intrinsic control over spurious polarisation signals. The HARPSpol pipeline then processes the data and the final products include the Stokes parameters as a function of wavelength.

HARPSpol: Performance

During commissioning we have measured several characteristics of HARPSpol. The most important ones for the observer are the total throughput of the system and the polarimetric sensitivity. The throughput (Figure 3) was measured by observing spectrophotometric standards, reducing the data, rebinning it to match the resolution of the spectrophotometry and deriving the sensitivity curves for each fibre. The total efficiency with HARPSpol is somewhat lower due

to the lower throughput of the “sky fibre” (used to carry one of the polarised beams), but still sufficient to reach rather faint targets.

Systematic errors limit both the polarimetric sensitivity and the accuracy. The sensitivity is the weakest polarisation detectable with HARPSpol. After accumulating enough photons we expect to see spurious polarisation present in the light coming to the telescope. We test this by observing a bright source and collecting many photons in a series of many short exposures. Figure 4 shows the results of the test for an inactive solar-type star, α Cen A, where we reach the median signal-to-noise ratio of 2400 per CCD column. Besides combining multiple exposures we also derive the mean Stokes profiles using the least squares deconvolution (LSD) technique (Donati et al., 1997; Kochukhov et al., 2010), which takes advantage of the fact that most of the spectral lines are affected by magnetic fields in a similar way. This increases the signal-to-noise even further. The top

plot in each panel of Figure 4 shows the so-called null spectrum, obtained by modifying the analysis in such a way as to destroy the polarisation signal in the incoming light (Bagnulo et al., 2009). What remains reflects the spurious polarisation induced inside the instrumentation or by the data reduction.

We do not expect any detectable polarisation signal from α Cen A and Figure 4 shows that our new instrument does not detect or induce any polarisation above the level of 10^{-5} , which is on a par with the best solar polarimeters like ZIMPOL (Ramelli et al., 2010). The accuracy (the level at which the HARPSpol measurements match the true polarisation signal) is assessed by observing objects with known polarisation spectra. Our observations of γ Equ demonstrate the high accuracy of HARPSpol. γ Equ is a well-studied magnetic star showing linear and circular polarisations. The lack of noticeable rotation makes γ Equ an excellent polarisation standard. Figure 5 shows the comparison of the HARPSpol polarisation

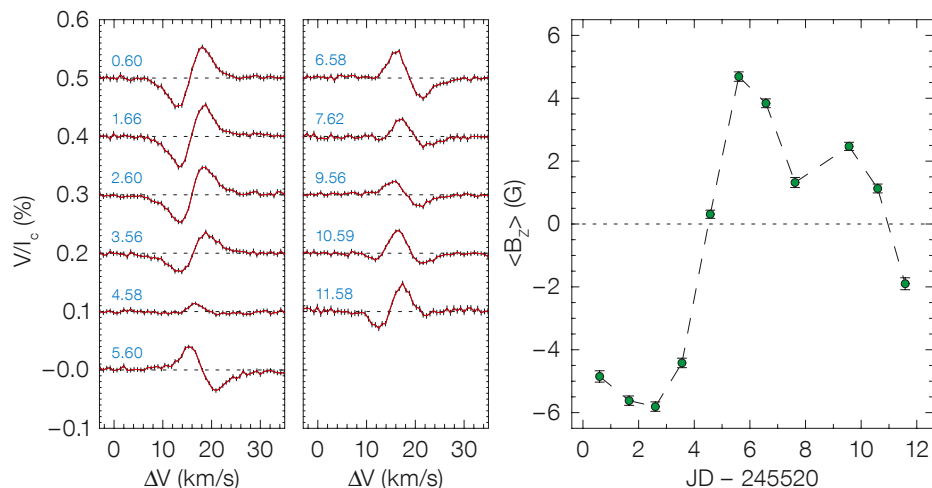


Figure 7. Spectropolarimetry of a K2 dwarf planet-hosting star ϵ Eri taken with HARPSpol. Circular polarisation profiles (left) are marked with observation times in days. Derived line-of-sight field strength and uncertainty in Gauss are shown against time (in Julian Day) on the right.

spectra of this star with those taken with the ESPADONS spectropolarimeter (Donati et al., 2006) at the Canada France Hawaii Telescope (CFHT) with a resolving power of 67 000.

HARPSpol: First results

One of the obvious applications of HARPSpol is in the study of the topology of magnetic fields on chemically peculiar (CP) stars. The goal is to understand the relationship between the field geometry and the surface/depth distribution of chemical elements. This task requires a series of observations well spread over the rotation period so as to see all visible parts of the stellar surface. Figure 6 shows an example of one measurement in such a series for a cool magnetic CP star HD 24712. Circular and linear polarisation were detected in all 13 phases covering the whole stellar rotation (bad weather prevented the collection of one set of circular polarisation data) and one can easily follow the evolution of polarisation spectra with stellar rotation. The low level of the noise makes the data quite adequate for reconstructing the field topology.

Another example is a chromospherically active cool dwarf ϵ Eri. This nearby star harbours at least two planets and a dust belt in orbit around it. Polarisation measurements of stars hosting planets may provide an important check for the presence of starspots that can mimic radial velocity variations. Detection of polarisation can reveal signatures of star-planet magnetic interactions. Our polarisation measurements for ϵ Eri are presented in Figure 7. Again, we applied the LSD technique to enhance the signal-to-noise ratio and we see an unambiguous signal in circular polarisation. A simplistic interpretation with a longitudinal field geometry shows field strength changing from -5.8 to $+4.7$ Gauss with median uncertainty of 0.1 Gauss! These values are comparable to the disc-averaged magnetic field of the Sun (Kotov et al., 1998).

Prospects

HARPSpol adds powerful polarimetric capabilities to the suite of ESO high-resolution spectroscopic instruments. It is fully integrated into the ESO operational environment and is equipped with

a pipeline producing science-grade data products. The tests and applications to various types of objects have demonstrated high sensitivity and a low level of systematic effects, making HARPSpol an ideal tool for detecting and studying weak magnetic fields, reconstructing field topology and many other magnetic phenomena.

References

- Bagnulo, S. et al. 2009, *PASP*, 121, 993
- Donati, J.-F. et al. 1997, *MNRAS*, 291, 658
- Donati, J.-F. et al. 2006, *Solar Polarization 4*, ASP Conf. Series, 358, 362
- Kochukhov, O. et al. 2010, *A&A*, 524, 5
- Kotov, V. A. et al. 1998, *ApJ*, 116, 103
- Mayor, M. et al. 2003, *The Messenger*, 114, 20
- Ramelli, R. et al. 2010, *SPIE*, 7735, 1
- Semel, M. et al. 1993, *A&A*, 278, 231
- Snik, F. et al. 2008, *SPIE*, 7014, 22
- Snik, F. et al. 2010, arXiv: 1010.0397

Tests of Radiometric Phase Correction with ALMA

Bojan Nikolic¹
 John Richer¹
 Rosie Bolton¹
 Richard Hills²

¹ Astrophysics Group, Cavendish Laboratory, University of Cambridge, United Kingdom

² Joint ALMA Observatory, Santiago, Chile

Of the many challenges facing ALMA, one of the greatest is overcoming the natural seeing limit set by the atmosphere to achieve very high resolution images. Its longest antenna separations (baselines) permit ALMA to synthesise the effect of a single antenna with a diameter exceeding 15 km, but an accurate radio “adaptive optics” system is required to ensure ALMA’s images are diffraction limited. With initial test data now available from the first ALMA antennas in Chile, we describe current progress towards this goal.

Atmospheric limitations to radio astronomy

ALMA aims to synthesise an antenna with an effective diameter of over 15 km: this would have a diffraction-limited resolution of 15 milliarcseconds at a frequency of 300 GHz. (Note, however, that for most projects with ALMA, we anticipate that a more modest resolution of 50–100 milliarcseconds will be requested by scientists.) In comparison, the uncorrected radio seeing at this frequency would typically limit the resolution of images to 700 milliarcseconds if no adaptive optics corrections were applied (see Evans et al., 2003).

The seeing at sub-millimetre and millimetre wavelengths arises due to atmospheric (specifically, tropospheric) instabilities that lead to fluctuations of the refractive index and consequent path errors in the propagating wavefront. As explained in a previous *Messenger* article (Nikolic et al., 2008), the process is analogous to that affecting the optical seeing, but the dominant contribution to the refractive index fluctuations is from inhomogeneities in water vapour, rather

than temperature fluctuations. ALMA is attempting to correct the effects of these fluctuations through a combination of two techniques: frequent observations of calibration sources; and direct measurement of atmospheric properties along the line of sight of each of the 54 12-metre diameter telescopes using mm-wave radiometers that measure emission of the 183 GHz water vapour line. ALMA is the first telescope to employ phase correction based on mm-wave water vapour radiometers.

Water in the atmosphere is poorly mixed and the concentration (and phase) of water varies rapidly with position in the atmosphere and with time. The underlying reason for this is of course that all three phases of water are accessible in the range of temperatures and pressures typical on the ground and in the atmosphere, leading to various localised sources and sinks of water vapour. Even at a very high and dry site like ALMA, changes of up to 50% in line-of-sight water vapour can be observed in a matter of minutes. Additionally, water vapour has a high effective refractive index at mm and sub-mm wavelengths: one millimetre of precipitable water vapour retards radiation by an equivalent of about seven millimetres of path in vacuum. The combination of poor mixing and high refractive index leads to a corruption of the wavefront of incoming astronomical radiation. When observing with an aperture synthesis array like ALMA, these wavefront errors lead to phase errors in the recorded visibilities.

In order to correct for these errors, each of ALMA’s 12-metre diameter antennas has an accurate millimetre-wave radiometer that measures the radiation passively emitted by water molecules in the atmosphere along the line of sight of the antenna. The radiometers cover frequencies around the $3_{13} \rightarrow 2_{20}$ rotation line of the para water molecule, which is centred at 183.3 GHz. This line lies about 200 K above the ground state and so is ideal for tracing atmospheric properties. The principle of radiometric phase correction is that these measurements can be used to compute the quantity of water vapour along the line of sight of each antenna and, consequently, the equivalent path error. Using these estimates the

observed astronomical data can be corrected for the effect of path fluctuations.

Water vapour radiometers

The water vapour radiometers (WVRs) are the devices that measure accurately the absolute brightness of downwelling radiation along the lines of sight of the antennas. The prototype WVRs for ALMA were developed by a collaboration between the University of Cambridge and Onsala Space Observatory. After successful laboratory and field testing of the prototypes, an industrial partner (Omnisys Instruments AB, Sweden) was contracted for delivery of the production units. The production stage is now already fully complete and ALMA has taken delivery of radiometers for all of the planned 54 12-metre antennas.

The ALMA radiometers are unique among the radiometers used for phase correction in that they measure sky brightness around 183 GHz, as opposed to 22 GHz, which is the spectral region where most other WVR systems are designed to observe. This has a number of advantages, primarily based on the very high strength of the water vapour line at 183 GHz (see Figure 1 for plots of brightness in typical conditions), which is about 150 times stronger than the line at 22 GHz. This means that fluctuations in water vapour content produce much higher, more readily observed fluctuations in the observed brightness at this frequency. Besides this, the high strength of the line means that radiation from sources other than atmospheric water vapour has a smaller influence on the predicted phase corrections. For example, clouds, spill-over past the primary reflector of the antenna and man-made radio frequency interference (RFI) all have a smaller effect relative to the strength of the line.

Measurements at these higher frequencies do, however, also present a number of challenges:

1. Design and production of the hardware is more complex and expensive, requiring custom components and high precision machining.
2. Calibration is more difficult as it needs to be based on very frequent (10 Hz

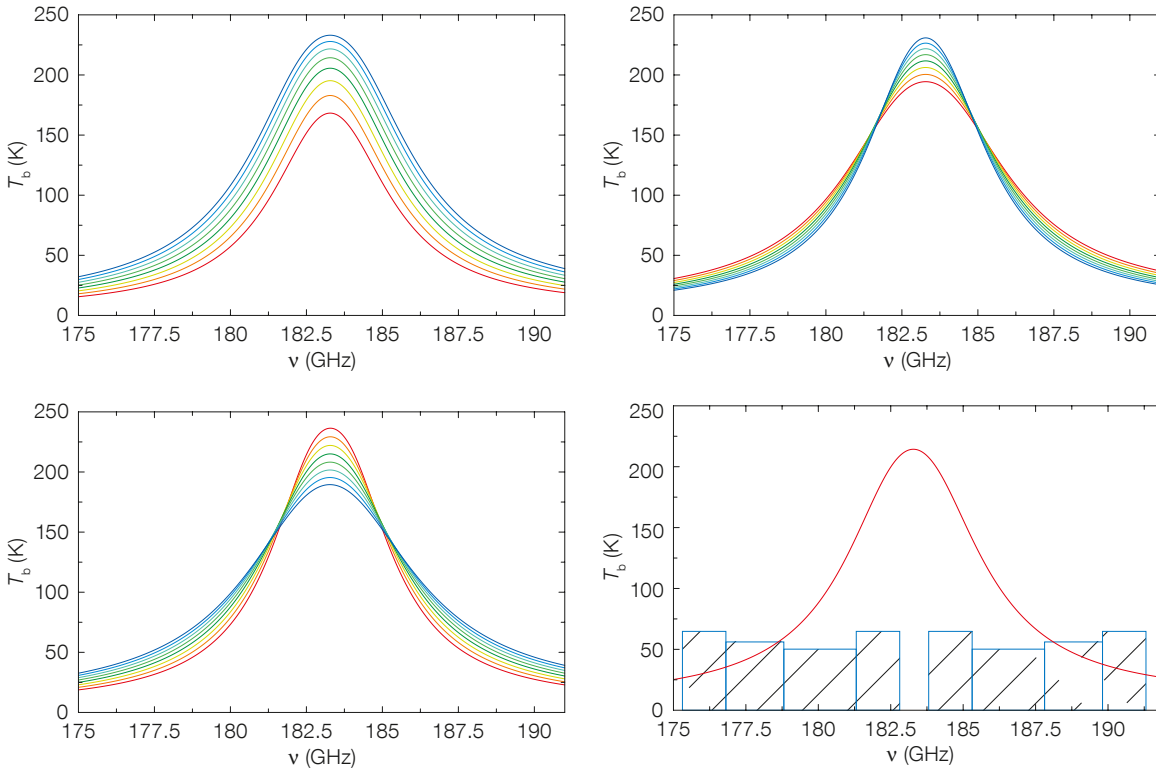


Figure 1. The water vapour line at 183 GHz. The upper left, upper right and lower left panels show how the simulated brightness of the atmospheric 183 GHz water vapour line varies with changes in total contents of the water vapour, the atmospheric temperature and atmospheric pressure. The lower right panel shows the nominal filter pass-bands for the ALMA 183 GHz water vapour radiometers. The detection system is double-sideband and so only the average signal of the two filters symmetric around the line centre is measured.

in the case of ALMA) observation of physical internal calibration loads.

3. The water vapour line is close to saturation and thus subject to non-linear effects, leading to significantly more complex software requirements.

Over the past twelve months, extensive testing of the first WVR systems has been carried out at the ALMA site. The preliminary results of these tests suggest that the development and production stage has successfully met these challenges. So far, the units installed on the ALMA antennas appear to be performing well in terms of noise, stability and reliability.

Technique

The WVRs provide measurements of sky brightness in the four filters illustrated in the lower right plot in Figure 1. As ALMA WVRs employ a double-sideband mixing system, only the average brightness of the sky at frequencies symmetric around the centre of the line is measured. The maximum readout frequency from the WVRs is 5 Hz, although normally

we read out at 1 Hz, which is fast enough to capture essentially all the path variations.

The task of the phase correction software is to turn these 1 Hz measurements in four filters into phase rotations to be applied to the observed astronomical signal. The first step in the analysis is to use the four observed sky brightness temperatures, together with ancillary weather information, to make an inference about the total quantity, temperature and pressure of the water vapour. This is important because the profile of the water vapour line is a strong function of these parameters, as shown in Figure 1, and because the near-saturation of the line means that the observed sky brightness is not in general linearly related to the total path error.

The second stage of analysis is to turn the *fluctuations* in the observed sky brightness into estimates of fluctuation of effective path to each of the antennas in the array. We only consider the fluctuations because, as an interferometer, ALMA is sensitive to only the difference in path errors to each of the antennas

and we do not need to try to retrieve the total extra path due to the water vapour in the atmosphere. Additionally, frequent observation of point-like sources will allow ALMA to calibrate the expected “zero” phase and it is only the departures from this that are important.

The close relationship between fluctuations in sky brightness and the path errors is illustrated in Figure 2, which is based on recent observations by ALMA. During this observation, the telescope was tracking a quasar (i.e., a point-like source) at a known location on the sky, so for a perfect interferometer we would expect to measure visibilities with constant phase and amplitude. The phase we actually measure is therefore an estimate of the differential path along the two lines of sight due to atmospheric fluctuations. This is plotted on the horizontal axis of the diagrams, and on the vertical axis we plot the difference in observations by the WVRs on these two antennas. What can be seen in Figure 2 is that there is a high degree of correlation between the two quantities, meaning that as long as we can forecast the slope of this correlation then we can convert

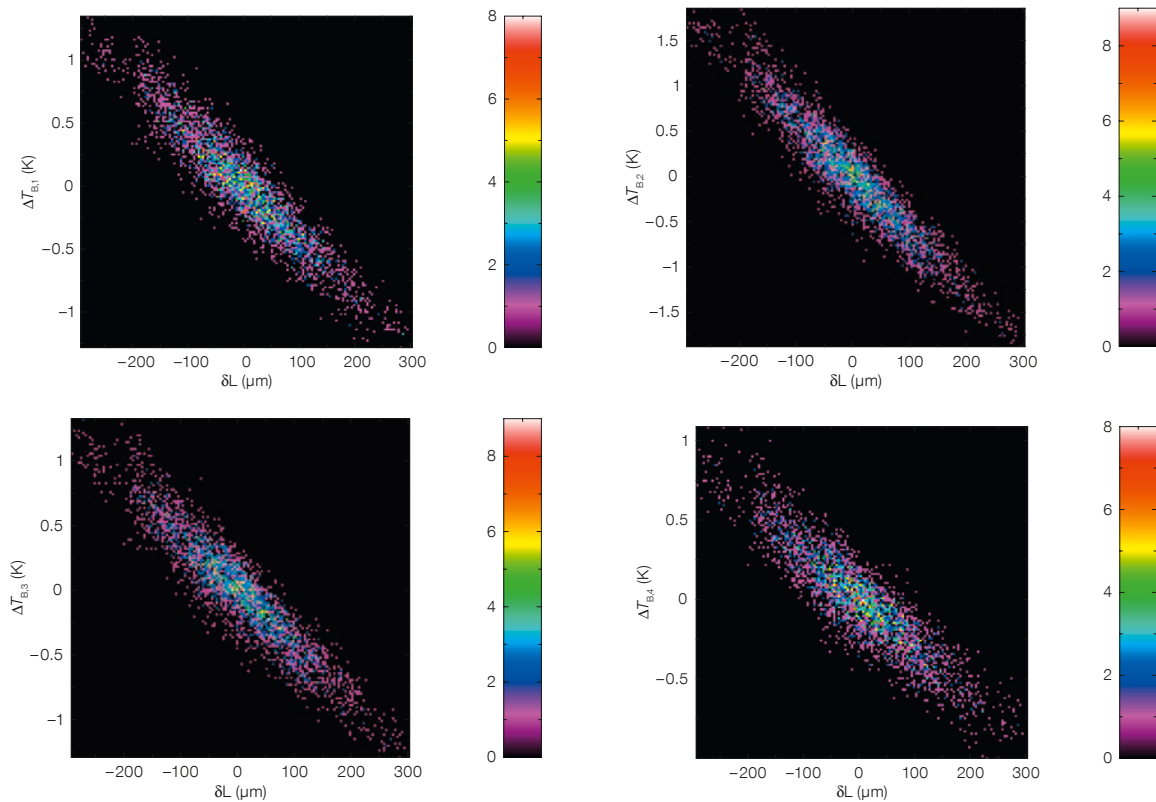


Figure 2. Correlation between the atmospheric path error estimated from observations of bright point-like objects (horizontal axis) and the differenced WVR signal (vertical axis). Each plot is a two-dimensional histogram where the colour scale shows how many points fall in each bin. The four panels correspond to the four channels of the radiometers (1–4 designated by the axis label).

fluctuations of WVR outputs to path fluctuations for a general observation.

The final stage of the analysis is to turn estimates of path fluctuations into a phase correction that needs to be applied to the astronomical data. This is generally straightforward, although it is important to take into account the dispersive effects of the atmosphere and also to ensure that rotations applied using estimates derived from WVR data interact correctly with other calibrations applied to the astronomical data.

Development of phase correction software for ALMA under FP6

Our recent involvement in WVR phase correction for ALMA has been primarily through development of software and algorithms that process the raw data observed by the WVRs and use these to calibrate and correct the astronomical data. This work is separate from the baseline ALMA software and has been funded as an ALMA enhancement by the European Union Framework Programme 6.

(This programme also supports development of Band 5 receivers for ALMA [see Laing et al., 2010], and on-the-fly interferometry techniques).

The software we have been developing is designed primarily for off-line phase correction, i.e., it operates on the observed data after these have been stored on disk. Some of the principal features of our software are:

- It is closely integrated with the official ALMA off-line data reduction suite (CASA), which allows it to be used in a straightforward manner by scientists.
- The software has a rapid development cycle, with new features and improved algorithms appearing regularly.
- It uses a robust Bayesian statistical inference framework to derive optimal corrections.
- When certain WVRs are missing from an observation, the software has the ability to interpolate available data to provide phase correction estimates at those antennas lacking accurate WVR measurements.

- The software is easy to distribute as a binary package that works in conjunction with CASA.

The software (`wvrgcal`) for phase correction is available freely under the Gnu Public License in both source code and binary formats¹. We also operate a mailing list² for discussion, improvement suggestions and community support of the software.

Tests of phase correction

Since about January 2010, ALMA has been collecting significant amounts of test observations designed to measure the effectiveness of WVR phase correction and to guide the further development of algorithms used to translate sky brightness measurements to the phase rotations. In order to fit with the numerous other ALMA commissioning activities, most of these observations were taken with the antennas in relatively compact configurations, i.e., most data are with baselines in range 30–100 m, with some data on baselines of up to 600 m. These

data have already provided a good demonstration of effectiveness of phase correction on these relatively modest baselines. However, we know that the phase correction will be most challenging on long baselines (up to 15 km in length for ALMA); this is because the root structure function of the atmosphere increases as roughly the 0.6 power of baseline on typical ALMA baselines. Long baseline test data are awaited to investigate the effectiveness of the technique when ALMA is making its highest resolution images.

Two typical examples of path fluctuations computed from WVR observations are shown in Figure 3. For these plots we have used data from three antennas, shown by different colours in these plots. Since these are absolute path estimates from the WVRs, it is the *differences* between the three traces that correspond to the phase rotations to be applied. For these observations, the antennas were relatively close to each other and therefore these differences are quite small. These plots illustrate very well the wide variety of conditions that are present at the ALMA site: total fluctuations are different by about two orders of magnitude between the two observations. It can be seen that the total (peak-to-peak) fluctuations on the upper panel of Figure 3 are about 50 μm on timescales of about five minutes; this is significantly less than 350 μm , the shortest wavelength at which ALMA will observe. On the lower panel of Figure 3, the fluctuations are greater than 3.5 mm, i.e. they are larger than the longest wavelength at which ALMA will initially observe.

Figures 4 and 5 show two examples of WVR phase correction at work. In both plots, the red trace represents the phase of the recorded visibilities while observing a quasar. In the absence of atmospheric and instrumental phase errors we would expect this phase to be constant in time — the variations actually observed are due to the combination of atmospheric effects and instrumental errors. The uncorrected phase in Figure 4 is varying by more than 360 degrees, i.e., by a full rotation, which means that in these conditions it would not be possible to make any measurements on faint sources. The blue line shows the phase after correction using our `wvrgcal` software.

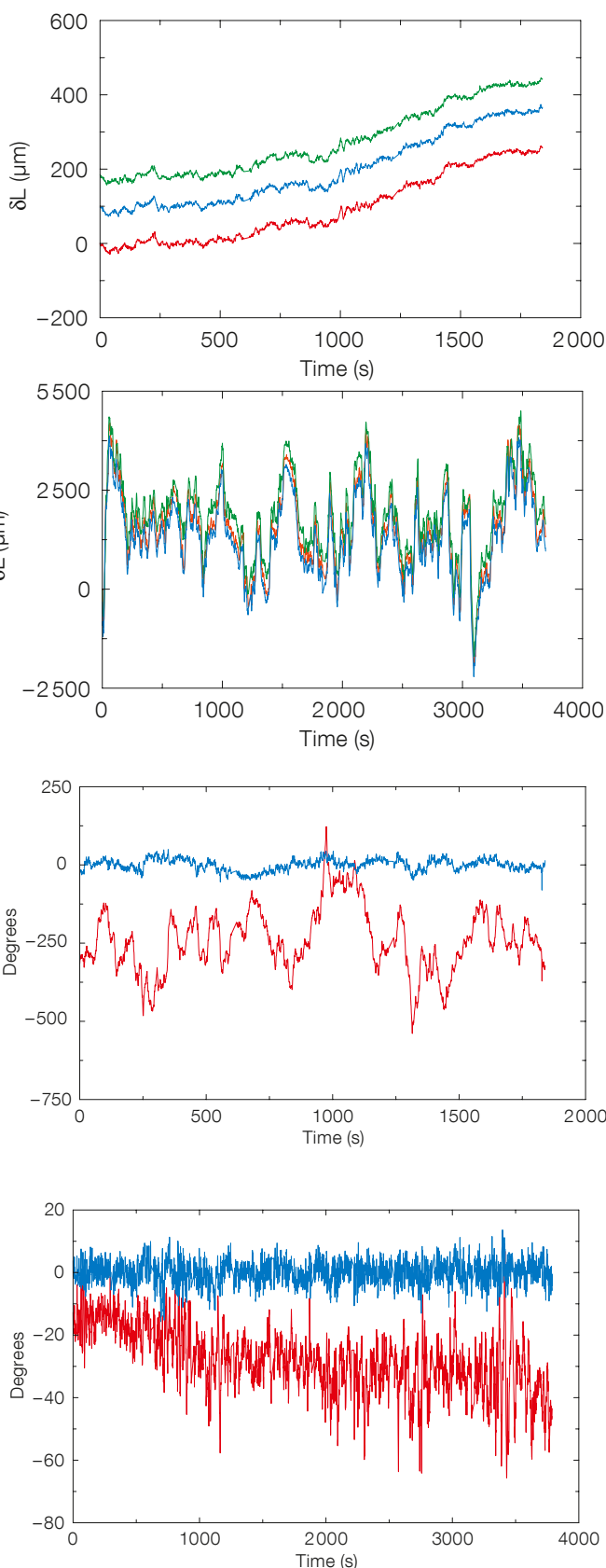


Figure 3. Path fluctuation estimated from WVR data for two observing sessions. Times are expressed in UT, so the upper panel corresponds to night-time, while the lower panel to a time around mid-day. Note that the vertical scale is different between the two panels.

Figure 4. Test observation of a sub-mm bright quasar on a roughly 650-metre baseline with ALMA. The red line is the phase (in degrees) of the observed (complex) visibility on this baseline — note that for a quasar (or other point-like) source at the tracking centre of the interferometer we expect a constant phase in time. The blue line is the visibility phase after correction of the data based on the WVR signals and using the `wvrgcal` program.

Figure 5. Like Figure 4, this is a test observation of a strong quasar, but on a baseline of around 60 m and during stable weather. The red line is again the uncorrected observed phase (in degrees) of the visibility, while the blue line is the phase after WVR-based correction. Note the change of vertical scale between Figure 4 and this figure.

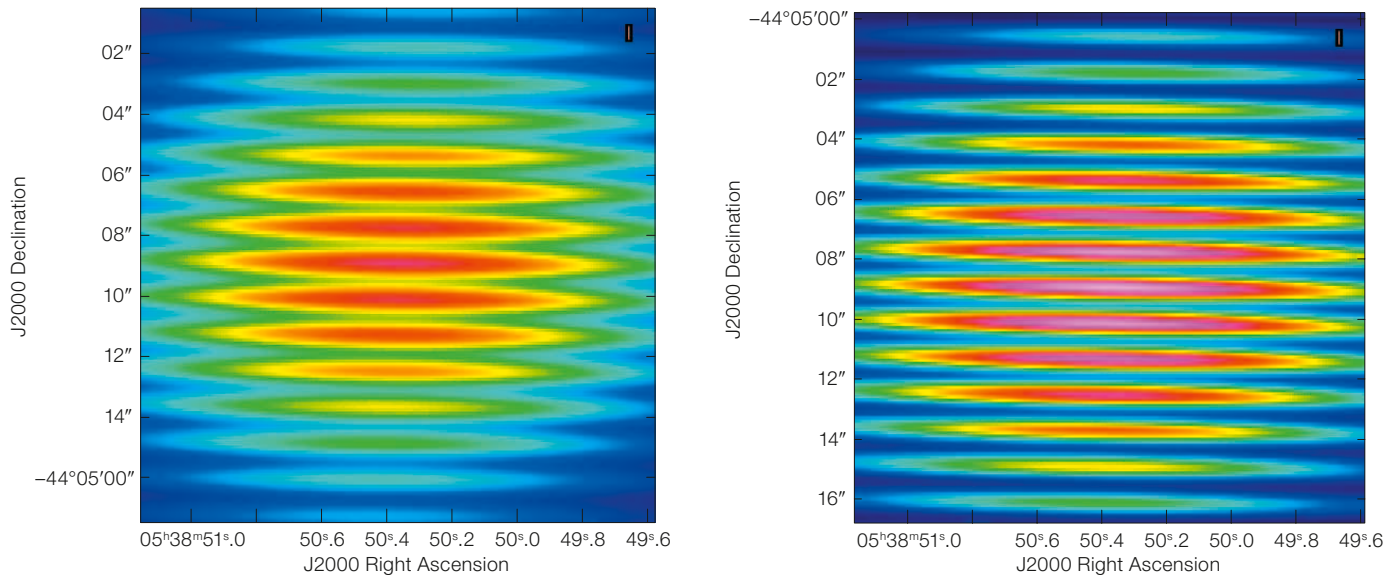


Figure 6. Un-deconvolved images of a quasar (which is unresolved) with ALMA in a very heterogeneous configuration: four of the antennas were very close together while the fifth was about 650 metres away. The heterogeneity leads to the rapid modulation in the north–south direction, which corresponds to the long baseline. The image on the panel on the left was made with no phase correction while the image in the panel on the right has had WVR phase correction applied. It can be seen that the phase fluctuations, when uncorrected, lead to an almost complete wash-out of fringes on the long baseline.

It can be seen that the fringes in the map made from corrected data (right panel) are much sharper and have much higher contrast compared to the map made from uncorrected data. After deconvolution (and completing the baseline coverage) this increase in sharpness directly corresponds to an increase in resolution and fidelity.

to use, so they can automatically remove the distorting effects of the atmosphere and allow them to focus on the novel science in their ALMA datasets. Nonetheless, ALMA already has made great progress towards this goal, and can already claim to have an effective and ground-breaking adaptive optics system.

The phase errors can be seen to be reduced by an order of magnitude, to a level where meaningful averaging of the data can be done.

The example shown in Figure 5 is less extreme — the uncorrected data have a phase root-mean-square deviation of about 20 degrees. However, even in these much more stable conditions, application of WVR phase correction leads to much improved phase stability. Also notable in this example is that variations in uncorrected phase at longer timescales are also very effectively reduced by WVR phase correction.

As an illustration of the effect of WVR-based phase correction on imaging, in Figure 6 we show an un-deconvolved (“dirty”) map of a point source with ALMA in an unusual configuration with north-south baselines much longer than the others. We have made the map both with the raw data, and with the data after WVR-based phase correction.

Future challenges

The data presented in this article represent by far the most extensive tests of the capabilities of 183 GHz phase correction ever attempted. They demonstrate that the technique should increase significantly the sensitivity of ALMA, by reducing the decorrelation caused by phase errors, and increase the fidelity of ALMA images by ensuring visibility phases are more accurately measured. In addition, they should improve the efficiency of ALMA operations, by permitting observations to take place when atmospheric instabilities cause rapid large amplitude phase fluctuations.

However, much work remains to be done. It is vital that ALMA can demonstrate that its phase correction strategy works to specification in a wide range of atmospheric conditions and on baselines all the way out to the maximum allowed by the configuration designs. In addition, it remains a challenge to ensure that the software tools are easy for astronomers

Acknowledgements

The results shown in these plots are of course the result of the efforts of many tens, if not hundreds, of people who have been involved in ALMA over the years. Phase correction tests require everything in the ALMA system to be working perfectly, so a great deal of credit is due to all of those involved, from the designers of the systems to those keeping the observatory running in Chile. The specific work described here, including the analysis of test data and development of the `wvrgcal` program has been carried out by the Astrophysics Group at the Cavendish Laboratory, University of Cambridge, as part of the ALMA Enhancement Programme, an enhancement to the baseline ALMA project. This work is funded by the European Union’s Sixth Framework Programme.

References

- Evans, N. et al. 2003, *Site properties and stringency*, ALMA Memo Series, 471, The ALMA Project
- Laing, R. et al. 2010, *The Messenger*, 141, 41
- Nikolic, B. et al. 2008, *The Messenger*, 131, 14

Links

- ¹ Source code for `wvrgcal` available at: <http://www.mrao.cam.ac.uk/~bn204/alma/wvrsoft.html>
- ² Mailing list for `wvrgcal` updates: <https://lists.cam.ac.uk/mailman/listinfo/mrao-wvrgcal>

GRAVITY: Observing the Universe in Motion

Frank Eisenhauer¹
 Guy Perrin^{2,10}
 Wolfgang Brandner³
 Christian Straubmeier⁴
 Karine Perraut⁵
 António Amorim⁶
 Markus Schöller⁹
 Stefan Gillessen¹
 Pierre Kervella^{2,10}
 Myriam Benisty³
 Constanza Araujo-Hauck⁴
 Laurent Jocou⁵
 Jorge Lima⁶
 Gerd Jakob⁹
 Marcus Haug¹
 Yann Clénet^{2,10}
 Thomas Henning³
 Andreas Eckart⁴
 Jean-Philippe Berger^{5,9}
 Paulo Garcia⁶
 Roberto Abuter⁹
 Stefan Kellner¹
 Thibaut Paumard^{2,10}
 Stefan Hippler³
 Sebastian Fischer⁴
 Thibaut Moulin⁵
 Jaime Villate⁶
 Gerardo Avila⁹
 Alexander Gräter¹
 Sylvestre Lacour^{2,10}
 Armin Huber³
 Michael Wiest⁴
 Axelle Nolot⁵
 Pedro Carvas⁶
 Reinhold Dorn⁹
 Oliver Pfuhl¹
 Eric Gendron^{2,10}
 Sarah Kendrew³
 Senol Yazici⁴
 Sonia Anton^{6,8}
 Yves Jung⁹
 Markus Thiel¹
 Élodie Choquet^{2,10}
 Ralf Klein³
 Paula Teixeira^{6,9}
 Philippe Gitton⁹
 David Moch¹
 Frédéric Vincent^{2,10}
 Natalia Kudryavtseva³
 Stefan Ströbele⁹
 Eckhard Sturm¹
 Pierre Fédou^{2,10}
 Rainer Lenzen³
 Paul Jolley⁹
 Clemens Kister¹
 Vincent Lapeyrière^{2,10}
 Vianak Naranjo³
 Christian Luciu⁹
 Reiner Hofmann¹

Frédéric Chapron^{2,10}
 Udo Neumann³
 Leander Mehrgan⁹
 Oliver Hans¹
 Gérard Rousset^{2,10}
 Jose Ramos³
 Marcos Suarez⁹
 Reinhard Lederer¹
 Jean-Michel Reess^{2,10}
 Ralf-Rainer Rohloff³
 Pierre Haguenaue⁹
 Hendrik Bartko¹
 Arnaud Sevin^{2,10}
 Karl Wagner³
 Jean-Louis Lizon⁹
 Sebastian Rabien¹
 Claude Collin^{2,10}
 Gert Finger⁹
 Richard Davies¹
 Daniel Rouan^{2,10}
 Markus Wittkowski⁹
 Katie Dodds-Eden¹
 Denis Ziegler^{2,10}
 Frédéric Cassaing^{7,10}
 Henri Bonnet⁹
 Mark Casali⁹
 Reinhard Genzel¹
 Pierre Lena²

- ¹ Max-Planck Institute for Extraterrestrial Physics, Garching, Germany
- ² LESIA, Observatoire de Paris, CNRS, UPMC, Université Paris Diderot, Meudon, France
- ³ Max-Planck Institute for Astronomy, Heidelberg, Germany
- ⁴ Physikalisches Institut, University of Cologne, Germany
- ⁵ UJF–Grenoble 1/CNRS-INSU, Institut de Planétologie et d'Astrophysique de Grenoble, France
- ⁶ Laboratório de Sistemas, Instrumentação e Modelação em Ciências e Tecnologias do Ambiente e do Espaço (SIM), Lisbon and Porto, Portugal
- ⁷ ONERA, Optics Department (DOTA), Châtillon, France
- ⁸ Centro de Investigação em Ciências Geo-Espaciais, Porto, Portugal
- ⁹ ESO
- ¹⁰ Groupement d'Intérêt Scientifique PHASE (Partenariat Haute résolution Angulaire Sol Espace) between ONERA, Observatoire de Paris, CNRS and Université Paris Diderot

GRAVITY is the second generation Very Large Telescope Interferometer instrument for precision narrow-angle astrometry and interferometric imaging. With its fibre-fed integrated optics, wavefront sensors, fringe tracker, beam stabilisation and a novel metrology concept, GRAVITY will push the sensitivity and accuracy of astrometry and interferometric imaging far beyond what is offered today. Providing precision astrometry of order 10 microarcseconds, and imaging with 4-milliarsecond resolution, GRAVITY will revolutionise dynamical measurements of celestial objects: it will probe physics close to the event horizon of the Galactic Centre black hole; unambiguously detect and measure the masses of black holes in massive star clusters throughout the Milky Way; uncover the details of mass accretion and jets in young stellar objects and active galactic nuclei; and probe the motion of binary stars, exoplanets and young stellar discs. The instrument capabilities of GRAVITY are outlined and the science opportunities that will open up are summarised.

Fundamental measurements over a wide range of fields in astrophysics

Much as long-baseline radio interferometry has done, GRAVITY infrared (IR) astrometry, with an accuracy of order 10 microarcseconds and phase-referenced imaging with 4-milliarsecond resolution, will bring a number of key advances (Eisenhauer et al., 2008). GRAVITY will carry out the ultimate empirical test to show whether or not the Galactic Centre harbours a black hole (BH) of four million solar masses and will finally decide if the near-infrared flares from Sgr A* originate from individual hot spots close to the last stable orbit, from statistical fluctuations in the inner accretion zone or from a jet. If the current hot-spot interpretation of the near-infrared (NIR) flares is correct, GRAVITY has the potential to directly determine the spacetime metric around this BH. GRAVITY may even be able to test the theory of general relativity in the presently unexplored strong field limit. GRAVITY will also be able to unambiguously detect intermediate mass BHs, if they exist. It will dynamically measure the masses of supermassive

BHs (SMBHs) in many active galactic nuclei, and probe the physics of their mass accretion, outflow and jets with unprecedented resolution. Furthermore, GRAVITY will explore young stellar objects, their circumstellar discs and jets, and measure the properties of binary stars and exoplanet systems. In short, GRAVITY will enable dynamical measurements in an unexplored regime, and it will increase the range and number of astronomical objects that can be studied with the Very Large Telescope Interferometer (VLTI) substantially. An overview of the key experiments that will become possible with GRAVITY is illustrated on the Telescopes and Instrumentation section page (p. 6, lower panel).

A unique combination with the VLTI

The VLTI is the largest array of 8-metre-class telescopes that explicitly included interferometry in its design and implementation. No other array is equipped with a comparable infrastructure. The VLTI, with its four 8-metre Unit Telescopes (UTs) and a total collecting area of 200 m², is the only interferometer to allow direct imaging at high sensitivity and high image quality. The VLTI is also the only array of its class offering a large (2-arcsecond) field of view and this unique capability will, for the first time, be utilised, providing simultaneous interferometry of two objects. This capability allows narrow-angle astrometry with a precision of order 10 microarcseconds. A second new and unique element of GRAVITY is the use of IR wavefront sensors to observe highly obscured objects suffering high extinction. GRAVITY is also the only instrument providing phase-referenced complex visibilities, which is a major advantage for the model independence and fiducial quality of interferometric maps. The combination of VLTI and GRAVITY will be the world-leading facility for many years to come.

Adaptive optics assisted interferometric imaging and astrometry

GRAVITY provides high precision narrow-angle astrometry and phase-referenced interferometric imaging in the astronomical K-band (2.2 μm). It combines the light

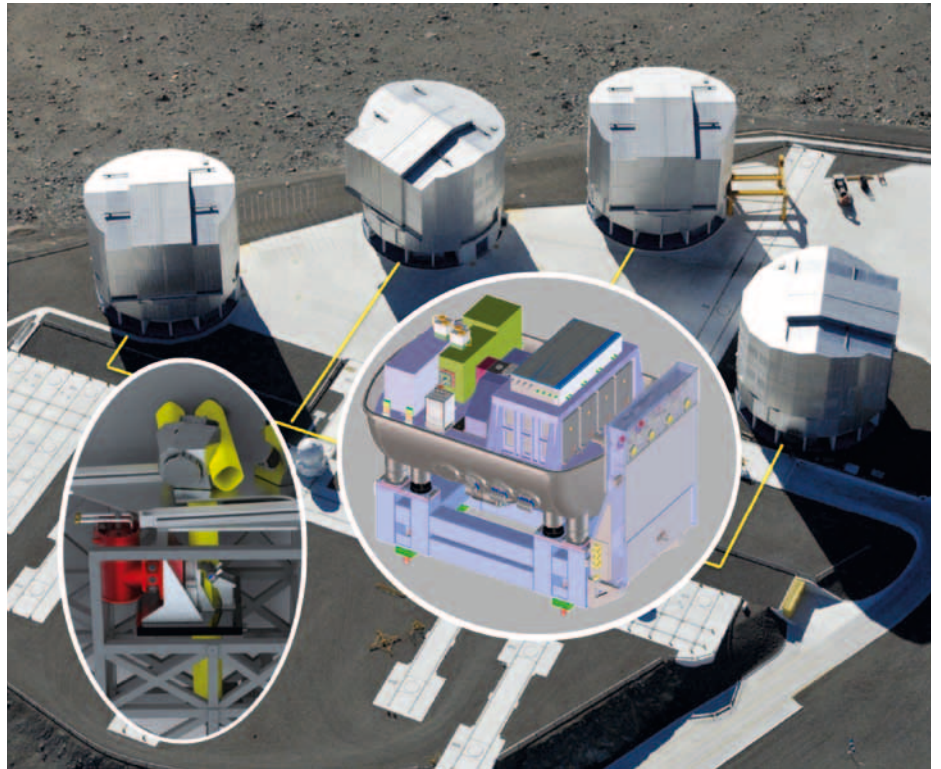
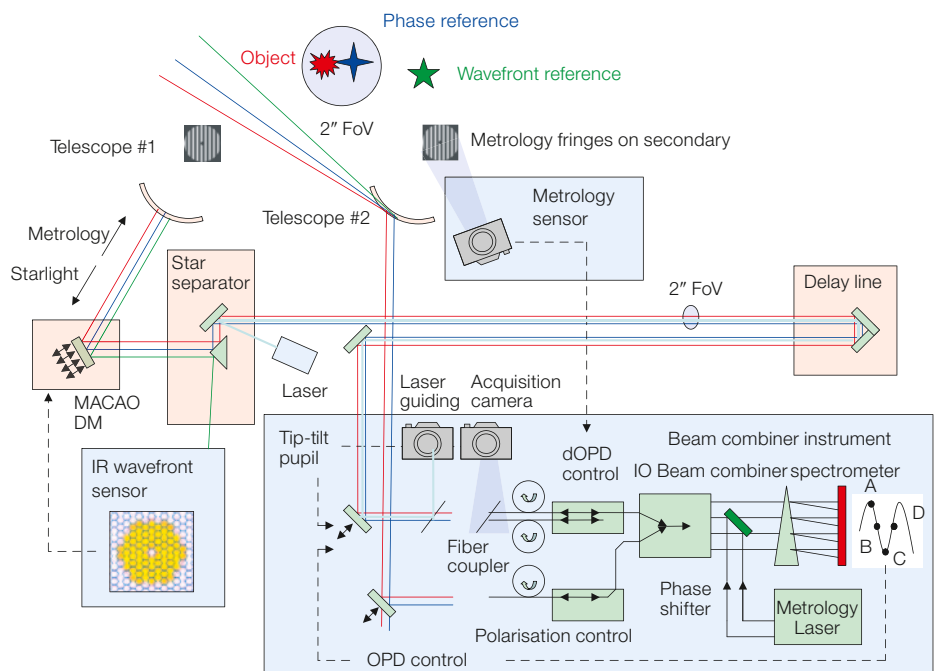


Figure 1. (Upper) GRAVITY at the VLT Interferometer. GRAVITY combines the light from four UT or AT telescopes, measuring the interferograms for six base-lines simultaneously, with a maximum baseline of 200 metres. The insets depict the GRAVITY beam-combiner instrument (middle), which is located in the VLTI laboratory, and one of the four GRAVITY IR wavefront sensors (left) for each of the UTs.

Figure 2. (Lower) Working principle of GRAVITY. The beam-combiner instrument (bottom right) is located in the VLTI laboratory. The IR wavefront sensors (bottom left) are mounted on each of the four UTs. The laser metrology is launched from the beam combiner and is detected at each UT/AT (top middle).



from four UTs or Auxiliary Telescopes (ATs), measuring the interferograms from six baselines simultaneously (see Figure 1). The instrument has three main components: the IR wavefront sensors (Clénet et al., 2010); the beam-combiner instrument; and the laser metrology — system (Bartko et al., 2010). Figure 2 gives an overview of the GRAVITY instrument. For clarity, only two of the four telescopes — i.e. one out of six baselines — are shown.

The GRAVITY IR wavefront sensors will be mounted in the Coudé rooms of the UTs and will command the existing Multiple Application Curvature Adaptive Optics (MACAO) deformable mirrors. The system can work on either of the two beams (on-axis or off-axis) behind the PRIMA star separators. Any additional tip/tilt from the beam relay down to the VLT laboratory will be corrected by a dedicated laser-guiding system. Low frequency drifts of the field and pupil will be corrected by GRAVITY's internal acquisition and guiding camera (Amorim et al., 2010). The interplay of these systems will guarantee an unperturbed and seeing-corrected beam at the entrance of the beam-combiner instrument in the VLT laboratory. The interferometric instrument will work on the 2-arcsecond (for UTs) or 4-arcsecond (for ATs) VLT field of view. Both the reference star and the science object have to lie within this field of view. The light of the two objects from the four telescopes is coupled (Pfuhl et al., 2010) into optical fibres for modal filtering, to compensate for the differential delay and to adjust the polarisation. The fibres feed two integrated optics beam

combiners (Jocou et al., 2010) and the coherently combined light is dispersed in two spectrometers (Straubmeier et al., 2010). A low resolution spectrometer provides internal phase- and group-delay tracking (Choquet et al., 2010) on the reference star, and thus enables long exposure times on the science target. Three spectral resolutions with up to $R \sim 4000$ are implemented in the science spectrometer, and a Wollaston prism provides basic polarimetry.

GRAVITY will measure the visibility of the reference star and the science object simultaneously for all spectral channels, and the differential phase between the two objects. This information will be used for interferometric imaging exploring the complex visibilities, and for astrometry using the differential phase and group delay. All functions of the GRAVITY beam-combiner instrument are implemented in a single cryostat for optimum stability, cleanliness, and thermal background suppression. The internal path lengths of the VLT and GRAVITY are monitored using dedicated laser metrology. The laser light is back-propagated from the beam combiner and covers the full beam up to the telescope spider above the primary mirror.

Highlights from the instrument development

A detailed description of GRAVITY's subsystems can be found elsewhere (Gillesen et al. [2010] and above references). Instead, we present a few

highlights from the ongoing prototype development: the world's first K -band ($2.2 \mu\text{m}$) integrated optics beam combiner for four telescopes, a high-speed photon-counting IR detector, and a novel laser metrology concept.

GRAVITY's beam combiner is an integrated optics chip, the optical equivalent of a microelectronic circuit, which combines several functions in a single component. It combines the advantages of compactness and stability, and provides outstanding visibility accuracies. Integrated optics is widely used in telecommunications up to $1.6 \mu\text{m}$, but does not cover the astronomically interesting K -band. GRAVITY has thus launched its own development programme between IPAG, LETI, and CIP to port the technology to longer wavelengths. Following a series of prototypes implementing individual functions, we now have the world's first K -band integrated optics beam combiner for four telescopes in hand (shown in Figure 3).

The second major breakthrough for GRAVITY is the recent success in the development of high-speed IR photon-counting detector arrays. All current astronomical IR fringe trackers and wavefront sensors suffer from the high readout noise of their detectors, which is ten or more electrons per pixel at frame rates of a few hundred Hz. The GRAVITY detectors overcome this noise barrier by avalanche amplification of the photoelectrons inside the pixels. Last year, SELEX-Galileo and ESO demonstrated for the first time a readout-noise of less



Figure 3. A recent breakthrough in integrated optics is shown (left) and an example image from the new avalanche photodiode detector arrays (right); both to be used in GRAVITY.

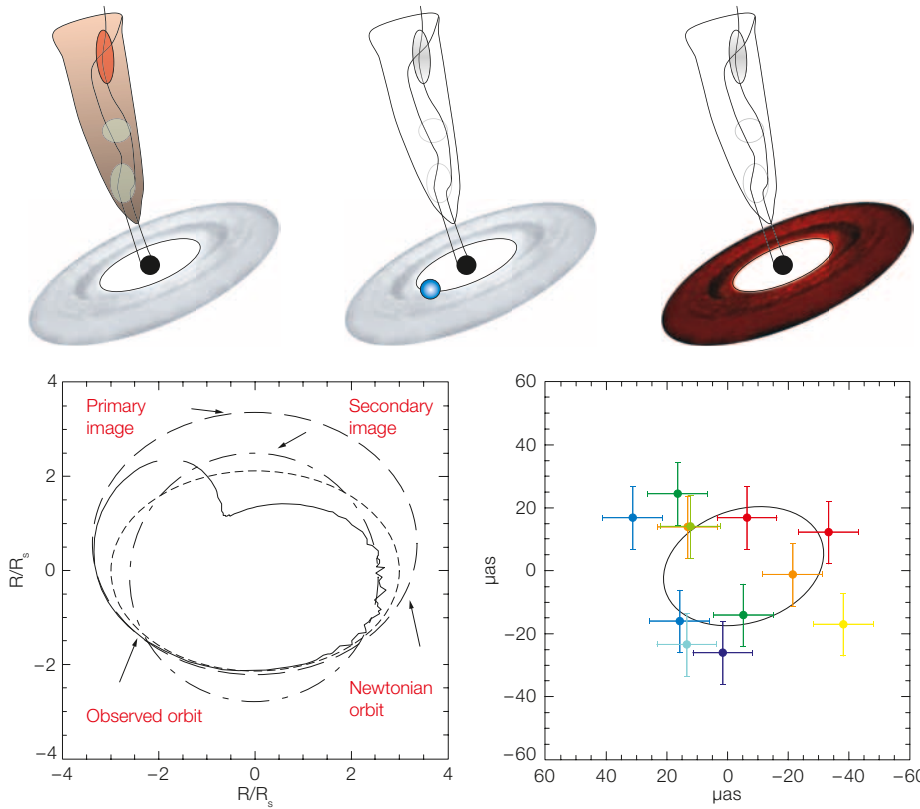


Figure 4. Uncovering the true nature of Sgr A* flares (upper three panels); probing spacetime close to the black hole event horizon (lower left); and measuring its spin and inclination (two lower right panels). GRAVITY will easily distinguish between the three most plausible flare scenarios: a jet (left), an orbiting hot spot (middle) and statistical fluctuation in the accretion flow (right). The detailed shape of the photo-centre orbit is dominated by general relativistic effects (lower left, from Paumard et al. 2008), and GRAVITY will thus directly probe spacetime close to the event horizon. The combination of time-resolved astrometry (lower middle) and photometry (lower right, from Hamaus et al., 2008) will also allow the spin and inclination of the BH to be measured.

than three electrons with their prototype detector array (see image in Figure 3). Based on this success, ESO and SELEX-Galileo are currently developing a next generation detector, which is tuned to GRAVITY's wavefront sensor and fringe tracker. Another example of a major breakthrough is in GRAVITY's laser metrology. It is based on a novel concept, and traces the starlight through the observatory, to allow the optical path to be measured at any desired point of the pupil up to the primary mirror. This concept and its implementation have been demonstrated in three technical runs at the VLTI.

Science cases for GRAVITY

In the following sections the science cases for GRAVITY are briefly outlined, beginning with the broad range of science opportunities that have opened up at the Galactic Centre of the Milky Way. The Galactic Centre is by far the closest galactic nucleus and the best studied SMBH (Genzel et al., 2010). There are still a number of fundamental open issues and just to name a few that we want to

answer with GRAVITY: What is the nature of the flares in Sgr A*? What is the spin of a BH? How can we resolve the "Paradox of Youth" of the stars in its vicinity? Even tests of fundamental physics may come into reach with GRAVITY: Does the theory of general relativity hold in the strong field around SMBHs? Do BHs really have "no hair"?

Uncovering the true nature of the Sgr A* flares

The Galactic Centre BH is surprisingly faint — its average luminosity is only about 10^{-8} of the Eddington luminosity, emitted predominantly at radio to sub-mm wavelengths. On top of this quasi-steady component there is variable emission in the X-ray and IR bands. Some of this variable emission comes as flares, typically a few times per day, lasting for about one to two hours, and reaching the brightness of massive main-sequence stars. The three most plausible explanations for the origin of these flares are: a jet with clumps of ejected material; hot spots orbiting a BH; or statistical fluctu-

ations in the accretion flow (Figure 4). The jet model seems natural from the presence of jets in active galactic nuclei. The orbiting hot-spot model would be a natural explanation for the observed quasi-periodicity in the light curves of flares and associated changes of the IR polarisation. However, the long-term light curves are well described by a pure, red power-law noise, indicating that statistical fluctuations in the accretion flow are responsible for the observed variability. Time-resolved astrometric measurements with GRAVITY will settle the debate (Eckart et al., 2010). Even without pushing GRAVITY to its ultimate performance, the observed distribution of flare positions and its periodic variation will distinguish between these models.

Measuring spin and inclination of the Galactic Centre black hole

The mass of the Galactic Centre BH is well known from stellar orbits. If the currently favoured orbiting hot-spot model is correct, GRAVITY will take the next step and measure its spin and inclination.

These measurements are more difficult because the astrometric signature from the spin is a factor few less than the orbital motion and lensing effects. However, the combined signal from the periodic light curves and astrometry is much stronger. Already the simple correlation between the observed position variation and flux variability is giving the first insights into the source geometry. The next step is a simultaneous fit to the observed motion and light curve to quantify the underlying model parameters (Figure 4). Finally, the periodic flux can be used to trace the orbital phase to coherently co-add measurements from multiple flares, such that higher order signatures can be directly identified.

Resolving the Paradox of Youth of the Galactic Centre stars

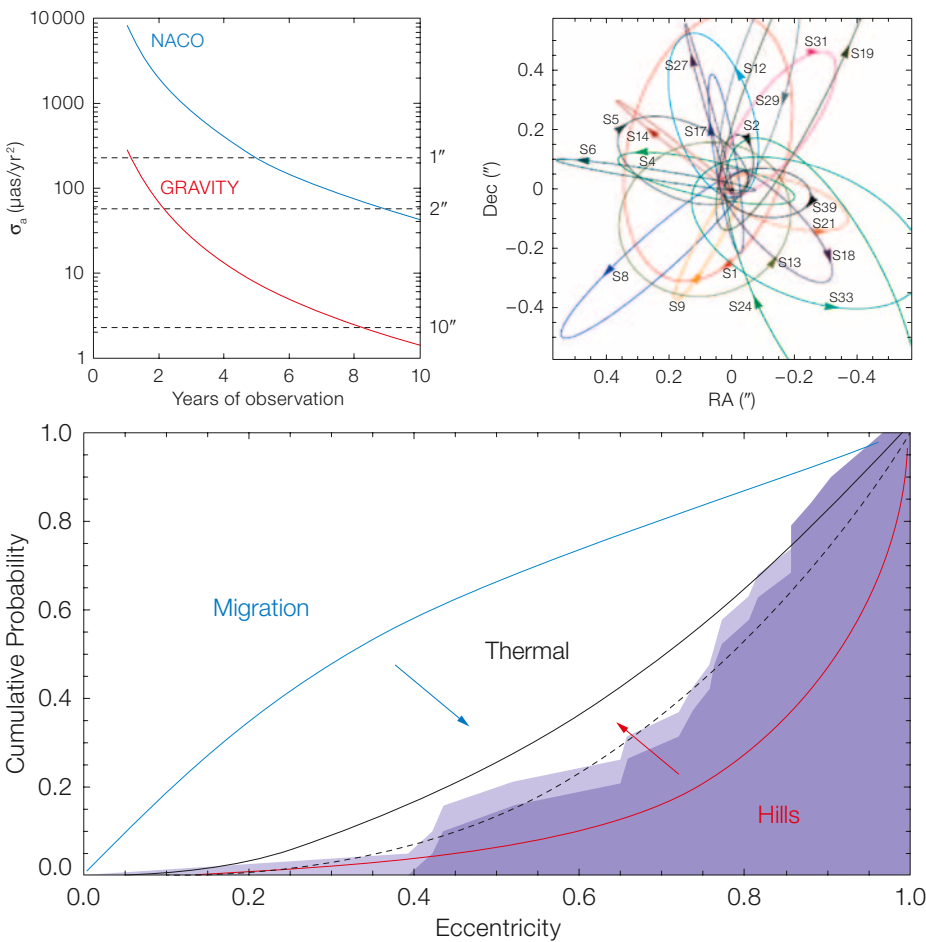
Most stars in the central light-month of the Galactic Centre are young, massive

early-type main sequence stars. It is currently not understood how these stars have formed or moved so close to the SMBH, because the tidal forces should have prevented *in situ* formation, and because these stars are too young to have migrated so far within the timescale of classical relaxation. Precise orbit measurements with GRAVITY offer a route to resolving this Paradox of Youth. In particular measurements of the orbital eccentricities can distinguish between the various scenarios. The currently favoured Hills scenario, in which massive binaries are scattered down to the BH and one component is ejected in a three-body interaction with the BH, will lead to predominantly high eccentricities. In contrast, the competing migration scenario, in which the stars migrate from circumnuclear stellar discs, will result mainly in low initial eccentricities. First results from adaptive optics observations slightly favour the Hills scenario, but the significance is still marginal. GRAVITY will

significantly enlarge the number of stars with known eccentricities, and will distinguish between the formation scenarios unambiguously (see Figure 5).

Testing general relativity in the strong field regime

The unprecedented astrometric accuracy of GRAVITY may even allow the theory of general relativity to be tested in the (so far) unexplored strong field around SMBHs. The observed orbit of a hot spot on the last stable orbit will be dominated by strong gravitational effects like gravitational lensing and redshift (Figure 4). GRAVITY observations of the flaring BH will thus directly probe spacetime in the immediate vicinity of the event horizon of the BH. The stellar orbits will be notably affected by higher order general relativistic effects, for example the relativistic periastron shift and the Lense-Thirring precession of the orbital angular momentum around the BH spin axis (Figure 6). These effects will be strongest for stars within the central light-week, which will be observed with GRAVITY in its interferometric imaging mode. In the most optimistic case, GRAVITY may even be able to test the so-called “no-hair” theorem (Will, 2008), which states that a BH is fully characterised by its mass and spin. In particular the BH spin and its quadrupole moment should be strictly related. Since spin and quadrupole moment couple differently to the inclination of stellar orbits, they can be measured independently (see Figure 6).



Active galactic nuclei

The standard unified model for active galactic nuclei postulates that an accreting SMBH is surrounded by an obscuring torus, whose orientation determines if the central engine is hidden

Figure 5. Solving the Paradox of Youth of the Galactic Centre stars. GRAVITY will be able to measure accelerations, i.e. individual orbits, out to about 10 arcseconds distance from the SMBH (upper left) and will significantly enlarge the number of S-stars (upper right) with precise eccentricities (from Gillessen et al., 2009). The improved eccentricity distribution (lower) can distinguish between the various formation scenarios proposed for stars in the central light-month.

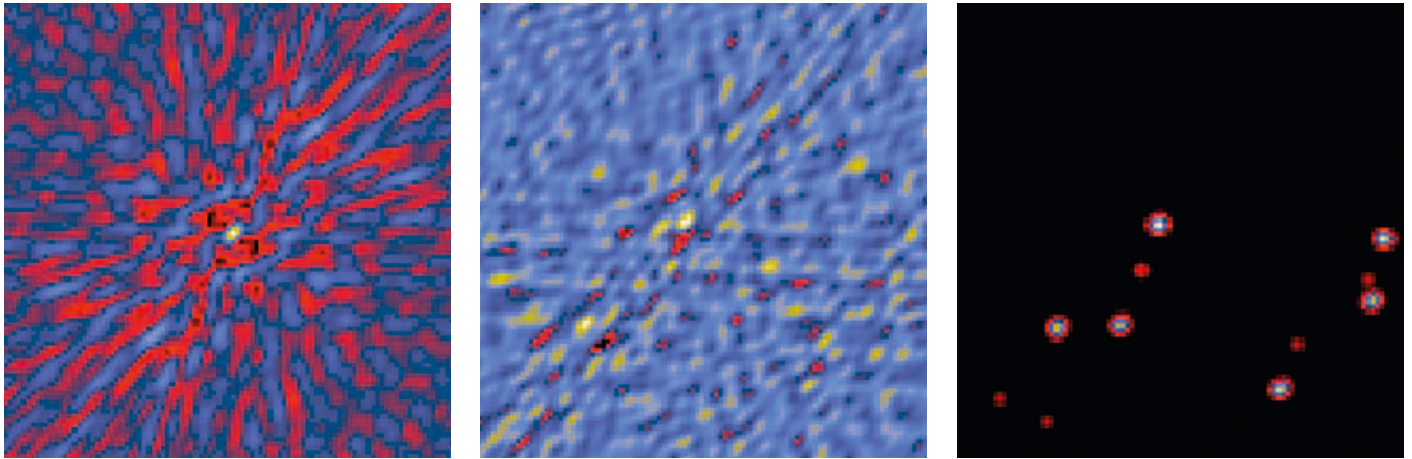


Figure 6. Testing the theory of general relativity with stellar orbits. GRAVITY will observe the orbits of stars within the central light-week of the Galactic Centre by means of interferometric imaging (upper panels: dirty beam with a resolution of four milliarcseconds (left), simulated dirty image (middle), cleaned image (right, from Paumard et al. 2008)). Stellar orbits (illustrated in the lower left panel) will be affected by the general relativistic periastron shift (red arrows) and the Lense-Thirring precession of the orbital angular momentum (blue arrows). For small distances to the BH, the timescale of these relativistic effects are short enough (lower right) to be in reach of GRAVITY (blue shaded area).

from the observer's view or not. The direct proof that this absorber is really a torus, rather than another structure, is still pending. Indeed most resolved gaseous structures on the putative scale of the torus appear more disc-like, for example the maser disc, the radio continuum emission and the mid-IR emission of the prototypical active galactic nuclei NGC 1068 (see Figure 7). Observing six baselines simultaneously, GRAVITY will image the inner edge of the torus with unprecedented quality, where the dust is close to the sublimation limit. GRAVITY will thus put strong constraints on the absorber models. These models are very much inspired by the observations of NGC 1068, but the few active galactic nuclei with interferometric observations show a puzzling variance. GRAVITY will significantly extend the sample to finally draw statistically sound conclusions.

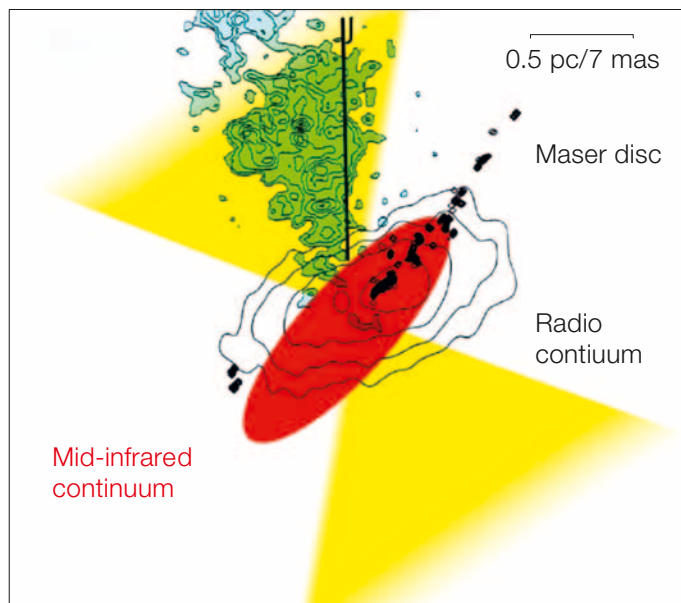


Figure 7. A sketch of the prototypical active galactic nucleus of NGC 1068 (from Raban et al., 2009). The gaseous structures and dust emission on the scale of the putative torus appear disc-like, while the unified model suggests a geometrically thick torus. Observing at NIR wavelengths, GRAVITY will image the inner edge of the absorber, putting strong constraints on the absorber geometry.

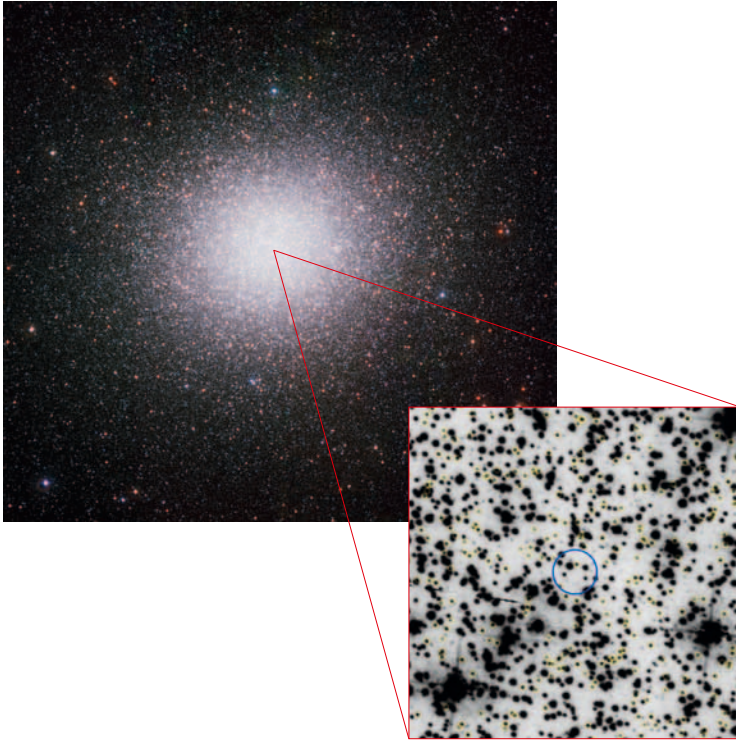


Figure 8. Discovering IMBHs in star clusters. The left panel shows the globular cluster ω Cen and a zoom into its centre (from Anderson et al., 2010). The blue circle has a radius of 1 arcsecond. The statistical analysis of the velocity dispersion is limited by having only a few stars within the sphere of influence of the BH. GRAVITY will make a clear-cut case in a few suitable clusters by measuring the accelerations of individual stars (right), directly probing the central gravitational potential.

Even the broad-line region may come in reach for GRAVITY. It is seen in those active galactic nuclei for which we have a direct view onto the SMBH. The size of the broad-line region can currently only be measured indirectly, looking at the time delay between the variations of the ultraviolet continuum and the emission lines. Broad-line regions of nearby active galactic nuclei are typically smaller than 0.1 milliarcseconds, and thus too small to be resolved in GRAVITY's images. But the astrometric accuracy of GRAVITY will allow measurement of the velocity gradient across it. This will strongly constrain the broad-line region geometry and determine dynamically the mass of the central BH.

Intermediate mass black holes

The tight correlation between the bulge mass of a galaxy and the mass of the central SMBH suggests that the rapid formation of a spheroidal stellar system also collects up to about 1% of the initial mass in a central BH. Such a core collapse and collisional build-up may have also led to the formation of intermediate

mass BHs in massive, dense star clusters. Recent searches in globular clusters show evidence for such IMBHs (Figure 8). However, the sphere of influence of the postulated BHs is typically less than a few arcseconds, such that only a few stars are available for these statistical studies. GRAVITY will dramatically change this situation in a few suitable cases for which accelerations can be detected, thus directly probing the gravitational potential without suffering from the small number statistics of velocity dispersion measurements.

X-ray binaries

X-ray binaries are the best place to study neutron stars and BHs. These neutron stars and BHs are very faint when isolated, but they can be observed as part of a X-ray binary, some of which are bright enough for GRAVITY. We expect that it will be possible to detect the orbital displacement from the compact companion in the interferometric closure phase. Even the absolute astrometric displacement of the binary system's photo-centre will be observable with GRAVITY in a few

nearby systems, for which a suitable astrometric reference star is available. Combined with spectroscopy, these observations will provide the orbital elements and distance of the system, as well as the mass of the two components. In addition GRAVITY will characterise the wind from the stellar companion at a scale of a few stellar radii. The physical properties of this wind are particularly interesting as it is the main source for feeding the compact object.

Masses of the most massive stars and brown dwarfs

There is still a discrepancy of up to a factor of two in the mass estimates for the most massive main sequence stars. It is not known what the maximum allowed mass for a star is. Comparison of spectra with atmospheric models yields upper mass limits of typically $60 M_{\odot}$, whereas evolutionary tracks and observed luminosities suggest a mass of up to $120 M_{\odot}$. Clearly, dynamical mass estimates are required. Quite a number of spectroscopic binary O-stars are known in the cores of starburst clusters like Arches,

30 Doradus and the Galactic Centre. GRAVITY will resolve some of the longer period spectroscopic binaries, and will monitor the astrometric motions of the photo-centres for the short period, close binaries. In this way, GRAVITY will directly yield dynamical mass estimates for many of these systems, and finally provide the crucial input required to calibrate stellar evolutionary tracks.

The situation is similar for brown dwarfs, which are the lowest mass stars. Most current mass estimates are based on evolutionary models and model atmospheres, which have not yet been accurately calibrated by observations. Dynamical masses for brown dwarfs have only been derived for a few objects. In general, the observed masses for sub-stellar objects with ages older than a few 100 million years seem to be in good agreement with theoretical models. But there are significant uncertainties and discrepancies for the very young, very low mass objects like AB Dor C. If indeed these objects are more massive than indicated by stellar evolutionary models, many putative planets would be rather in the brown dwarf than the planetary

mass regime. GRAVITY will probe many more multiple systems like AB Dor C, deriving the individual component masses, and even probe the sub-stellar companions themselves for binarity, thus clarifying this situation.

Jet formation in young stars

Jets are omnipresent in the Universe, from gamma-ray bursts to active galactic nuclei, from young stars to micro-quasars. Understanding the formation of jets is still one of the “big” open challenges of modern astrophysics. It is now known that jets are powered by magneto-hydrodynamic engines, tapping the energy of the accretion disc. Young stars are ideal objects to study these processes at the highest resolution. Matter from the disc surface couples to the open, highly inclined star–disc magnetic field lines, and is accelerated up to the Alfvén surface. The rotating magnetic field lines then become more and more twisted, wind up and collimate the jet. But surprisingly, some stellar jets are found only on one side of the disc. Clearly, some basic ingredient is missing in our

understanding of jet formation. The relevant processes take place within about one astronomical unit from the star, which at the typical distance to the nearest star-forming regions of about 150 pc translates into an angular size of about 6 milliarcseconds, slightly larger than GRAVITY’s 4-milliarcsecond angular resolution. By repeatedly imaging the time-dependent ejection just outside the engine at high spectral resolution, GRAVITY will provide key observational tests of time-dependent jet simulations (Figure 9). Furthermore, the astrometric signal across the emission line will directly probe the central engine on the sub-milliarcsecond scale, i.e. well within one astronomical unit.

Planet formation in circumstellar discs

Circumstellar discs are the cradles of planet formation. Planets are thought to form rapidly in a few million years through the fast evolution of the disc structure. Dust processing, settling and coalescence are accompanied by an increase of particle size, leading to the formation of planetesimals that eventually aggregate to form planetary systems. The planet formation process is expected to leave strong imprints in the disc structure, such as inner disc clearing, gap opening and tidally induced spiral structures. GRAVITY will hunt down all these signs. Its unique sensitivity in the NIR will allow the sample of observed young stars to be increased towards the poorly explored solar-mass regime. This will be done at sub-astronomical unit resolutions for the closest star-forming regions. It will reveal the disc structure evolution, the so-called transitional step, search for disc disruption signatures, and be used to probe the presence of hot, young sub-stellar and planetary companions.

Astrometric planet detection

Many hundreds of exoplanets have been detected to date, mostly from radial

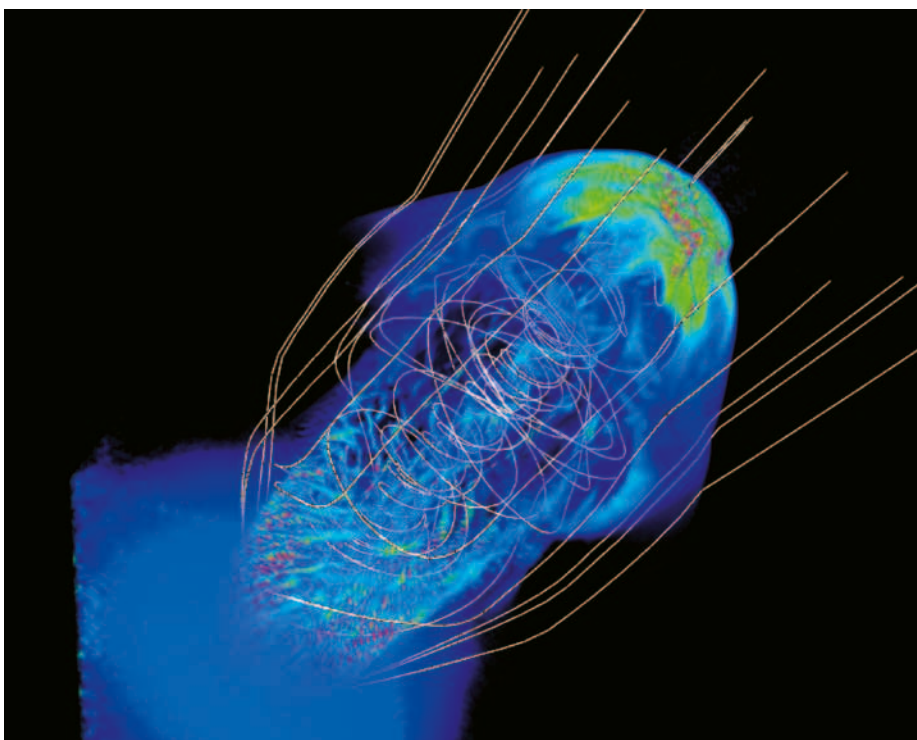


Figure 9. 3D simulation of a large-scale jet from a nearby young star. In this picture the bow shock has propagated roughly 400 milliarcseconds out from the jet engine (from Staff et al., 2010).

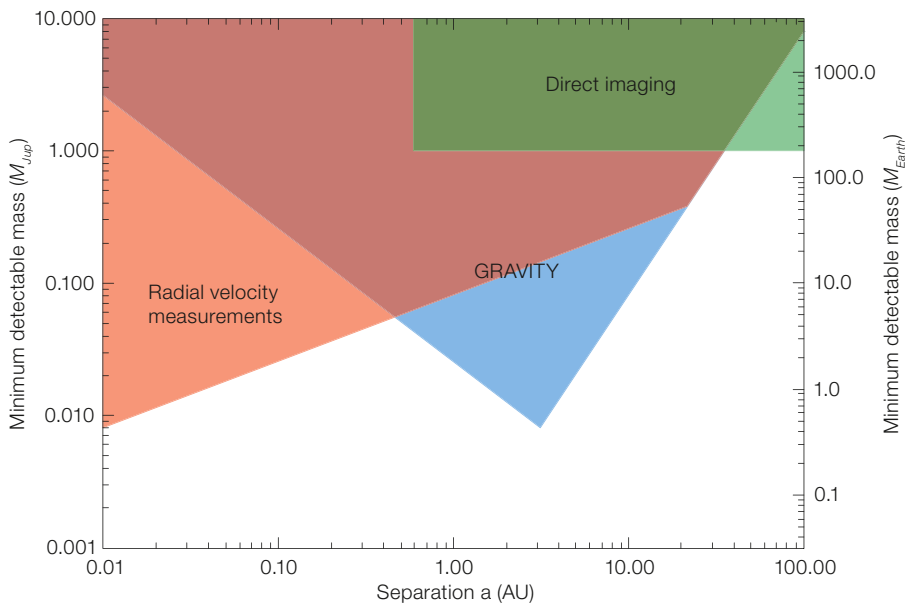


Figure 10. The realm of GRAVITY exoplanet search among very low-mass stars is shown. The blue shaded area depicts the discovery space of GRAVITY for planets around a late M dwarf at a distance of 6 pc. The green and red areas indicate roughly the parameter space probed by radial velocity observations and direct imaging.

velocity measurements and photometric transit observations. However, these methods are biased towards detecting massive planets in close orbits. Moreover, radial velocity measurements alone cannot provide the inclination of the orbit, and can thus only give a lower limit for the mass of the planet. In contrast, the reflex motion of a star observed by astrometry allows the orbital solution to be retrieved, resulting in an unambiguous measurement of the mass of the planet.

Astrometric planet detection is also a scientific goal of the PRIMA facility, currently being commissioned at the VLTI (Delplancke, 2009). While planet searches with PRIMA mostly target isolated stars or wide binaries, GRAVITY will focus on detecting brown dwarfs and exoplanets in close binary systems. For Sun-like stars, GRAVITY's survey volume would extend out to more than 200 pc. Even the much fainter M-stars, with just 20% of the mass of the Sun, can be observed out to about 25 pc (Figure 10). GRAVITY has the potential to detect exoplanets as small as three Earth masses around an M5V star at a distance of 5 pc, or less than two Neptune masses around an M3V star at a distance 25 pc.

Transiting exoplanets

The transit of a planet in front of its host star causes an apparent motion of the photo-centre of the star and introduces a slight asymmetry in the image of the star. The former effect can be measured using GRAVITY's astrometric observing mode, the latter effect can be seen in the closure phases of the interferograms (van Belle, 2006). GRAVITY observations of such transits have the potential to measure the radius of the planet and its parent star.

For a star like HD 189733, a $0.8 M_{\odot}$ star at a distance of about 20 pc, and its Jupiter-sized planet on a very close, two-day orbit, the apparent motion is about 10 microarcseconds. This is at the limit of GRAVITY's capability, but transiting planets around later-type dwarfs would be easier to detect. This type of measurement will also give the position angle of the orbit on the sky, which, combined with the direction and amount of polarisation of the light reflected by the planet, might ultimately even place constraints on the distribution of surface features like clouds and weather zones.

On sky in 2014

The GRAVITY project emerged from ESO's second generation VLTI instrument workshop in 2005. Following the initial Phase A study in 2006/7, ESO's Science and Technical Committee's recommendation and ESO Council's endorsement in 2008, and the preliminary design review in 2010, the project is currently in its final design phase. First astronomical light at the VLTI is planned for 2014.

References

- Amorim, A. et al. 2010, Proc. SPIE, 7734, 773415
- Anderson, J. et al. 2010, ApJ, 710, 1032
- Bartko, H. et al. 2010, Proc. SPIE, 7734, 773421
- van Belle, G. 2008, PASP, 120, 617
- Choquet, E. et al. 2010, Proc. SPIE, 7734, 77341Z
- Clénet, Y. et al. 2010, Proc. SPIE, 7736, 77364A
- Delplancke, F. 2008, NewAR, 52, 199
- Eckart, A. et al. 2010, Proc. SPIE, 7734, 77340X
- Eisenhauer, F. et al. 2008, *The Power of Optical/IR Interferometry: Recent Scientific Results and 2nd Generation Instrumentation*, ed. Richichi, A. et al., ESO Astrophysics Symposia, 41, 431
- Genzel, R. et al. 2010, RvMP, 82, 3121
- Gillessen, S. et al. 2010, Proc. SPIE, 7734, 77340Y
- Gillessen, S. et al. 2009, ApJ, 692, 1075
- Jocou, L. et al. 2010, Proc. SPIE, 7734, 773430
- Paumard, T. et al. 2008, *The Power of Optical/IR Interferometry: Recent Scientific Results and 2nd Generation Instrumentation*, ed. Richichi, A. et al., ESO Astrophysics Symposia, 41, 431
- Pfuhl, O. et al. 2010, Proc. SPIE, 7734, 77342A
- Raban, S. et al. 2009, MNRAS, 394, 1325
- Staff, J. E. et al. 2010, ApJS, 722, 1325
- Straubmeier, C. et al. 2010, Proc. SPIE, 7734, 773432
- Will, C. M. 2008, ApJL, 674, 25

The E-ELT has Successfully Passed the Phase B Final Design Review

Roberto Gilmozzi¹
Markus Kissler-Patig¹

¹ ESO

The European Extremely Large Telescope (E-ELT) recently achieved a critical milestone by passing its Phase B final design review. The top-level question posed to the Review Board was whether the technical maturity of the design of the E-ELT is sufficient to warrant the programme entering the construction phase. It was the unanimous conclusion of the Review Board that the answer to this question is "Yes".

This comprehensive design review of the E-ELT project was held at ESO Headquarters in Garching on 21–24 September 2010. The Review Board consisted of 11 distinguished members: Steve Szechtman (Carnegie/GMT, chair), Chuck Claver (NOAO/LSST), Matt Johns (GMT), Doug

MacMynowski (Caltech/TMT), Buddy Martin (Steward Observatory Mirror Lab), Harald Nicklas (University of Gottingen), Roberto Ragazzoni (INAF), Francois Rigaut (Gemini), Luc Simard (HIA/TMT), Doug Simons (Gemini) and Larry Stepp (TMT). Six weeks before the review, the Telescope Construction Proposal with over 300 ancillary documents was made available to the Board, to which it responded with over 300 written questions and comments. The review ran over four days during which the design was probed in great depth. The outcome was praise, constructive feedback and the unanimous agreement that the E-ELT is ready to enter the construction phase.

The Review Board not only addressed technical issues but also commented on cost/contingency and the schedule (the executive summary of the board report can be downloaded¹). The project saw it as due diligence to address in more depth some of these points in a Delta Phase B study, which is now underway.

In the meantime, Brazil has signed the formal accession agreement becoming ESO's 15th Member State (see the announcement by Tim de Zeeuw on p. 5 and the ESO press release 1050²), bringing new resources and skills to the organisation at the right time for them to make a major contribution to this exciting project.

All the pieces are now in place to go for Council approval this year and to break ground on Cerro Armazones in 2012, then head for first light of the biggest eye on the sky at the end of this decade.

Links

¹ Executive summary of E-ELT Board report:
<http://www.eso.org/sci/facilities/eelt/docs>

² Press release on Brazil joining ESO:
<http://www.eso.org/public/news/eso1050/>



Figure 1. The members of the E-ELT Phase B Final Review Board, together with the ESO team, share the picture with some of the prototypes of the E-ELT components.



Near-infrared colour image of the core of the nearby star formation region Monoceros R2 formed by combining VISTA images in the Y-, J- and Ks-bands. Monoceros R2 is part of a large association of embedded high and intermediate mass star-forming regions, reflection nebulae and molecular clouds. See eso1039 for further details.

Ozone: Twilit Skies, and (Exo-)planet Transits

Robert Fosbury¹
George Koch²
Johannes Koch²

¹ ESO

² Lycée Français Jean Renoir, München, Germany

Although only a trace constituent gas in the Earth's atmosphere, ozone plays a critical role in protecting the Earth's surface from receiving a damaging flux of solar ultraviolet radiation. What is not generally appreciated, however, is that the intrinsically weak, visible Chappuis absorption band becomes an important influence on the colour of the entire sky when the Sun is low or just below the horizon. This effect has been explored using spectra of the sunset and also of the eclipsed Moon; phenomena that involve a similar passage of sunlight tangential to the Earth's surface. This geometry will also be relevant in future attempts to perform transit spectroscopy of exo-Earths.

Introduction

The colours seen by an observer of the Earth's sky, from within or from without

the atmosphere, can be rich and varied. The processes that result in this palette are geometrically complex, but comprise a limited number of now well-understood physical effects. This understanding was not gained easily. From the time when early humans first consciously posed the question: "*What makes the sky blue?*", to the time when the processes of scattering by molecules and molecular density fluctuations were elucidated, thousands of years passed, during which increasingly intensive experiments and theories were developed and carried out (Pescic, 2005).

Most physicists, if asked why the sky is blue, would answer with little hesitation: "*Because of Rayleigh scattering by molecules.*" With the Sun above the horizon in a clear sky, this is worth a good mark. During twilight, however, things get more complicated.

Twilight has a special place in the life of an observational (optical/near-infrared) astronomer who is privileged to witness it from some of the most spectacular sites on the planet. The geometry of the illumination of the atmosphere at twilight is also very pertinent to the study of transiting exoplanets, when the path of starlight is tangential to the planetary sphere.

This article is about the effect of ozone on the colour of the twilit sky and, in the same vein, its appearance as the strongest telluric absorption feature in the visible spectrum of the Earth as it would be seen by a distant observer watching it transit in front of the Sun. We present and analyse spectrophotometric observations of sunset and also discuss observations of the eclipsed Moon reported by Pallé et al. (2009).

Ozone

Ozone (O₃ or trioxygen) is an unstable allotrope of oxygen that most people can detect by smell at concentrations as low as 0.01 parts per million (ppm). When present in the low atmosphere as a pollutant, it has many damaging effects, including to lung tissue. At higher altitudes, typically between 15 and 40 km, however, it produces the beneficial effect of preventing damaging ultraviolet (UV) radiation from reaching ground level. The Hartley band, extending between 200 and 300 nm, absorbs very strongly in this region with a maximum at 255 nm. The UV absorption extends, more weakly, in the Huggins band up to around 360 nm. In the visible spectrum, a radial path through the atmosphere exhibits very little ozone absorption but, as the column increases at greater zenith distances, the Chappuis band begins to have an appreciable effect by absorbing across the entire visible spectrum with a maximum close to 600 nm. More absorptions, in the Wulf bands, appear in the infrared at 4.7, 9.6 and 14.1 μm.

By absorbing red and orange light, the Chappuis band has the effect of imparting a pale blue colour to pure ozone gas in the laboratory. As the Sun approaches the horizon, the increasing optical depth in the Chappuis band begins to have an effect on the sky colour that, at twilight, dominates the effect due to Rayleigh scattering (Hulbert, 1953). The colour of the clear zenith sky as the Sun

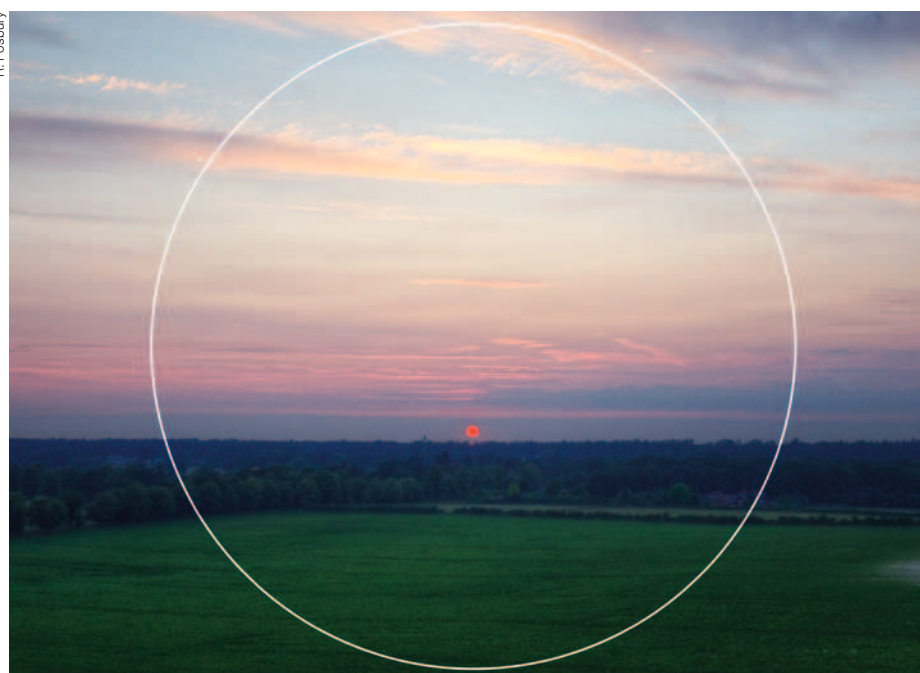


Figure 1. A few minutes before sunset at the Appleton Water Tower in Norfolk on 27 June 2010. The white circle shows the approximate pointing and acceptance aperture of the fibre input to the spectrometer. The deep red Sun and the haze at the horizon suggest a high atmospheric aerosol content which is reflected in the model fit to the spectrum.

sets is far bluer than can ever be achieved by Rayleigh scattering alone and simple models demonstrate that, in the absence of ozone, it would be a pale grey–yellow shade at this time. Observations of the sky and/or the setting sun with a spectrometer show what a profound effect the ozone has on the telluric spectrum, as it far exceeds the effects produced by water and diatomic oxygen absorption (so familiar to optical spectroscopists) on the visible spectral energy distribution.

Spectral measurements and models

We have made a series of spectrophotometric measurements of both the sky and the Sun, covering a period from several hours before sunset up to a short period afterwards. These have been made under both clear and overcast skies using a fibre input to a spectrometer, which results in an effective input aperture with a full width half maximum (FWHM) of 25° . The spectrometer, an Ocean Optics Jaz, covers a wavelength range of 350–1000 nm in 2048 spectral channels with a spectral resolution of 1.5 nm (FWHM). Exposure times range from 3 to over 100 ms per integration with each observation being the average of 32 or 64 individual exposures.

Sunset

Reported here are data collected from the top of a tower (the Appleton Water Tower¹) in Sandringham, Norfolk, England on the evening of the 27 June 2010 with the axis of the input fibre tracking the position of the Sun to within a few degrees. The scene just preceding sunset is shown in Figure 1, where it can be seen that the sky is partially cloudy and quite hazy on the horizon, suggesting a relatively high atmospheric aerosol concentration. With our large angular input aperture, and especially at the shorter wavelengths, the scattered light from the sky becomes the major contributor to the signal when the Sun is below a few degrees in altitude.

Figures 2a and 2b show a spectrum (black line) constructed as an average of four observations taken during the half

hour before sunset. In order to remove the Fraunhofer lines originating in the solar atmosphere, the observed spectrum is divided by one taken five hours before sunset. This shows the very strong telluric water and diatomic oxygen absorptions expected at large zenith distances. It also shows the very broad dip, centred at about 585 nm, due to the Chappuis band of ozone. Note the coincidence of a pair of water bands with the central structure of the ozone Chappuis absorption between 560 and 600 nm. This ozone feature is prominent in the spectrum of sunset viewed with a visual spectroscopist.

In order to model the overall shape of this spectrum we have used an analytic representation of molecular Rayleigh scattering, taken from Allen (1973), expressed per atmo-cm (thickness of atmospheric layer in cm when reduced to standard temperature and pressure, STP). This gives a scattering cross-section which varies as wavelength to the power -4.05 to take account of the scattering and the wavelength variation of refractive index. It is normalised to give an optical depth of 0.098/atmo-cm at 550 nm. For dust and aerosols, we use Allen's wavelength exponent of -1.3 , normalised to give an optical depth of 0.195/atmo-cm at 550 nm, which corresponds to normally clear conditions. For the ozone cross-section we use data from the project Spectroscopy & Molecular Properties of Ozone², normalised to give an optical depth of 0.0268 at 550 nm for 0.3 atmo-cm (taken as the standard ozone depth).

We consider two types of atmospheric path to compute the spectrum ratios relative to the high Sun. The first is the direct line of sight to the Sun, where we account for Rayleigh and aerosol scattering out of the beam and ozone absorption. The optical depth is derived from the atmospheric path as a function of solar zenith distance, choosing scaling factors of order unity for the aerosol and ozone contributions relative to the Rayleigh scattering.

The second contributor is scattered skylight summed from a set of twelve equal logarithmically-spaced atmospheric paths up to 100 atmo-cm. Each path is given a weighting factor chosen to match

the spectral shape. The initial values were chosen based on the geometry of the observation, but then adjusted to give the best match. The aerosol and ozone scaling factors can be chosen independently from those applied to the direct solar path. Each sky path has a source term that is proportional to the sum of the Rayleigh and aerosol cross-sections and a negative exponential sink term that represents ozone absorption and molecular and aerosol scattering out of the beam, both scaled for pathlength. Finally, the relative contributions of direct sunlight and skylight are adjusted to take account of the balance imposed by the large input aperture.

Although this model serves the purpose of a rather complicated fitting function, rather than an *ab initio* calculation, it does give a very good feel for how the skylight we see is influenced by the geometry it has to negotiate on its path through the atmosphere. We stress that the complexity derives from the geometry rather than the physics of absorption and scattering.

Figure 2 (upper) shows the separate components of direct sunlight (brown line) and the combination of a set of different paths involving a single scattering from the sky (dark blue line). The combination of the two is shown as a red line, and the ratio of the data to the model gives a normalised telluric spectrum containing the O₂ and H₂O features that we do not model (light blue line). Figure 2 (lower) shows the same model except for the ozone contribution that is set to zero for both the direct and the scattered paths.

Lunar eclipse

The deep, copper-coloured illumination of the eclipsed Moon represents the extinction and forward scattering of the Sun's light by a tangential passage through the Earth's atmosphere summed over the entire range of altitudes where the optical depth is significant (see Figure 3 for a sequence of photographs of the 2010 winter solstice lunar eclipse). This geometry is similar to that which applies when a transiting planet is seen against the disc of its parent star. This

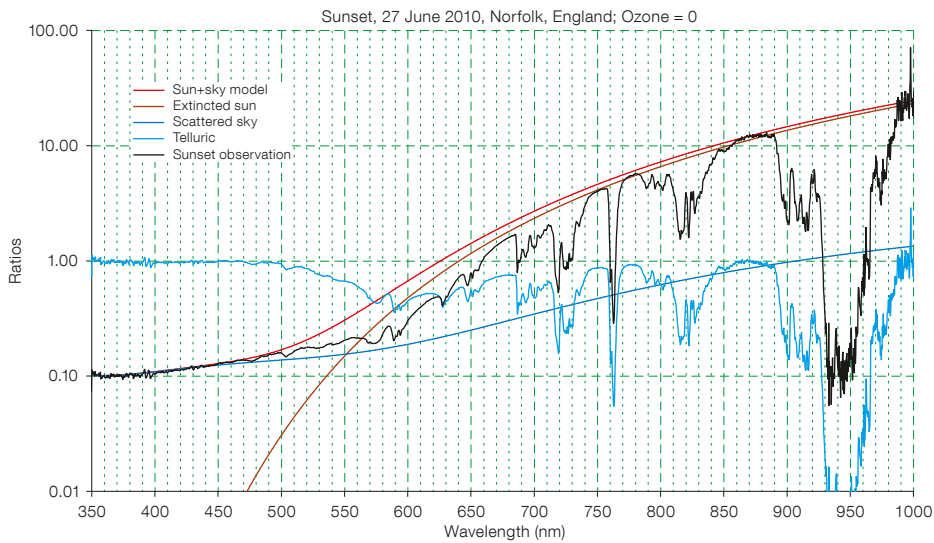
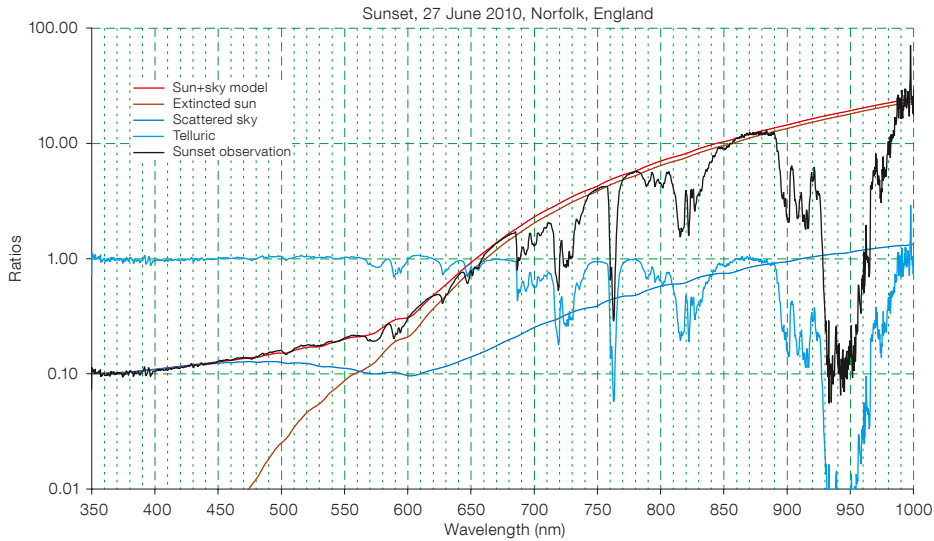


Figure 2. Upper: The visible and near infrared spectrum of the setting Sun (black line). The red line shows our model fit to this observed ratio, comprising the addition of the direct extincted light from the Sun (brown line) and the combination of a set of different paths involving a single scattering from the sky (dark blue line). The light blue line shows the ratio of the observed spectrum to the model fit and so reveals the telluric absorption due to diatomic molecular oxygen and water vapour. Lower: The same model fit but with the ozone content of the atmosphere set to zero. This gives a good idea of the extent of the ozone effect on the spectrum when the Sun is at large zenith distances.



Figure 3. A photo-montage of the Moon during the eclipse coinciding with the 2010 winter solstice on 21 December. This gives an excellent representation of the orange/copper colour of the illumination within the umbra of the Earth.

recognition prompted Pallé et al. (2009) to make the first comprehensive optical/infrared observations of an eclipsed Moon with modern, digital spectrophotometers. Using a combination of measurements of the uneclipsed Moon and the penumbra and umbra during the eclipse, they were able to cancel the solar spectral features (Fraunhofer lines) and the effects of the lunar albedo and also to minimise the effect of variations in the telluric spectrum caused by the path from the telescope to the Moon during the observations.

Within the umbra of the Earth's shadow, the residual illumination is produced by refracted and forward-scattered sunlight passing almost tangentially through all levels of the Earth's atmosphere. The integral of these paths is complex and depends on the distribution of clouds in the troposphere and above. The penumbra, as seen from the Moon, is analogous to sunset, with contributions both from direct sunlight and scattered skylight.

We have taken the visible and near-infrared eclipse spectrum from Pallé et al. and performed a fit to it using a model similar to the one we used for the sunset spectrum. We assume that, in the visible, the umbral spectrum does not contain a significant contribution from direct sunlight, so we have restricted our fitting to the use of multiple scattering paths from the sky. Figure 4 shows the result of this fitting, both with and without the contribution of ozone. The ability of the ozone model to match the small wiggles in the spectrum, especially around 500 nm, is to be noted.

A good physical insight into the formation of this spectrum is obtained by looking at examples of sunset and sunrise seen from Earth orbit. Astronauts on the International Space Station have obtained many such images and we have chosen one of them for Figure 5. This shows the illuminating source as it would appear at the boundary between the umbra and penumbra of an eclipse. There are several things to note in this image. At low altitudes there is strong but highly red-ened forward scattering. This produces the steeply rising spectrum longward of 600 nm. At high altitudes, there is a large solid angular contribution from optically thin Rayleigh scattering that is responsible

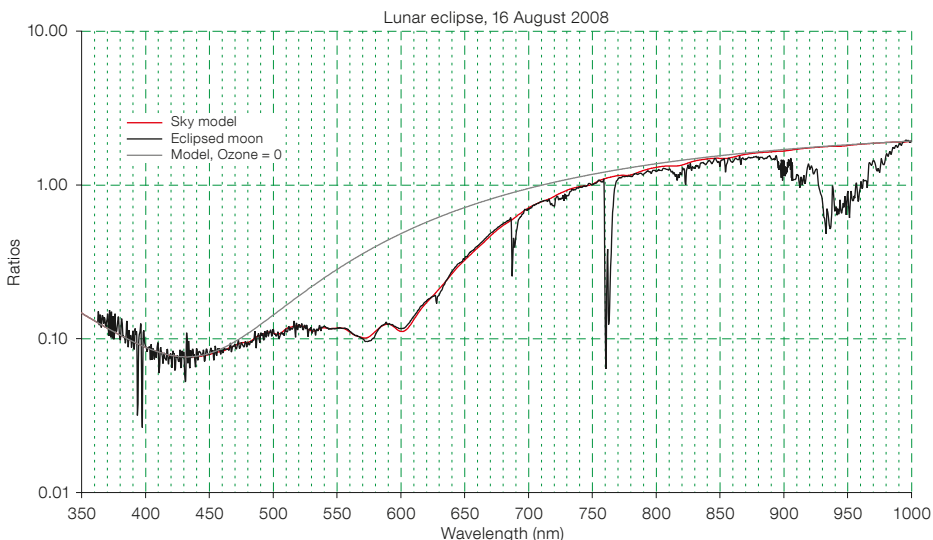


Figure 4. The visible and near-infrared part of the spectrum of the August 2008 lunar eclipse (black line) published by Pallé et al. (2009). This is the ratio of the umbral to the penumbral spectrum taken at the same average airmass, resulting in the removal of the solar and lunar spectral signatures as well as minimising the telluric features resulting from the

path between the telescope and the Moon. The red line shows our model fit to the data. The smooth grey line is the same model without ozone absorption. The sharp upturn in the blue is due to pure, unabsorbed Rayleigh scattering contributed by the very outer regions of the Earth's atmosphere illuminating the eclipsed Moon.



Figure 5. An image of a sliver of direct sunlight photographed from the International Space Station [ISS015-E-10471, 3 June 2007, courtesy of NASA]. This illustrates the colour of the light source that illuminates the eclipsed Moon at the boundary between the umbra and penumbra of the Earth's

shadow (see Figure 4). We note that the darker, dirty yellow band dividing the troposphere from the stratosphere corresponds to the region of maximum ozone absorption and so demonstrates that the Chappuis band is visible without the use of a spectrometer!

for the spectral rise shortward of 420 nm. We do not see this latter effect so strongly from the surface of the Earth at sunset because there is no path to the Sun with a length of less than an atmosphere (except at high altitude of course). Perhaps the most remarkable feature of the image, however, is the presence of the dark, dirty-yellow band just above the clouds at the troposphere/stratosphere boundary. We propose that this is the visible representation of the Chappuis ozone absorption at heights above 15 km. In other words, the vertical sequence of horizontal bands of colour in the image of sunset/rise map directly on to the eclipse spectrum.

Earth-like exoplanets

With current capabilities, notably the space-based transit monitors, the detection of Earth-like planets has become feasible. Characterising their atmospheres, however, requires new generations of telescopes and instruments (Perryman et al., 2005; Vázquez, Pallé & Montañés Rodríguez, 2010) and is extremely technically challenging. Also, as we know from studies of the evolutionary

history of the Earth's own atmosphere, the inference of the presence of life from the detection of individual molecular species is not without ambiguity. The efforts taking place now to assemble high quality observations of long-pathlength telluric spectra over a wide wavelength range will prove to be of great value in future experiment design. In the visible spectrum, it is fascinating to perceive the direct connection between the telluric spectra and some of the atmospheric phenomena we can see from the surface of our planet.

The colours of the sky are beautiful, rich and varied and the interplay between complex geometry and a small number of scattering and absorption processes can produce the great variety of effects. In addition to developing a close understanding of the formation of the colours we can see, certain geometries allow us to observe rather close analogues of what we might expect to see if we could catch a transiting exo-Earth with a sufficiently large telescope at some — hopefully not too distant — future time. In the visible spectrum, ozone is likely to be one of the most sought after indicators of the state of the atmosphere.

Acknowledgements

We thank Enric Pallé for providing the lunar eclipse digital data and Andreas Seifahrt for providing pointers to atmospheric data. Zolt Levay provided his beautiful photo-montage of the December 2010 lunar eclipse.

References

- Allen, C. W. 1973, *Astrophysical Quantities*, 3rd Edition, (London: Athlone Press)
 Hulbert, E. O. 1953, *JOSA*, 43, 113
 Pallé, E. et al. 2009, *Nature*, 459, 814
 Perryman, M. et al. 2005, *ESA-ESO Working Group Report No. 1, Extra-Solar Planets, Space-Telescope – European Coordinating Facility*
 Petic, P. 2005, *Sky in a Bottle*, (Cambridge, MA: The MIT Press)
 Vázquez, M., Pallé, E. & Montañés Rodríguez, P. 2010, *The Earth as a Distant Planet*, (New York: Springer)

Links

- ¹ Appleton Water Tower: http://bookings.landmark-trust.org.uk/BuildingDetails/Overview/129/Appleton_Water_Tower
² Spectroscopy & Molecular Properties of Ozone project: <http://smpp.iao.ru/1188x1216/en/home/>



ESO/José Francisco Salgado (josefrancisco.org)

Four antennas of the Atacama Large Millimeter/submillimeter Array (ALMA) on the Chajnantor plateau profiled against the night sky. The Moon illuminates the scene on the right, while the Plane of the Milky Way stretches across the upper left.

Planet-forming Regions at the Highest Spectral and Spatial Resolution with VLT–CRIRES

Klaus M. Pontoppidan¹
 Ewine van Dishoeck^{2,3}
 Geoffrey A. Blake⁴
 Rachel Smith⁵
 Joanna Brown^{6,3}
 Gregory J. Herczeg³
 Jeanette Bast²
 Avi Mandell⁷
 Alain Smette⁸
 Wing-Fai Thi^{9,10}
 Edward D. Young⁵
 Mark R. Morris⁵
 William Dent⁹
 Hans Ulrich Käufel⁸

- ¹ Space Telescope Science Institute, Baltimore, USA
² Leiden University, the Netherlands
³ Max Planck Institute for Extraterrestrial Physics, Garching, Germany
⁴ California Institute of Technology, Pasadena, USA
⁵ University of California at Los Angeles, USA
⁶ Harvard-Smithsonian Center for Astrophysics, Cambridge, USA
⁷ NASA Goddard Space Flight Center, Greenbelt, USA
⁸ ESO
⁹ University of Edinburgh, Scotland, United Kingdom
¹⁰ University of Grenoble, France

The inner regions (< 10 AU) of discs surrounding young pre-main sequence stars are thought to be places of active planet formation. The disc surfaces are traced by molecular emission lines in the infrared. We have carried out a spectroscopic 3–5 μm survey at the highest spectral resolution (as high as $R = 100\,000$) using CRIRES on the VLT, and have used the data to map the dynamics and chemistry of molecular gas, with the aims of constraining disc evolution and learning more about the process of planet formation. In this paper, we provide a brief overview of our CRIRES observing campaign and discuss the results obtained.

The era of exoplanetary science, starting with the first radial velocity detection of a planet orbiting a star other than our own Sun more than 15 years ago, is certain to be remembered as a truly remarkable

time in the history of astronomy. We now know that planetary systems are common in our Galactic neighbourhood, and that many of them are very different indeed from the Solar System: some giant planets orbit very close to their parent stars — the so-called hot Jupiters, while others orbit at larger distances from their parent stars. As planet detection methods become increasingly refined, the hunt for true Earth analogues is in full swing, and few doubt that it is only a matter of time before we discover the first terrestrial (rocky) planets orbiting their stars at distances suitable for life as we know it.

Yet, we are far from having a comprehensive understanding of the formation of planets and planetary systems. In parallel with the emergence of exoplanetary science, the field of circumstellar discs around young stars has come into full swing. While discs have long been predicted to be the inevitable outcome of the collapse of a rotating cloud, firm proof of their existence came only in the mid-1990s with the Hubble Space Telescope optical images of proplyds in Orion and the detection of gas in Keplerian rotation at millimetre wavelengths. Surveys have shown that many young stars retain gas-rich circumstellar discs with enough material to form a planetary system for a few million years after the formation of the star.

However, the connection between discs, exoplanetary systems and the formation of planets is not at all understood yet. Much of the observed structure of exoplanetary systems is thought to be the result of the protoplanets interacting with their parent disc. This is particularly true for the hot Jupiters, which are thought to migrate from a birthplace at disc radii of several astronomical units (AU) to a fraction of an AU, by way of angular momentum exchange with a gas-rich disc. The idea that circumstellar discs are actively forming planetary systems, at least up to the point of making gas giants, is so strong that these discs are often labelled as being protoplanetary, in spite of the fact that, as of now, no unambiguous protoplanet within a circumstellar disc has ever been seen.

It can be argued that the lack of understanding of planet formation and the paucity of detected protoplanets relative to mature planetary systems primarily results from a deficiency in observational capabilities, rather than insufficient theoretical tools or ideas, which currently are quite advanced and in dire need of constraints. It is clear that planets do form, protoplanetary discs must contain planetesimals and planetary embryos, and gas giants must accrete most of their mass during the gas-rich phase of the disc. In a nutshell, the problem is one of spatial resolution. The nearest protoplanetary discs are located at distances in excess of 100 pc, with a few exceptions, meaning that protoplanets are expected to exist on angular scales of 10–100 milliarcseconds — or less. The aim of our ESO large programme was to characterise the physical and chemical conditions as well as the kinematics of these planet-forming zones of discs.

Probing gas in the inner disc

Gas-rich discs are not flat, but flare in such a way that the disc surface is exposed to direct energetic stellar radiation. This gives rise to a warm layer of gas, extending from the inner edge of the disc out to at least tens of AU. Lines tracing the temperatures and densities prevalent within 10 AU are therefore found at infrared (IR) wavelengths (3–40 μm). The topmost layer is atomic, as harsh ultraviolet radiation dissociates molecules faster than they can form. Deeper in the disc, as densities rise and as the gas becomes shielded from the stellar radiation, molecules begin to dominate the gas. Even deeper, temperatures drop rapidly, and many molecular species freeze out, thus becoming invisible at IR wavelengths, due to a combination of high opacities and low excitation conditions. The intermediate, so-called warm molecular layer, on the other hand, gives rise to a veritable forest of molecular emission lines. The most prevalent species is CO, but other carbon-bearing molecules such as CO₂, C₂H₂ and HCN, and oxygen-dominated molecules, H₂O and OH, can be detected as well.

The fundamental rovibrational band of CO centred in the atmospheric *M*-band

window at 4.5–5.2 μm turns out to be the best spatio-kinematic tracer available to the high spatial and spectral resolution of large aperture ground-based telescopes. CO has the highest feature-to-continuum ratio of all species observed and produces a simple spectrum with a regular series of lines originating from levels with a wide range of energies, up to several thousand Kelvin. Moreover, lines of CO isotopologues lie in the same wavelength range, so that both temperature and optical depth can be determined. All of these lines (typically a few dozen) can be observed simultaneously in just a few spectral settings, allowing accurate relative calibration. This ease of observing is in contrast with millimetre lines of CO and its isotopologues, which often require different receivers (and even different telescopes) to observe a wide range of excitation conditions. Figure 1 shows an example of different types of CO, H₂O and OH IR emission from T Tauri stars. Warm gas (typically > 400 K) is seen in emission, whereas colder gas is detected in absorption against the continuum or line emission.

A CRIRES large programme

The CO rovibrational band was the main target of an ESO large programme (179.C-0151) carried out with the Very Large Telescope CRYogenic high-resolution InfraRed Echelle Spectrograph (CRIRES) over the course of about 30 nights during the period 2007–2009. Significant additional time was allocated to survey water and OH lines at around 3 μm , as well as exploratory forays to search for H₃⁺, HCN, CH₄ and NH₃.

The final dataset¹ includes high quality spectra of about 100 young, mostly low-mass, stars, spanning a range of evolutionary stages, from sources still surrounded by a natal envelope, to discs in the process of clearing out their inner regions, the final stage at which inner disc molecular gas can be observed. In total, nearly 600 individual spectral settings were observed. The targets were selected from nearby star-forming clouds, including Ophiuchus, Lupus, Chamaeleon, Corona Australis, Taurus, Serpens and Orion. The main selection criterion was the IR brightness of the sources, typically

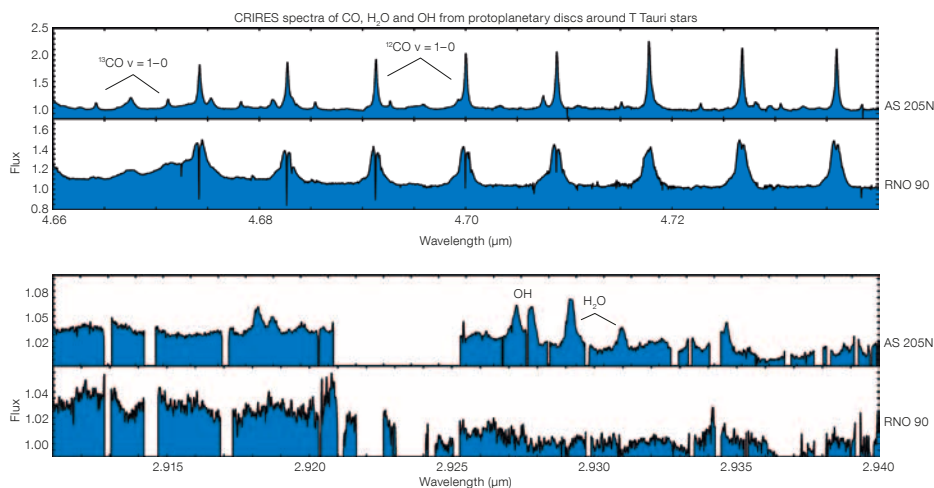


Figure 1. Examples of two types of molecular spectra seen in classical T Tauri stars. The highly accreting star AS 205N (K7) shows single-peaked CO line profiles indicative of a disc wind, along with strong rovibrational water and OH lines at shorter wavelengths tracing hot gas (Bast et al., 2011; Pontoppidan et al., 2011). RNO 90 (G5) shows clas-

sical double-peaked emission line profiles from a disc in Keplerian rotation, and much weaker or absent line emission from hot water and OH. Note that numerous patches of the water spectra around 3 μm are missing due to strong absorption from telluric water vapour.

$F_{4.7\mu\text{m}} > 0.5$ Jy to generate a relatively uniform sample of spectra with high signal-to-noise ratios.

Until the completion of the European Extremely Large Telescope (E-ELT), CRIRES offers, to our knowledge, the highest combined spatial and spectral resolution available for molecular line imaging. The typical adaptive optics (AO)-assisted imaging resolution at 3–5 μm is 0.1–0.2 arcseconds and the resolving power is of order $R = 95\,000$. The aim of the large CRIRES programme was to fully exploit these unique capabilities to explore the dynamics and chemistry of warm molecular gas as an ingredient for planet formation. Central questions identified at the beginning of the programme included: What is the timescale for the dissipation of (molecular) gas in protoplanetary discs? What is the distribution of the molecular gas, as compared to the dust, in the terrestrial planet-forming zones of discs? Are radial motions present in discs and, if so, what drives them? Are inner discs turbulent, and can this turbulence be measured and quantified? Is there a relation between embedded discs and those surrounding T Tauri stars? What is the temperature structure of inner envelopes and discs? What is the extent of hot chemistry producing water

and organic molecules of astrobiological interest?

Pushing beyond the diffraction limit

Since 0.1 arcseconds still corresponds to at least ~ 10 AU at the distance of our sources, a significant fraction of the survey was dedicated to the development of a spectro-astrometric mode for CRIRES that can provide even higher spatial resolution (Pontoppidan et al., 2008; 2011). Infrared spectro-astrometry is a pioneering capability of CRIRES that exploits the combination of AO-assisted imaging, stable optics and high spectral resolution to image lines at sub-milliarcsecond resolution, several orders of magnitude below the formal diffraction limit. Spectro-astrometry works by measuring the centroid offset of a spectrum as a function of wavelength (or line velocity), essentially generating position-velocity diagrams. There is no fundamental limit to how accurately astrometric offsets can be measured, but in practice the accuracy achieved with CRIRES is 0.1–0.5 milliarcseconds (a fraction of an AU!) for the 4.7 μm CO band for typical protoplanetary discs around solar-mass stars, essentially limited by photon statistics. We developed, in collaboration

with ESO staff, an observing template that ensures optimal stability of the instrument. This accuracy resolves the molecular line emission in nearly all nearby protoplanetary discs. This spectro-astrometry template has been available for use by the general ESO community since Period 81.

To summarise the results of the spectro-astrometric campaign; some discs are, as expected, dominated by emission from gas in Keplerian motions around the central star, having line profiles and astrometric position-velocity spectra that can be modelled simultaneously by simple Keplerian models. Moreover, the basic geometries (size, position angle and inclination) of the discs can be determined with much less ambiguity than is possible from pure continuum imaging and interferometry. We found that CO emission from Keplerian discs obeys a size-luminosity relation, such that more luminous stars have larger line-emitting regions: the size of the CO emitting region is found to be proportional to the square root of the stellar luminosity (see Figure 2). This result is similar to that found for the near-IR continuum (Monnier et al., 2005), except that CO is found to emit at larger radii corresponding to theoretical equilibrium dust temperatures of about 350 K (the gas excitation temperature is actually significantly higher, 1000 K, demonstrating that it is not in thermal equilibrium).

A particularly exciting result generated by the spectro-astrometry is that many transitional discs, in which the small grains have been cleared out to several tens of AU, still harbour significant amounts of warm molecular gas inside these gaps or holes. This is a strong indication that, if the clearing is due to dynamical interaction with a companion, this object is less massive than a few Jupiters. Alternatively, the dust may not have been cleared and lost, but rather has grown to form an inner swarm of unseen planetesimals. Either way, the observation of warm molecular gas very close to the protostar seems to be directly related to the process of planet formation. Furthermore, the survival of CO in the absence of small dust grains may indicate that molecular self-shielding is operating to ensure the survival of the observed CO molecules

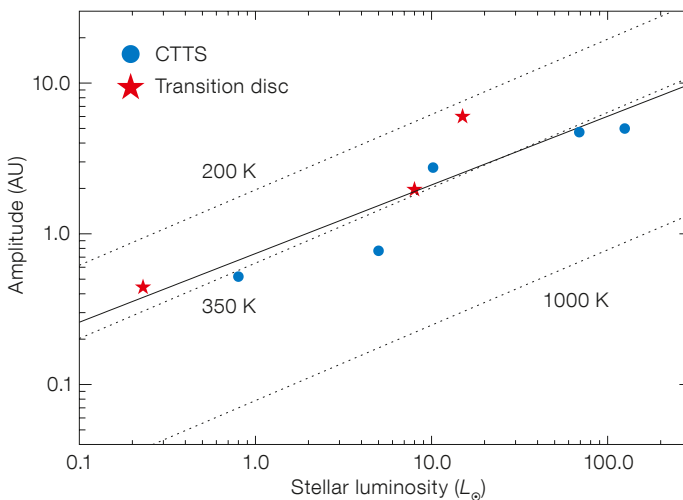
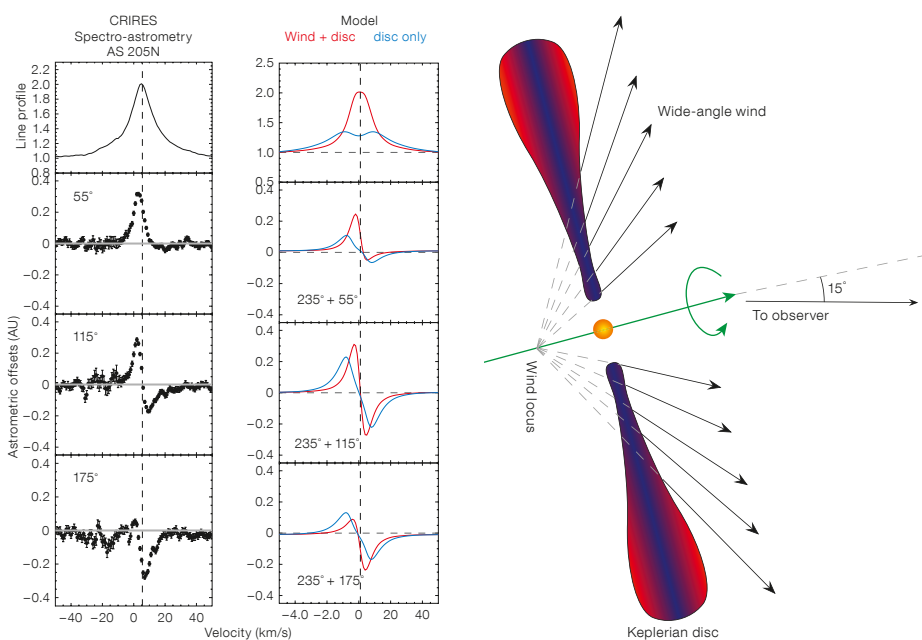


Figure 2. The size-luminosity relation, as measured with CRIRES spectro-astrometry, for discs showing CO emission from gas in Keplerian motion. Adapted from Pontoppidan et al. (2011).



against the ultraviolet radiation field from the central star.

Molecular disc winds

While some discs follow convention and display clear signatures of Keplerian motions, most of our observed sample does not match a simple Keplerian velocity field. In fact, one of the surprises of our survey is the large diversity in observed line profiles (Brown et al., 2011). One class of sources — the so-called single-peaked sources — shows indications of radial motions of the gas (Bast et al., 2011). Specifically, they show low

Figure 3. Example of the spectro-astrometry for a wind-dominated disc. The left panels show CRIRES data of the classical T Tauri star AS 205N with the regular line flux spectrum at the top and spectro-astrometry at three different slit position angles. The middle panels show radiative transfer models with (red curves) and without (blue curves) a wind component. The illustration to the right sketches the wind geometry that is consistent with the data. Adapted from Pontoppidan et al. (2011).

velocity gas (< 3 km/s offset from the stellar velocity) at less than a few AU from the central star, as measured directly with spectro-astrometry (see Figure 3 and Pontoppidan et al., 2011). This signature can be modelled as outflowing gas with an azimuthal velocity vector (rotation) that

is slowed significantly relative to Keplerian rotation due to conservation of angular momentum.

Thus a key finding of the spectro-astrometric survey is that slow molecular disc winds are prevalent in the inner few AU of classical T Tauri stars. Because the winds are so slow, it is not certain that the gas is able to escape the disc, and may even fall back onto the disc at larger radii; if so, these winds may serve as efficient redistributors of disc material. The implied mass flow rates of the winds are of order 10^{-8} – $10^{-9} M_{\odot}/\text{yr}$, corresponding to the entire inner disc being cycled through the wind over the disc lifetime (Pontoppidan et al., 2011). It is tempting to speculate that if the wind is able to carry dust grains with it, it may be able to contribute to the annealed (crystalline) dust found in the outer disc and in comets, the origin of which is a longstanding, and much debated, problem. Similar ideas were discussed in the 1990s in the context of fast magnetic winds (Shu et al., 1994). However, this type of wind appears to be very different than that observed by CRILES.

Exo-cosmochemistry

The absorption components seen in many CO spectra, both toward embedded protostars as well as some T Tauri stars, allow an investigation of isotope ratios with unprecedented precision. A central objective of this subprogramme was to search for rare isotopologues of CO, in particular C^{17}O and C^{18}O , and obtain accurate measurements of their relative ratios. Why is this particularly interesting? The field of cosmochemistry deals, in part, with high precision measurements of the composition of early Solar System material, specifically primitive meteorites, to infer conditions of the Solar Nebula at the time of planet formation. Ratios of elemental isotopes provide important clues not only to the timing of formation of the meteorites, but also of the chemical and radiative environment of the material. For instance, the oxygen in meteorites is found to be heavy (^{18}O - and ^{17}O -rich with respect to ^{16}O) with a re-relative, mass-independent ratio that indicates the action of a photon-induced process rather than thermal chemistry. A leading hypothesis to explain this non-

terrestrial oxygen isotopic relationship is CO self-shielding, i.e. that the Solar System oxygen was once part of gas that was exposed to strong ultraviolet radiation, likely generated by either the central protostar or hot stars in the vicinity of the Solar Nebula (e.g., Clayton, 2002). The effect arises because the light isotopologue C^{16}O is much more abundant than the heavier isotopologues C^{17}O and C^{18}O and therefore self-shields against photo-dissociation at much lower column densities.

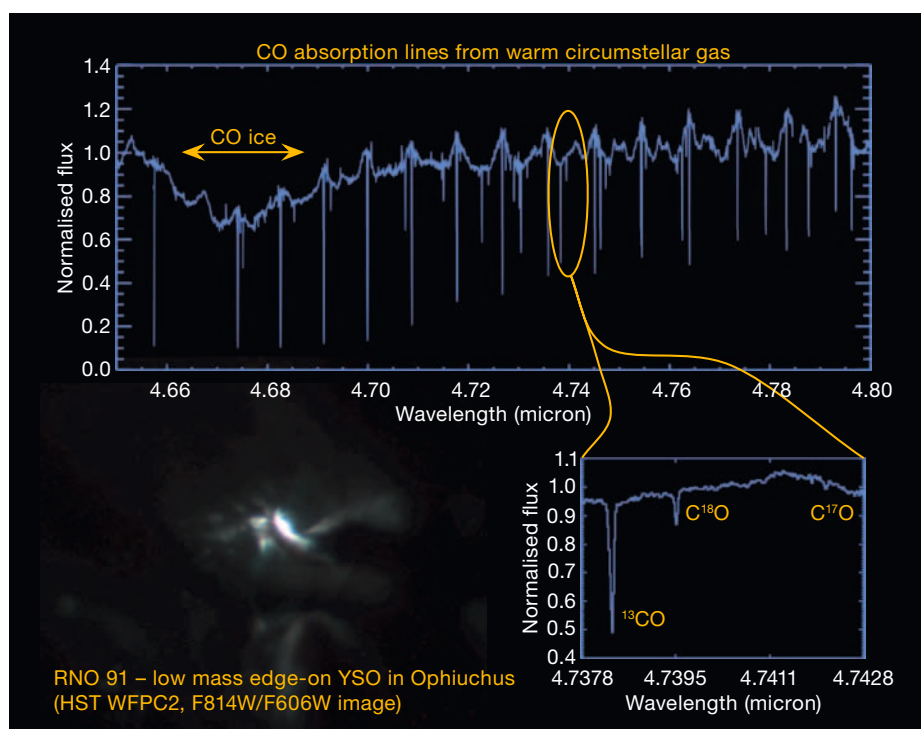
Due to its high spectral resolving power, CRILES is, in principle, capable of measuring column densities of the four main CO isotopologues ($^{12}\text{C}^{16}\text{O}$, $^{13}\text{C}^{16}\text{O}$, $^{12}\text{C}^{18}\text{O}$ and $^{12}\text{C}^{17}\text{O}$) to high precision in discs, given a favourable geometry in which the gas is seen in absorption. This opens up the exciting possibility for directly comparing protoplanetary disc chemistry, as it is unfolding, with that inferred from 4.6 billion year old rocks from the ancient Solar System. As part of our CRILES large programme, we have carried out a mini-survey of discs and protostars with CO absorption lines deep enough to allow an accurate measure of isotopologue ratios to a relative precision as high as 5 % (Smith et al., 2009).

The analysis is aided by *K*-band absorption spectra of the ^{12}CO $v = 2-0$ overtone band at 2.3 μm , which has much smaller oscillator strengths and thus low optical depth. The first results are indeed consistent with isotope selective photo-dissociation in other planetary systems, in support of the model for Solar System oxygen fractionation. Remarkably, the oxygen isotopic data have also been used as evidence for supernova enrichment of the Solar Nebula (Young et al., 2011). Finally, our survey has uncovered anomalously high $^{12}\text{CO}/^{13}\text{CO}$ ratios in many absorption components in the protostellar sample, the origin of which is still undetermined (Smith et al., 2011; see Figure 4).

Embedded discs

While our understanding of fully formed protoplanetary discs is rapidly improving, in part due to fundamental improvements in the spatial resolution of continuum and line imaging data across the wavelength

Figure 4. CRILES spectrum of CO absorption lines from the young low-mass star RNO 91. The insert shows detected lines from ^{13}CO , C^{18}O and C^{17}O (adapted from Smith et al., 2011).



range, the formation of the discs during the embedded phase of star formation is still very poorly understood. Because the mid-IR molecular forest may provide a unique tracer of such young discs at scales of a few AU, an important part of our CRIRES programme was to investigate whether molecular emission from embedded discs shares the properties of the emission from T Tauri discs. Even though AO was not possible on these optically weak sources, we were fortunate to have several nights of exceptional natural seeing (down to 0.3 arcseconds at visible wavelengths) which we used to observe these sources. Our results showed that, while complexities such as absorption from cloud material and (episodic) outflowing gas (Thi et al., 2010) interfere with the emission components, embedded discs appear similar to the inner regions of highly accreting T Tauri stars (Herczeg et al., 2011).

In some cases, embedded protostars also show highly extended CO emission, an example of which is shown in Figure 5, where a continuum-subtracted two-dimensional spectrum of rovibrational ^{12}CO is compared to a NACO K -band image of the source. The high resolution of CRIRES reveals narrow (~ 3 km/s full width half maximum [FWHM]) line emission extending to more than 2 arcseconds from the source along both outflow cavities. The mechanism forming the extended narrow emission is unclear, but it may be related to combined UV heating and shock interaction between a wind and the outflow cavity surrounding the young star (see Herczeg et al. [2011] for a discussion). The detail seen along a single slit alludes to the potential for line imaging with an integral field unit operating at high spectral resolution in the M -band.

Outlook

The fundamental outcome of our large programme is a database of high precision $R \sim 95\,000$ spectra of molecular gas from many, and perhaps more than half, of the bright protoplanetary discs around T Tauri stars in the southern hemisphere, as well as a significant sample of low-mass protostars. The high quality of the data and the richness of the spectra

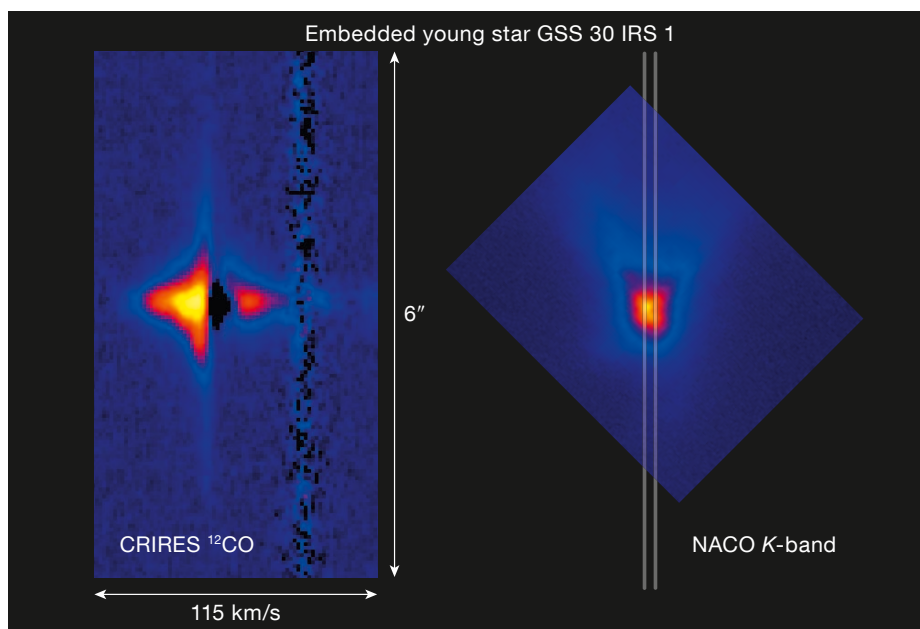


Figure 5. Long-slit spectrum of the ^{12}CO $v = 1-0$ lines of the embedded young star GSS 30 IRS 1, showing highly extended line emission (from Herczeg et al., 2011). The slit is oriented along the outflow cavity axis, as seen in an archival K -band image obtained by NACO (right). The K -band image is scaled to correspond to the spatial axis of the CRIRES two-dimensional spectrum.

demonstrate the potential of sub-arcsecond resolution imaging spectroscopy in the mid-IR, in particular for tracing warm molecular gas in circumstellar environments.

The potential of CRIRES is by no means exhausted. The spectro-astrometric mode is a very powerful capability that still has great potential for discovery. For instance, imaging sub-milliarcsecond structure goes beyond protoplanetary discs, and may be applied to other circumstellar (or even stellar) structures and active galactic nuclei. We also foresee significant synergies with the VLTI, as well as potential time-domain investigations. The detail observed even along a single slit (Figures 2 and 3) suggests a high potential for line imaging with an integral field unit operating at high spectral resolution in the M -band, such as the E-ELT instrument concept METIS (Brandl et al., 2010). Finally, both CRIRES and METIS will be highly complementary to ALMA, which can observe the dust distribution down to ~ 1 AU but is limited in its imaging of the gas to radii larger than a few AU.

Acknowledgements

We wish to thank ESO for producing CRIRES, a truly magnificent instrument, as well as for their generous support of our science programme. Support for Klaus Pontoppidan was provided by NASA through Hubble Fellowship grant #01201.01 awarded by the Space Telescope Science Institute, which is operated by the Association of Universities for Research in Astronomy, Inc., for NASA, under contract NAS 5-26555. Some data shown were based on observations made with the NASA/ESA Hubble Space Telescope, obtained from the data archive at the Space Telescope Science Institute.

References

- Bast, J. et al. 2011, *A&A*, in press
- Brandl, B. et al. 2010, *The Messenger*, 140, 30
- Brown, J. M. et al. 2011, *ApJ*, in preparation
- Herczeg, G. et al. 2011, *A&A*, submitted
- Clayton, R. 2002, *Nature*, 415, 860
- Mandell, A. et al. 2011, *ApJ*, in preparation
- Monnier, J. et al. 2005, *ApJ*, 624, 832
- Pontoppidan, K. M. et al. 2008, *ApJ*, 684, 1323; ESO Press Release 0827, *Mind the Gap*
- Pontoppidan, K. M. et al. 2010, *ApJ*, 720, 887
- Pontoppidan, K. M. et al. 2011, *ApJ*, submitted
- Shu, F. et al. 1994, *ApJ*, 429, 781
- Smith, R. L. et al. 2009, *ApJ*, 701, 163
- Smith, R. L. et al. 2011, in preparation
- Thi, W.-F. et al. 2010, *MNRAS*, 406, 1409
- Young, E. D. et al. 2011, *ApJ*, in press

Links

- ¹ Reduced spectra are made available for download at: <http://www.stsci.edu/~pontoppi/>

The SINFONI Integral Field Spectroscopy Survey for Galaxy Counterparts to Damped Lyman- α Systems

Céline Péroux¹
 Nicolas Bouché^{2,3}
 Varsha Kulkarni⁴
 Donald York⁵
 Giovanni Vladilo⁶

¹ Laboratoire d'Astrophysique de Marseille, OAMP, Université Aix-Marseille & CNRS, France

² Department of Physics, University of California, Santa Barbara, USA

³ Laboratoire d'Astrophysique de Toulouse-Tarbes, CNRS, Observatoire Midi-Pyrénées, France

⁴ Department of Physics and Astronomy, University of South Carolina, Columbia, USA

⁵ Department of Astronomy and Astrophysics and The Enrico Fermi Institute, University of Chicago, USA

⁶ INAF-Osservatorio Astronomico di Trieste, Italy

A complete picture of galaxy formation can only be obtained by detailed study of the processes by which galaxies convert their gas into stars. One approach is to relate the H I gas and the stars in galaxies. Damped and sub-damped Lyman- α systems (DLAs), which are galaxies probed by the absorption they produce in the spectra of background quasars, are purely selected on H I gas, but identifying the galaxy responsible for the absorber with more traditional methods remains challenging. Integral field spectroscopy provides an efficient way of detecting faint galaxies near bright quasars, further providing immediate redshift confirmation. Here, we report on the detection of DLA and sub-DLA systems identified in H α emission with VLT/SINFONI at near-infrared wavelengths.

Tremendous progress has been made over the last decade in establishing a broad cosmological framework in which galaxies and large-scale structure develop hierarchically over time, as a result of gravitational instabilities in the density field. The next challenge is to understand the physical processes of the formation of galaxies and structures and their interactions with the surrounding

medium. Of particular importance are the processes through which these galaxies accrete gas and subsequently form stars. The accretion of baryonic gas is complex. Recently, several teams have realised that, in halos with mass $< 10^{11.5-12} M_{\odot}$ baryonic accretion may not involve the traditional shock heating process. But the observational evidence for accretion is scarce. A related signature is that the total amount of neutral gas in the Universe, H I, is almost constant over most of the cosmic time (Péroux et al., 2005; Noterdaeme et al., 2009), unlike the history of the star formation rate, which peaks around $z = 1$. This shows the importance of ongoing global gas accretion and the conversion of atomic gas to molecular gas in the star formation process.

One way to tackle these problems is to relate the H I gas and the stars in galaxies. While radio observations now provide detailed constraints on the H I content of large samples of galaxies, they are still limited to redshift $z \sim 0$. Conversely, the study of quasar absorbers, the galaxies probed by the absorption they produce in a background quasar spectrum, is insensitive to the redshift of the object. Indeed, the H I content of the strongest of these quasar absorbers, the so-called damped Lyman- α systems, have been measured in samples of several hundreds of objects from the Sloan Digital Sky Survey (SDSS).

A new observational technique

Nevertheless, studying the stellar content of all these systems turns out to be rather challenging: the galaxies that produce such DLA absorption may be faint, thus requiring deep observations to detect their stellar/interstellar emission; in addition, they have small angular separations from the bright background quasars, which makes it difficult to disentangle the light of the galaxy from that of the quasar. Any broadband identification of a candidate absorber galaxy requires follow-up spectroscopy to confirm that the emission redshift of the object corresponds to the absorption redshift measured in the quasar spectrum. This time-consuming step is sometimes missing, thus complicating the interpretation of the

observations made so far. As a result of these issues, only 15 spectroscopically confirmed identifications of DLA/sub-DLA galaxies with measured $N_{H I}$ are known at cosmological redshift $z < 1$ and five at $z > 1$.

Imaging spectroscopy at near-infrared (NIR) wavelengths with adaptive optics can be used to solve the above-mentioned problems efficiently. The advantages afforded by this technique are manifold:

- 1) The contribution from the quasar is deconvolved from the absorber in the spectral dimension, thus allowing virtually zero impact parameters to be reached if the flux of the galaxy is greater than the quasar continuum flux.
- 2) The data provide a spectrum of the absorbing galaxy for immediate redshift confirmation.
- 3) The detection of nebular emission lines such as H α , a robust estimator of star formation rate, redshifted to the NIR at $z > 0.6$, can give clues to the stellar content of the galaxy and metallicity of the warm gas producing the nebular lines.
- 4) The spatially resolved kinematic data provide information on the dynamical state of the system.

The powerful combination of an 8-metre class Very Large Telescope (VLT) and the SINFONI instrument has been successfully pioneered by Bouché et al. (2007). These authors have detected 67% (14 out of 21) of the systems in a sample of Mg II absorbers at $z \sim 1$. The H α detections are used to derive star formation rates of the order 1–20 M_{\odot}/yr . Their observations are sensitive to fluxes $F(\text{H}\alpha) > 1.2 \times 10^{17} \text{ erg s}^{-1} \text{ cm}^{-2}$, corresponding to star formation rates of $\sim 0.5 M_{\odot}/\text{yr}$. Interestingly, lower detection rates are found at higher redshifts around $z \sim 2$ (Bouché et al., 2011). Here, we report the first results of our H I-selected survey aimed at detecting the host galaxies via their H α signature. In the present work, we report the detections of two DLA/sub-DLAs at $z \sim 1$ for which $N_{H I}$, and hence absorption metallicities, are known from high resolution spectroscopy out of five quasar fields with intervening absorbers (one with two sub-DLAs) searched.

New detections

The observations presented here were carried out with the NIR integral field spectrometer SINFONI on Unit Telescope 4 of the VLT during three separate observing runs (ESO 79.A-0673, 80.A-0330 and 80.A-0742). In Péroux et al. (2011a), we have reported detections of a DLA with $\log N_{\text{H I}} = 20.36 \pm 0.11$ at $z_{\text{abs}} = 1.009$ towards Q0302-223 (see Figure 1) and a sub-DLA with $\log N_{\text{H I}} = 19.48 \pm 0.05 - 0.06$ at $z_{\text{abs}} = 0.887$ towards Q1009-0026 (see Figure 2). We detect galaxies associated with the quasar absorbers at impact parameters of 25 and 39 kpc away from the quasar sight-lines, respectively.

For the field of Q0302-223 where the quasar is bright enough, we have used the quasar itself as a natural guide star for adaptive optics in order to improve the spatial resolution. Using the $\text{H}\alpha$ luminosity we derived the star formation rate assuming the Kennicutt (1998) flux conversion, corrected to a Chabrier (2003) initial mass function. These findings are summarised in Table 1. We find low star formation rates; these values of star formation rates are among the lowest that have ever been possible to detect in quasar absorber searches with ground-based observations at $z \sim 1$.

Comparison with other detected absorbers

We have made a careful reappraisal of published reports of detections of galaxies responsible for DLA and sub-DLAs. Figure 3 shows the relation between several of the properties. The triangles represent limits and the measurements reported in the present article are circled in red. From this figure, it appears that the detected objects in the sample are mostly low luminosity and low star formation rate galaxies, yet the galaxies have a wide range of luminosities. We also note

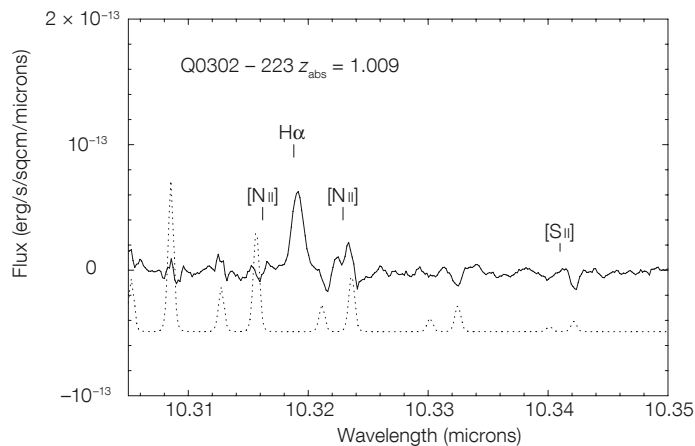


Figure 1. The integrated spectrum of the corresponding DLA galaxy with the expected $\text{H}\alpha$, $[\text{N II}]\lambda 6585$ and $[\text{S II}]\lambda 6718$ doublet positions indicated at $z_{\text{em}} = 1.00946$. The dotted spectrum at the bottom of the panel is the sky spectrum indicating the position of the OH sky lines. In this case, $[\text{S II}]$ is not detected and an upper limit is derived due to contamination by an OH sky line.

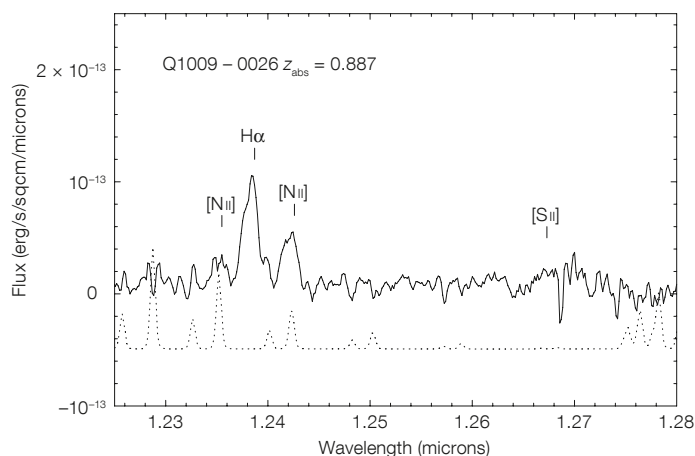


Figure 2. The integrated spectrum of the galaxy with the expected $\text{H}\alpha$, $[\text{N II}]$ and $[\text{S II}]$ line positions indicated at $z_{\text{em}} = 0.88637$. $[\text{N II}]\lambda 6585$ is affected by an OH sky line but this is much narrower than the line we detect and $[\text{S II}]$ is not detected.

that small impact parameters ($b < 30$ kpc) dominate and that very few galaxies are identified beyond 40 kpc, which matches the search radius in our SINFONI study well. Removing the outlier with $\log N_{\text{H I}} = 21.71$ and $b = 44$ kpc, we find a weak negative correlation, where higher $N_{\text{H I}}$ absorbers have smaller impact parameters. Also it is interesting to note that the highest $N_{\text{H I}}$ column density seems to have higher L/L_* ratio. The Spearman rank correlation coefficient indicates that the two are weakly correlated. Although the scatter is large, the reported absorption metallicities do not vary much

with impact parameter. It is also clear that abundances reported in absorption are not well-correlated with emission abundances.

Metallicity

Unlike most of the objects in Figure 3, and other objects reported at these redshifts, the galaxies that we have detected in this study have well-known absorption metallicities from high resolution UV spectroscopy. Using the N_2 parameter (Pettini & Pagel, 2004) based

Table 1. Summary of the properties of two Ly α absorber galaxies detected with SINFONI.

Quasar	z_{abs}	$\log N(\text{H I})$ (atoms/cm ²)	$[\text{Zn}/\text{H}]$	Impact parameter (kpc)	$F(\text{H}\alpha)$ (erg/s/cm ²)	Lum($\text{H}\alpha$) (erg/s)	SFR M_{\odot}/yr
Q0302-223	1.009	$20.36^{+0.11}_{-0.11}$	-0.51 ± 0.12	25	$7.7 \pm 2.7 \times 10^{-17}$	$4.1 \pm 1.4 \times 10^{41}$	1.8 ± 0.6
Q1009-0026	0.887	$19.48^{+0.05}_{-0.06}$	-0.25 ± 0.06	39	$17.1 \pm 6.0 \times 10^{-17}$	$6.6 \pm 2.3 \times 10^{41}$	2.9 ± 1.0

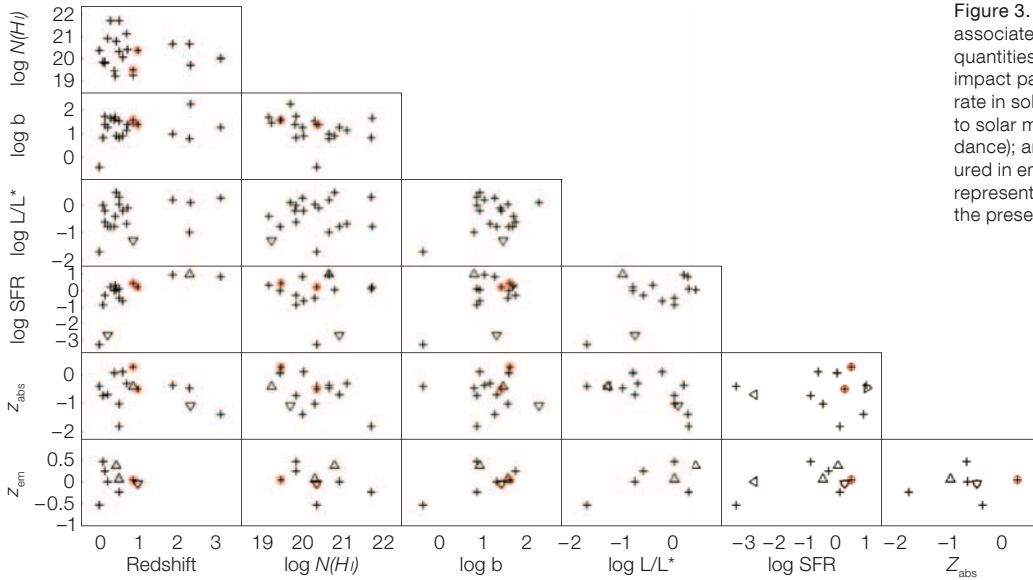
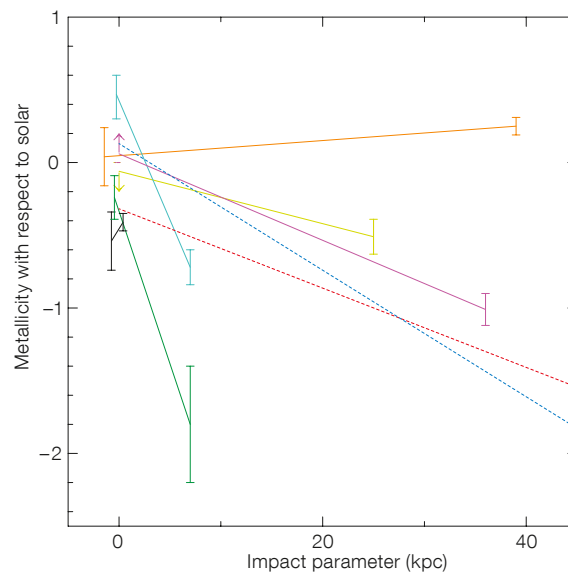


Figure 3. Correlation plots for the detected galaxies associated with DLAs and sub-DLAs. The following quantities are plotted: redshift; $N_{\text{H I}}$ column density; impact parameter in kpc; luminosity; star formation rate in solar masses per year; metallicity with respect to solar measured in absorption, Z_{abs} (H I abundance); and metallicity with respect to solar measured in emission, Z_{em} (H II abundance). The triangles represent limits and the measurements reported in the present article are circled in red.

Figure 4. Metallicity with respect to solar measured in emission at impact parameter $b = 0$ and in absorption at given impact parameters in kpc. The two metallicities arising from the same galaxy are linked by coloured lines. The arrows indicate upper and lower limits on the measure of the emission metallicities. The errors on the emission metallicities are artificially offset from $b = 0$ for clarity. The two dotted lines are the H II region oxygen abundance gradients measured in M101 (slope = -0.043 dex/kpc, in blue) and M33 (slope = -0.027 dex/kpc, in red) for comparison.



on $[\text{N II}]\lambda 6585/\text{H}\alpha$ ratio, we can derive an estimate of the emission metallicity. For the DLA towards Q0302-223, we find about solar abundance, compared to the one-third solar metallicity reported in absorption ($[\text{Zn}/\text{H}] = -0.51 \pm 0.12$). For the sub-DLA towards Q1009-0026, we find slightly above solar metallicity, compared with a super-solar absorption metallicity ($[\text{Zn}/\text{H}] = +0.25 \pm 0.06$).

In order to investigate the role that gradients might play in the difference between the emission and absorption

abundances, we have plotted the metallicity with respect to solar as a function of the impact parameter in Figure 4.

Clearly, in most of the six cases plotted here, the metallicity measured at a larger radius is lower than the one measured in the centre, sometimes with a slope steeper than that observed in local galaxies. In the case of Q1009-0026, however, the metallicity at the centre of the galaxy (seen in emission) is lower than the metallicity at 39 kpc radius (seen in absorption). This surprising result might just be the result of an uncertain

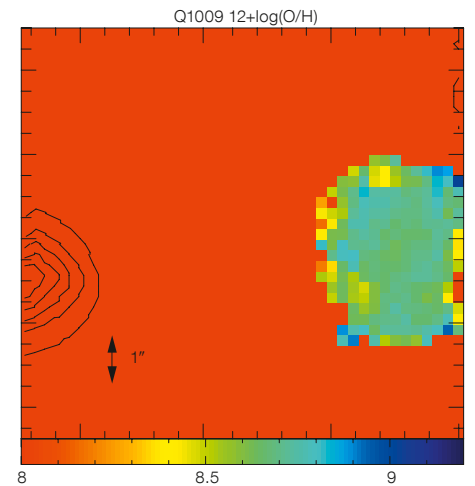


Figure 5. This figure presents the metallicity in units of $12+\log(\text{O}/\text{H})$ derived from the N_2 parameter, i.e. the ratio of $[\text{N II}]\lambda 6585/\text{H}\alpha$, in Q1009-0026. The metallicity appears to be rather uniform on this scale, as expected from the magnitude of the gradients observed in such objects (see Figure 4).

measurement as reflected by the large error bar (see Figure 4). It might also be partly explained by the use of the metallicity indicator. Indeed, Pettini & Pagel (2004) have demonstrated that the N_2 -parameter/metallicity relation has a rather large scatter at high metallicities, where these data lie. In addition, it should be emphasised that these measurements are not tracing the same gas phase (neutral versus ionised gas). However, it is interesting to note that at $z \sim 3$,

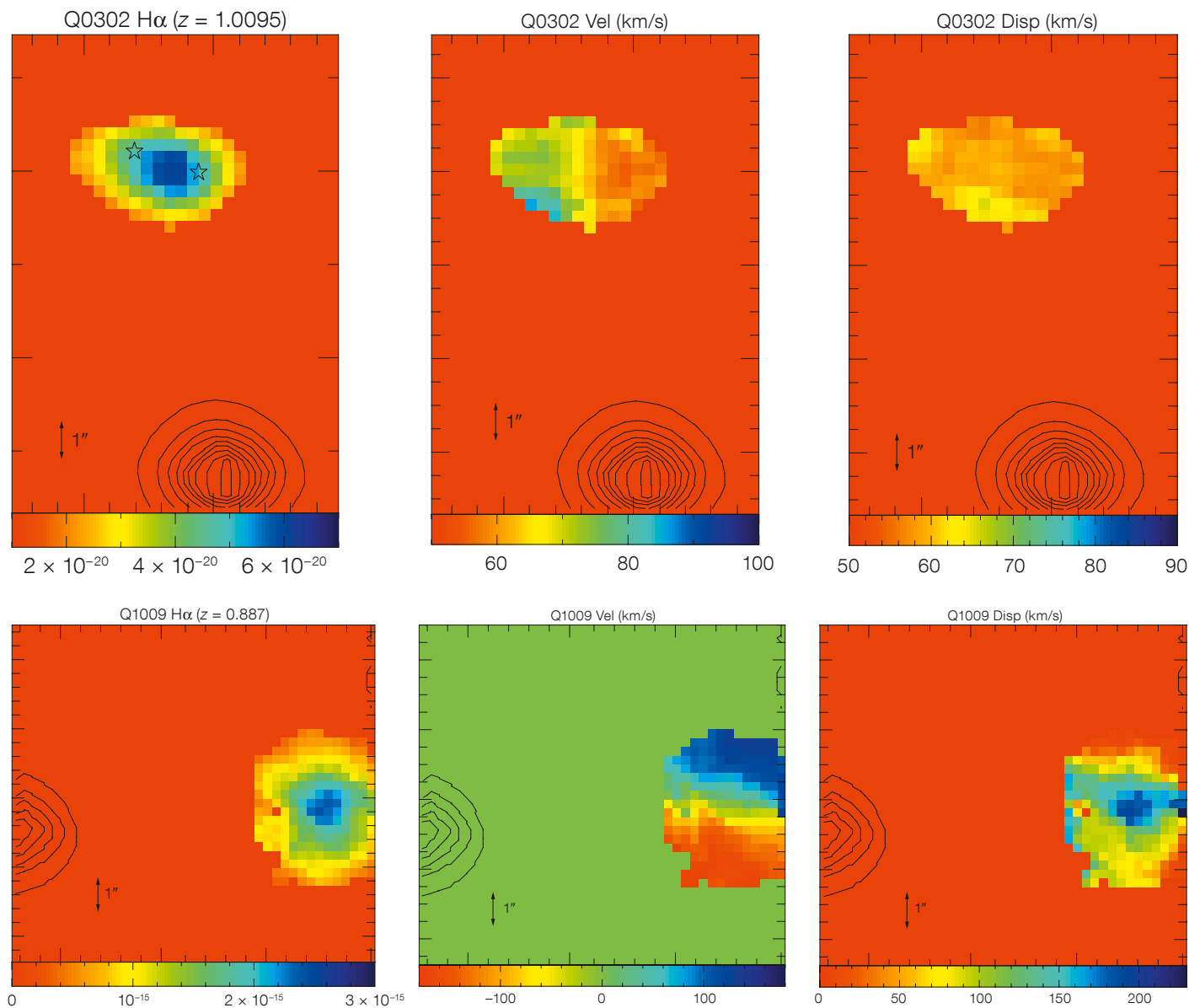


Figure 6. $H\alpha$ flux map, $H\alpha$ velocity field and $H\alpha$ velocity dispersion maps of the quasar absorbers Q0302–223 (upper) and Q1009–0026 (lower). The colour scale indicates the flux in $\text{erg s}^{-1} \text{cm}^{-2}$ in the $H\alpha$ flux map on the left and the velocities and velocity dispersions in km/s for the middle and right set of panels. North is up and east is to the left. The thin black contours indicate the position of the quasar.

there have been detections of inverted gradients, interpreted as a signature of accretion, but on a much smaller distance scale (Cresci et al., 2010).

Finally, we use the spatial information made available to us from the 3D spec-

troscopy to compute a metallicity map of Q1009–0026. Figure 5 presents the metallicity in units of $12+\log(\text{O}/\text{H})$ derived from the N_2 parameter (Pettini & Pagel, 2004), i.e. the ratio of $[\text{N II}]\lambda 6585.27/\text{H}\alpha$. The metallicity gradient appears to be rather uniform on that scale, as expected from the magnitude of the gradients observed in such objects (see Figure 4).

Kinematics

In addition to the identification and redshift confirmation of the galaxy responsible for

the quasar absorbers, the SINFONI data allow for a study of the dynamical properties of the galaxies. We extracted maps of the velocity-integrated line fluxes, relative velocities, and velocity dispersion from the reduced data cubes (Figure 6). Using these maps, critical information on the dynamical state and properties of the galaxies associated with quasar absorbers can be derived.

The galaxy associated with the $Z_{\text{abs}} = 1.009$ DLA towards Q0302–223 shows little sign of rotation or significant amounts of dispersion. It has an axis

Quasar	$\sin i$	v/σ	$r_{1/2}$ (")	Σ_{SFR} ($M_{\odot}/\text{yr}/\text{kpc}^2$)	M_{dyn} (M_{\odot})	Σ_{gas} (M_{\odot}/pc^2)	M_{gas} (M_{\odot})	M_{halo} (M_{\odot})	M_{*} (M_{\odot})
Q0302–223 ^a	0.88	0.19	0.7	0.13	$10^{10.3}$	$10^{1.9}$	$10^{9.1}$	–	$10^{9.5}$
Q1009–0026	0.60	1.45	0.5	0.31	$10^{10.9}$	$10^{2.2}$	$10^{9.2}$	$10^{12.6}$	–

ratio of $b/a = 0.47$ corresponding to an inclination of $\sin i = 0.88$. The maximum velocity is $V_{max} = 11$ km/s. The ratio v/σ in this object is 0.19 (see Table 2), much smaller than seen in local disc galaxies ($v/\sigma = 10$ – 20 km/s), and at high redshift. This might indicate that this object is pressure-supported, and early-type morphologies come to mind. However, the morphology of this object indicates that this galaxy might be a late-type object. The SINFONI data show that it is highly elongated. This is supported by the archival HST/WFPC2 images covering this field (Le Brun et al., 1997). In these data, two separate components can be seen, but their redshifts cannot be estimated (see the two stars in Figure 6 [upper flux map] which indicate the positions of the components). The two individual components are not resolved in the SINFONI observations and might explain the elongated shape; alternatively only one component is seen but the detection of H α emission at the position of the absorber provides secure identification. One interpretation is that we might be seeing a dispersion due to a small difference in redshift of two interacting galaxies. However, the H α light profile appears to be exponential with a scale length of 0.6 arcseconds. Thus, an alternative explanation is that this galaxy is dispersion-dominated, although it already has a disc-like morphology. This is indicative of a young attenuated object, with effective radius (containing half of the light) of $R_e = 0.5$ arcseconds, or 4 kpc, whose kinematics show that sustained rotation has not yet occurred. In other words, this object will have to contract further.

By contrast, the absorber toward Q1009–0026 has a morphology and kinematics consistent with that of a disc, with a normal dispersion profile ($v/\sigma = 1.45$) peaking at the centre $\sigma_{peak} = 190$ km/s and flattening in the outer parts to $\sigma_{disc} = 60$ – 70 km/s (see Table 2). This object is more face-on with an estimated inclination of $\sin i = 0.60$ derived from

an axes ratio $b/a = 0.80$. It shows clear signatures of rotation with systematic velocity gradients. Its v/σ is not typical of local disc galaxies, which have $v/\sigma = 10$ – 20 , but the systematic gradient still favours a spiral galaxy.

We also use the kinematic maps to estimate the sizes of the systems. These, in turn, are used to compute the area of the objects assuming that the inclined discs appear as ellipses. Using these estimates of the sizes of the detected galaxies, we compute their star formation rate surface densities (see Table 2).

Mass estimates

The observations provide direct observational estimates of dynamical masses for galaxies selected on neutral gas H I content (see Table 2). In order to estimate the mass of gas in these objects, we start from the observed H α surface brightness and compute gas surface brightness using an inverse Schmidt–Kennicutt relation. The results indicate a low gas fraction in the objects. In addition, both objects show clear exponential light profiles indicative of discs. Thanks to our kinematical data based on the H α emission line widths, we are able to estimate the mass of the halo in which the system towards Q1009–0026 resides. The halo mass we derive is comparable with the one from the Milky Way. In the case of the DLA towards Q0302–223, we use the broadband magnitudes from HST/WFPC2 (Le Brun et al., 1997) and ground-based NIR observations (Chen & Lanzetta, 2003) which cover the Balmer break of the object to constrain the age of the stellar population in the galaxy with a spectral energy distribution fitted to the integrated light of the galaxies. The spectroscopic redshift and star formation rate derived from our SINFONI spectra are used as an input to the code, thus allowing the stellar mass of the object to be constrained with relatively high confidence, and, in turn, allows us to put

Table 2. Kinematic properties and mass estimates of the two N_{HI} absorbers detected.

Note: The inclination is the main source of uncertainties and is estimated to be around 30 %.

^a The higher resolution HST/WFPC2 data from Le Brun et al. (1997) clearly shows that the object is subdivided into two sub-components, consistent with the elongated shape seen in the SINFONI data presented here. In this table, however, the object is treated as single.

constraints on the baryonic mass fraction in this galaxy. We derive a gas fraction of one third. Such gas fractions are in the low range of the typical values derived in $z \sim 2$ – 3 galaxies by others. When comparing these various mass estimates, we see that these systems have little room for molecular gas, which is consistent with the low star formation rates derived.

Future prospects

The observational set-up of SINFONI has demonstrated the power of integral field spectroscopy for deriving a number of emission properties for quasar absorbers, a type of high-redshift galaxy that has been difficult to identify in the past. These new tools are now available to study these objects systematically and work is continuing to expand the survey with three new additional detections recently reported (Péroux et al., 2011c). This type of study illustrates that detailed studies of quasar absorbers can offer entirely new insights into our knowledge of the interaction between stars and the interstellar gas in galaxies.

References

- Bouché, N. et al. 2007, ApJ, 669, L5
- Bouché, N. et al. 2011, MNRAS, submitted
- Cresci, G. et al. 2010, Nature, 467, 811
- Le Brun, V. et al. 1997, A&A, 321, 733
- Noterdaeme, P. et al. 2009, A&A, 505, 1087
- Pettini, M. & Pagel, B. E. J. 2004, MNRAS, 348L, 59
- Péroux, C. et al. 2005, MNRAS, 363, 479
- Péroux, C. et al. 2011a, MNRAS, 410, 2237
- Péroux, C. et al. 2011b, MNRAS, 410, 2251
- Péroux, C. et al. 2011c, MNRAS, submitted

The VLT VIMOS Lyman-break Galaxy Redshift Survey — First Results

Tom Shanks¹
Rich Bielby¹
Leopoldo Infante²

¹ Department of Physics, Durham University, United Kingdom

² Departamento de Astronomía y Astrofísica, Pontificia Universidad Católica de Chile, Santiago, Chile

We have completed the largest spectroscopic survey of Lyman-break galaxies (LBGs) at $z \approx 3$, using the uniquely wide field of the VLT VIMOS multi-object spectrograph. The survey now contains about 2100 galaxy redshifts over the range $2 < z < 3.5$ and is being used to investigate gas outflows from galaxies and large-scale structures at $z \approx 3$. These results are having an immediate impact on theories of galaxy formation and producing new tests of the standard cosmological model. In particular, we find: further evidence from their clustering that LBGs may be the progenitors of spiral galaxies; new evidence for gas outflows from star-forming galaxies as required by theoretical galaxy formation models; and new evidence for gravitational infall of galaxies into clusters at a rate that is consistent with the standard cosmology.

The Lyman-break technique uses the redshifting of the Lyman- α forest and Lyman-break into the U -band to detect $2.5 < z < 3.5$ galaxies. Use of this technique originated in the mid-1980s when it was applied to find $z > 3$ QSOs (Shanks et al., 1983). Further development of the method for selecting $z > 3$ galaxies came in the subsequent years as deeper optical imagery became available (Guhathakurta et al., 1990; Steidel & Hamilton, 1993). However, the first significant galaxy redshift surveys at $z \approx 3$ did not come until the mid-1990s when surveying of these objects was begun with the Keck LRIS spectrograph (e.g., Steidel et al., 1996) and secure galaxy redshifts could be determined.

Faint blue galaxies at high redshift

The early scientific results from these surveys were intriguing. Prior to the confirmation of these faint blue objects as $z > 2$ galaxies, there was a perception that star formation should be suppressed at $z > 1$ in line with predictions from cold dark matter models. This was supported by the sparsity of observations of $z > 1$ galaxies at the time, which was in fact a selection effect, i.e. the redshift desert due to the [O II] line leaving the optical bands had conspired to produce false agreement with the model predictions.

Metcalf et al. (1991, 1996) suggested that these faint blue galaxies, which dominate blue galaxy counts, may well be high redshift galaxies with their ultraviolet light from star formation redshifted into the visible bands. Only with the arrival of larger telescopes (such as Keck and the Very Large Telescope, VLT) armed with sensitive slit spectrographs did it become possible to cross the desert and pick up the UV light and, crucially, the Lyman- α emission line as it entered the optical bands at $z > 2$. At this point, it was found that a large fraction of faint blue galaxies were faint because they were at high redshifts and not intrinsically subluminescent lower redshift galaxies. These galaxies, selected via the Lyman-break technique, and therefore termed Lyman-break galaxies, were more clustered than expected, leading to suggestions that they were the progenitors of early-type galaxies. They were predicted to have a morphology that was chaotic, appropriate for proto-galaxies, however in more recent years the results show that in fact many may have rotation curves rather like spiral galaxies.

Starburst outflows from forming galaxies?

Interestingly, the Keck LBG redshift data showed evidence for significant velocity offsets (≈ 600 km/s) between Lyman- α ($\text{Ly}\alpha$) emission and absorption lines originating in the interstellar medium (ISM) in the LBG spectra, whilst at the same time the $\text{Ly}\alpha$ emission appeared to be asymmetric. These observations led to the development of the shell model for LBG structure in which a central star-forming region is surrounded by a shell of out-

flowing gas powered by the star formation in the central region. In this way the $\text{Ly}\alpha$ emission is scattered and absorbed by outflowing material, leading to the asymmetry and the velocity offsets between emission and absorption lines.

Further evidence for star formation feedback was also found in results showing LBGs close to the line of sight of $z > 3$ QSOs, which appeared to be associated with a deficiency of neutral hydrogen in the Lyman- α forest. The suggestion was that this was caused by the LBG outflows heating the surrounding gas (Adelberger et al., 2003). However, subsequent observations then contradicted this conclusion with no such deficit being observed in the larger, albeit somewhat lower redshift, sample presented by Adelberger et al. (2005).

VLT VIMOS LBG Redshift Survey

A key advantage of the VLT VIMOS is its large field of view. In one pointing, it covers a field of view of approximately 17×18 arcminutes, considerably larger than the field of view of approximately 6×8 arcminutes of the LRIS on Keck. Taking advantage of this, the VLT LBG survey has observed a total of 18 VIMOS fields, covering a total area of around 2.6 square degrees (Bielby et al., 2011; Crighton et al., 2011). A subset of the LBG fields is shown in Figure 1, where spectroscopically confirmed LBGs, identified using VIMOS, are denoted by blue circles and $z \approx 3$ QSOs from a range of sources are shown by red stars. In total the survey comprises around 2100 spectroscopically confirmed $z > 2$ galaxies, and in Figure 2 we show a number of example spectra of $R \approx 24.5$ mag LBGs taken using VLT VIMOS.

The spectroscopic observations that form the survey have relied on high quality deep imaging, which for the most part has been obtained using the MOSAIC imagers at the NOAO KPNO and CTIO facilities. These large MOSAIC imagers have provided the survey with 35×35 minute coverage of the fields (a large enough area to allow four VIMOS pointings per imaging dataset — the lower panels of Figure 1), each of these being centred on a bright $z \approx 3$ QSO.

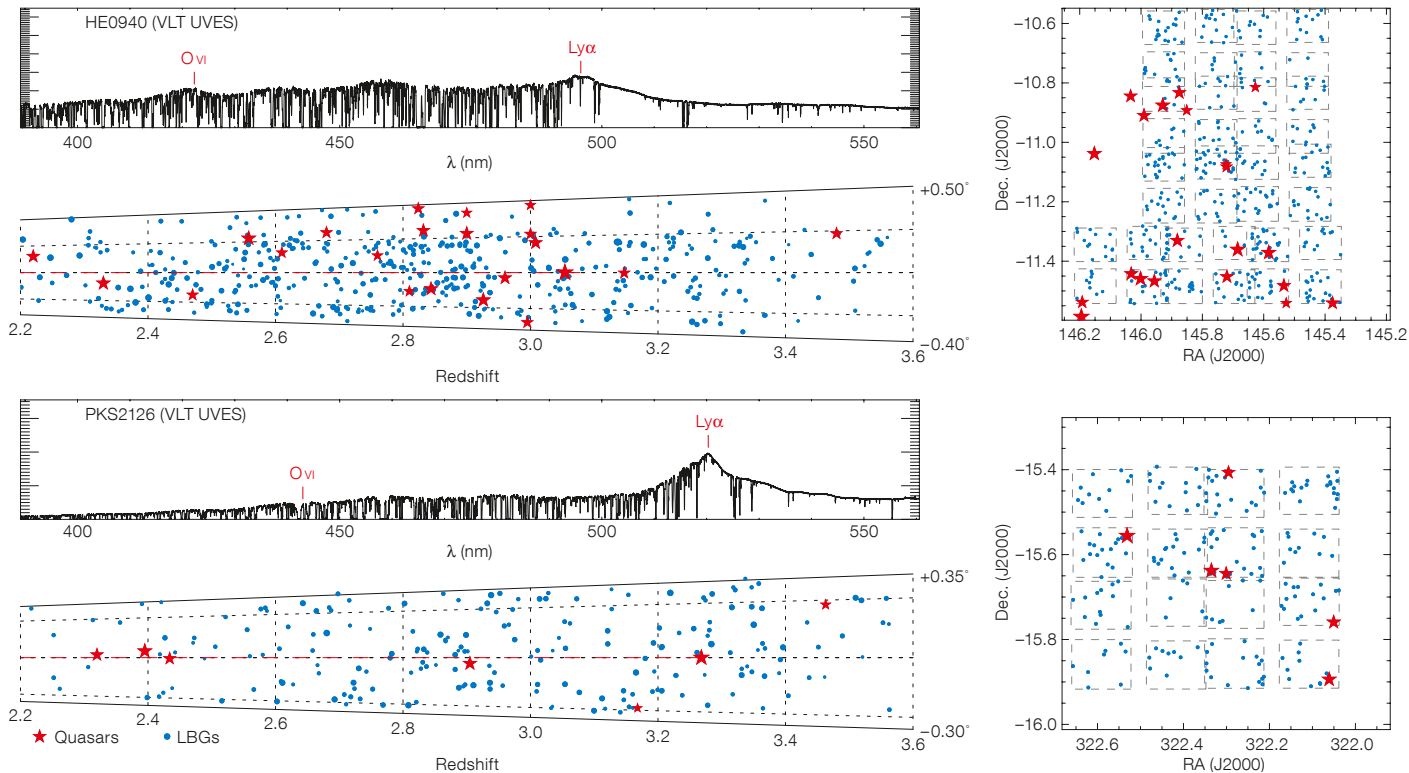


Figure 1. Left: The distribution in redshift and declination of LBGs and QSOs in two of our nine survey fields. LBGs spectroscopically confirmed using VIMOS are shown by blue circles; QSOs spectroscopically observed using AAT AAOmega or VLT UVES are shown by filled red stars. The UVES spectra of the central QSO is pictured above each cone and these show the Lyman- α absorption forest extending below the QSO Lyman- α emission line.

Other metal lines can be seen at longer wavelengths. These hydrogen and metal absorption lines allow us to probe the intergalactic gas in the vicinity of the star-forming LBGs. Right: The same two fields, now shown projected onto the sky. The dashed grey boxes show the VIMOS observation areas for the VLT LBG Survey. The upper field contains nine VIMOS pointings and the lower field contains four VIMOS pointings.

More recently, a larger area capability has been added using the MegaCAM instrument at CFHT, which provides a field of view for the deep imaging of 1×1 degrees (allowing nine VIMOS pointings for each set of imaging data — the upper panels of Figure 1). Using these combinations of data, the VLT LBG survey has broken new ground in the observation of large-scale structure of galaxies at $z \approx 3$.

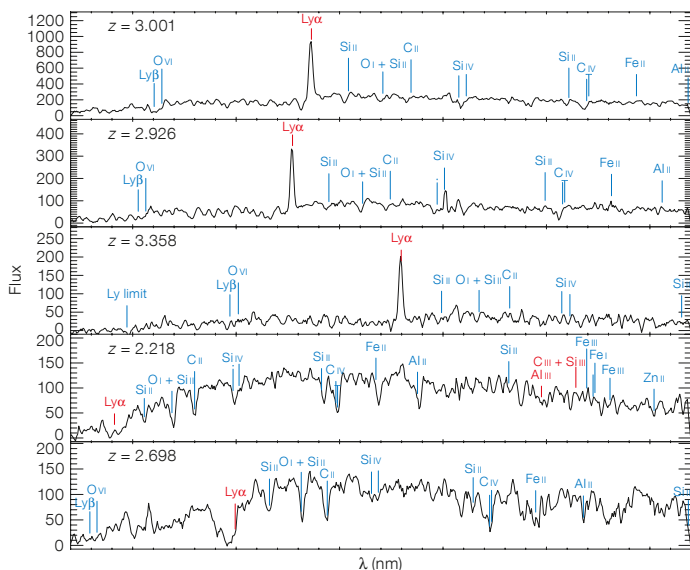


Figure 2. LBG spectra taken with VIMOS as part of the VLT LBG survey. The LBGs have $R \approx 24.5$ mag and the typical VIMOS on-sky exposure time was 3 hrs, using the low resolution LR-blue grism. Most of our redshifts are obtained via the Lyman- α line either in emission or absorption, but many other interstellar absorption lines can also be seen.

In order to probe the intergalactic medium, the survey also requires spectroscopic observations of $z \approx 3$ QSOs, which trace out the hydrogen content of the Universe along the line of sight. Where available we have made use of high resolution/high signal-to-noise spectra using VLT UVES and available through the ESO public archive. These only provide 1–2 QSO sightlines per field and we have added to this with a QSO survey within the VLT LBG fields using the AAOmega instrument on the Australian Astronomical Telescope (AAT). The AAOmega spectrograph easily encompasses our fields with its 2-degree field of view and in total has provided data on about 100 $z \approx 3$ QSOs in the VLT LBG fields, adding considerably to the available sightlines. For the brighter QSOs identified via these

lower resolution AAOmega observations, we then measure high resolution/high signal-to-noise spectra using the VLT's X-shooter to provide improved maps of the Ly α -forest and metal-line distribution in many additional sightlines in our fields.

Galaxy clustering evolution

We first looked at the clustering of the LBGs. The first aim is to measure the amplitude of clustering which can discriminate between models for the evolution of the galaxies. We measured the clustering amplitude and then compared it to a simple model that assumes that the LBG is a progenitor of a spiral. For biased populations that assumption leads to a simple prediction for the clustering when dark matter haloes can grow by merging, but the galaxies are not allowed to merge. We find that there is then agreement with the clustering of high luminosity spirals or low luminosity early-types at $z = 0$ (see Figure 3). This is consistent with previous results where the luminosity function of LBGs at $z \approx 3$ was found to be consistent with an evolved luminosity function for local spiral galaxies.

LBG z-space distortions and cosmology

The LBG clustering was further investigated for z -space distortions. The observed LBG clustering is measured in redshift-space, where Hubble's Law is naively used to convert redshifts into distances in the z direction. By comparing the clustering in the angular direction and the redshift direction the effect of velocity errors and peculiar velocities can be found. At small galaxy separations root mean square peculiar velocities and errors dominate, producing "fingers-of-god" elongated clusters in the redshift direction. At larger separations, dynamical infall dominates and flattens the clustering in the line of sight. Generally we have found LBG velocity dispersions of about 500 km/s, higher than found previously from the Keck survey, both in our re-analysis of that survey and in the VLT survey data. As well as having intrinsic interest, we shall see that the LBG velocity dispersion is a crucial parameter in interpreting the galaxy-gas relationship below. At larger scales we can estimate

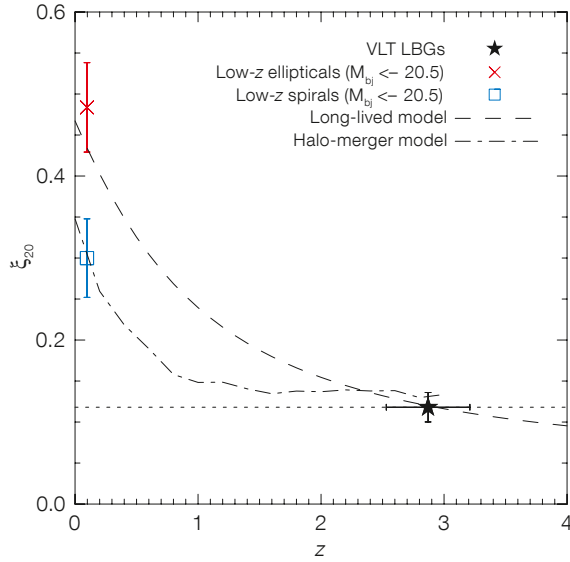


Figure 3. Predicted evolution of LBG clustering to the present day from Bielby et al. (2011). ξ_{20} measures galaxy clustering averaged out to $20 h^{-1}$ Mpc scales. A model where the LBGs are long-lived is consistent with them evolving into early-type galaxies by the present day, while a halo merger model could see them evolving into present-day spiral galaxies.

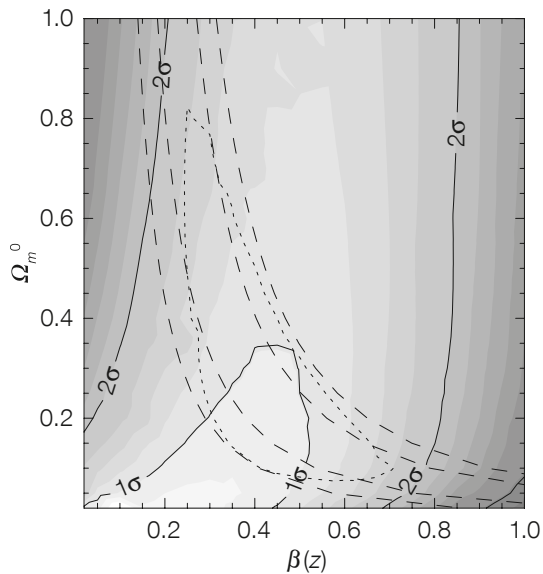


Figure 4. Fitting of the present-day value of Ω_m ($z = 0$) and the $z = 3$ infall parameter (β) based on the clustering measurements of the VLT LBG survey sample. The greyscale contours come from LBG redshift-distortions and the dashed contours come from the overall amplitude of the LBG clustering. These techniques provide reasonably independent constraints on the two unknowns, Ω_m ($z = 0$) and β ($z = 3$), allowing for their joint solution (dotted contours). The data suggest Ω_m ($z = 0$) ≈ 0.3 and $\beta \approx 0.45$, both consistent with the predictions of the standard cosmological model.

the parameter β that measures the rate of dynamical infall of galaxies into clusters. For standard gravity, $\beta = \Omega_m^{0.6}/b$ where Ω_m is the cosmological density parameter and b is the bias, or how much more the galaxies are clustered than the underlying mass. At these redshifts the cosmological density parameter should effectively be around one, whatever its value at $z = 0$. This makes it easy to determine the bias and we have found values which are pretty consistent with the standard Lambda Cold Dark Matter (Λ CDM) cosmological model, i.e. the amplitude of mass clustering implied by the LBG infall is about that predicted by Λ CDM (see Figure 4).

Gas outflows

One of the key goals of the VLT LBG survey has been to investigate the presence of galaxy outflows at $z \approx 3$. As discussed earlier, a key piece of evidence for the presence of outflows is the velocity offset between Ly α emission and ISM absorption lines (e.g., C II, O II, Si IV). Figure 5 shows the histogram of redshift differences between the Ly α emission line redshifts and the interstellar absorption line redshifts. There is evidence of a significant offset in the sense that the Ly α line is blue-shifted with respect to the interstellar lines. We have therefore confirmed the results of the Keck group

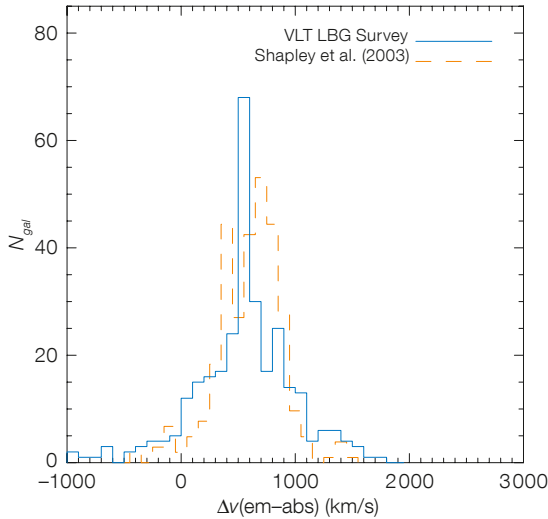


Figure 5. Velocity offsets between the Ly α emission line and the ISM absorption lines in the VLT LBG sample. The Ly α emission lines are redshifted relative to the ISM absorption lines, providing direct evidence for gas outflows from the star-forming galaxies at $z \approx 3$. Our VLT results agree with those from the Keck (Shapley et al., 2003).

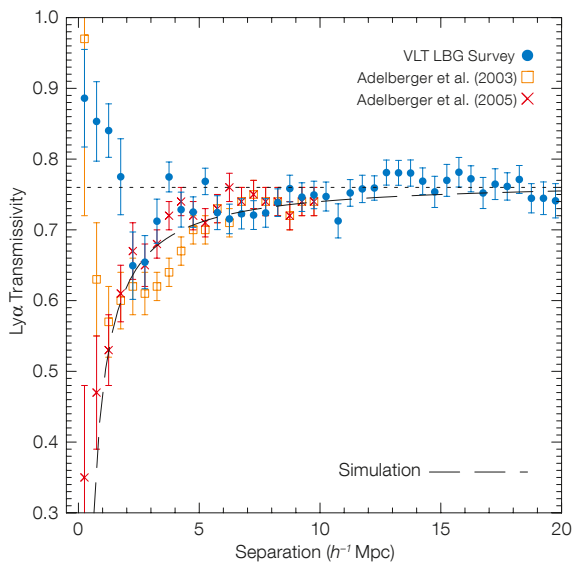


Figure 6. Average Ly α transmissivity as a function of distance from a $z = 3$ galaxy. Blue points show our results. Orange crosses and asterisks show results from Adelberger et al. (2003) and (2005) respectively. All datasets show a decrease in transmissivity (i.e. increased absorption) within $5 h^{-1}$ Mpc of an LBG, similar to the prediction from a hydrodynamical galaxy formation simulation. At smaller separations ($< 2 h^{-1}$ Mpc) the rise in transmissivity in our VLT data provides evidence for star formation feedback. Outflows from star-forming galaxies may be heating the surrounding gas, preventing further star formation. We note that this is highly preliminary however and further data will be added to this measurement from our latest VLT observations.

on this basic question about star-forming galaxies at $z \approx 3$.

Building on this result, we then performed a cross-correlation of the LBG sample with the underlying neutral hydrogen gas density as probed by QSO sightlines, based on the method of Adelberger et al. (2003, 2005). By tracing the relationship between gas and galaxies using cross-correlation analysis, we can find the extent of outflows around high redshift galaxies. We confirmed (Crighton et al., 2010) that as you get closer to an LBG ($< 5 h^{-1}$ Mpc), the neutral hydrogen Ly α absorption in the forest increases (see Figure 6). We also improved the modelling of the Ly α cross-correlation function by studying the effect of LBG

peculiar velocities and redshift errors on the gas-galaxy cross-correlation function. These can be quite sizeable since the LRIS/VIMOS velocity error is ~ 300 km/s or $3 h^{-1}$ Mpc. Nevertheless, in our latest results, with the full sample of 2100 LBGs, at separations below $1-2 h^{-1}$ Mpc the transmissivity increases again in a manner more like the result of Adelberger et al. (2003), rather than the Adelberger et al. (2005) result. This is direct evidence of the presence of galaxy formation feedback on the intergalactic medium immediately surrounding the galaxy, in line with the results shown in Figure 5. Peculiar velocities and measurement errors may contribute to the scale affected by feedback apparently extending to several megaparsecs in Figure 6.

Future work

Analysis of the VLT LBG survey is still continuing. On the galaxy evolution side, an immediate aim will be to analyse the redshift distortions in the LBG-Ly α cross-clustering in Figure 5 to understand better gas infall and outflows from galaxies. Fainter Lyman- α -emitter (LAE) galaxies have also been observed at $z = 3$ in all our fields via narrowband observations at the Subaru 8-metre, the CTIO 4-metre and the ESO 2.2-metre telescopes — these will allow the effect on the intergalactic gas of star formation in fainter galaxies to be measured. Further into the future, we want to determine better redshifts for the galaxies from nebular lines such as H α in the near-infrared. The new VLT spectrograph KMOS (Sharples et al., 2010) should be ideal for this task and the KMOS integral field units will also afford dynamical information about the brighter targets.

There are also proposals to extend the cosmological aspects of the survey. Here the main aim will be to measure the baryon acoustic oscillations scale at $z \approx 3$ and test for evolution of the dark energy equation of state. This will require a formidable increase in survey size — more than an order of magnitude — but might still be feasible as a VIMOS large programme. Such a survey of around 25000 LBGs could also be used to analyse redshift-space distortions and make a new cosmological test by looking for deviations from the spherical symmetry of LBG clusters in the redshift and angular directions in order to make a further basic test of cosmological models.

References

- Adelberger, K. L. et al. 2003, ApJ, 584, 45
- Adelberger, K. L. et al. 2005, ApJ, 629, 636
- Bielby, R. et al. 2011, MNRAS, accepted, arXiv:1005.3028
- Crighton, N. et al. 2011, MNRAS, accepted, arXiv:1006.4385
- Guhathakurta, P. et al. 1990, ApJ, 357, 9
- Metcalfe, N. et al. 1991, MNRAS, 249, 498
- Metcalfe, N. et al. 1996, Nature, 383, 236
- Shanks, T. et al. 1983, Nature, 303, 156
- Shapley, A. E. et al. 2003, ApJ, 588, 65
- Steidel, C. C. & Hamilton, D. 1993, AJ, 105, 2017
- Steidel, C. C. et al. 1996, ApJL, 462, L17
- Steidel, C. C. et al. 2003, ApJ, 592, 78

This new image of the reflection nebula Messier 78 was captured using the Wide Field Imager camera on the MPG/ESO 2.2-metre telescope at the La Silla Observatory, Chile and was awarded the first prize in ESO's Hidden Treasures competition. Igor Chekalin from Russia uncovered the raw data for this image in ESO's archives, processed the raw data with great skill and claimed first prize in the contest (see Hainaut et al., p. 57).



Spiral Structure in the Milky Way: Confronting Observations and Theory

held at Bahía Inglesa, Copiapó, Chile, 8–11 November 2010

Preben Grosbøl¹
Giovanni Carraro¹
Yuri Beletsky¹

¹ ESO

The main objectives of the workshop were to review current observational evidence for spiral arms in our Galaxy and confront them with models of spiral structure in order to arrive at a consistent picture. Of primary importance was to understand just what additional information is required to resolve outstanding issues related to the spiral structure in the Milky Way, especially as new survey instruments (e.g., ALMA, VISTA and VST) are coming online and major space missions like GAIA will be launched in the near future.

More than 50 years ago, the spiral arms of the Milky Way were identified in the distribution of OB-stars, H II-regions and neutral hydrogen. An overview of the early results was presented in the proceedings of the IAU Symposium 38 held in 1969, in Basel, Switzerland. Our knowledge of the evidence for spiral arms in the Milky Way and the kinematics in the Solar Neighbourhood has increased significantly over the last few decades. Despite this, there is still no consensus on the basic parameters of the spiral structure in our Galaxy, such as the number of major spiral arms and their location, its pattern speed(s) and amplitude, and its relation to the central bar. Major new and future observational facilities (such as ALMA, GAIA, LSST, VISTA, VST and APOGEE) will provide a wealth of data on the spatial and kinematic distributions of the material in the Galaxy. Thus, it seemed appropriate to perform a census of our current data, confront them with theory and models of spiral structure, and thereby map the path towards a consolidated view of the spiral pattern in the Milky Way. The workshop was held at the small, beautiful seaside resort of Bahía Inglesa in Central Chile over a period of three and a half days. It was a pleasure to see many students among the 55 participants (see Figure 1), the number being limited by the off-season availability of accommodation.



Figure 1. The participants by the swimming pool at the conference venue, the Hotel Rocas de Bahía in Bahía Inglesa.

Observations

Recent observational data suggesting a spiral structure in the Milky Way were reviewed during the first two days of the workshop. H I/CO maps of the Galaxy have much improved both in sensitivity and resolution (presentation by T. Dame; see the workshop web page¹ for more details). This has led to a better outline of the spiral arms, especially on the far side of the Galaxy, even though uncertainties in the rotation curve and the distance ambiguity still present issues. The identification of a symmetric counterpart to the 3-kiloparsec arms was made possible by the high resolution radio data. Accurate parallaxes to numerous masers have been determined using very long baseline interferometry (VLBI) techniques (talks by M. Reid, M. Sato and M. Honma). Since masers are located in Giant Molecular Clouds (GMCs), this has led to much better estimates of the shape of the arms. Measurements of parallaxes and the proper motion of the central source in the Galaxy provide a new independent estimate of the rotational velocity of the Sun. H I self-absorption observed in the second Galactic quadrant (GQ) suggests a shock in the gas associated with the Perseus arm. New all-sky radio maps in

the range 45–408 MHz show four tangential points associated with synchrotron radiation in spiral arms, consistent with a four-armed pattern (A. Guzmán).

GMCs and the massive stars in the southern Milky Way were identified by combining the new Columbia survey and IRAS data (P. Garcia-Fuentes). They follow the spiral structure with some scatter and include several massive GMCs in the Norma arm. New spectrophotometric distances have significantly improved the mapping of young stellar clusters in the Galaxy (A. Moitinho & A. Daminelli). There seems to be a lack of giant H II regions on the far side of the Milky Way. The Perseus arm is well defined by CO clouds, but is deficient in clusters. Using near-infrared (NIR) surveys such as GLIMPSE, a global view of the most massive, young stellar clusters was assembled (M. Messineo). Only clusters younger than 30 Myr display spiral structure in the Solar Neighbourhood (A. Lokin & M. Popova). Their ages and relative locations suggest a co-rotation radius just outside the Sun. A survey of early-type stars in the anti-centre direction using Strömgren photometry, which provides accurate distances to individual stars, indicates a density enhancement associated with the Perseus arm (M. Menguío). The IPHAS survey questions the existence of a sharp truncation of the stellar disc (S. Sale).

The general spiral structure displayed by young objects and gas agrees well with, and is best fitted by, a four-armed pattern (D. Russeil). Kinematic distance estimates are not always reliable due to possible systematic perturbations by a density wave. NIR star counts using 2MASS and GLIMPSE can give structural information when the underlying stellar population has features in its magnitude distribution like the red clump (R. Benjamin & P. Poldo). In integrated longitude–magnitude diagrams, structures in the bar and bulge can be seen as tangential points of spiral arms and the truncation of the disc. The distribution of CS emission sources in the Galactic Plane shows a squared feature which resembles the orbital shape near the 4:1 resonance (J. Lépine). Spiral and bar perturbations in external galaxies and possible implications for the Galaxy were also discussed (M. Arnaboldi & M. Dumke).

Theory

The third day of the workshop was dedicated to theoretical models and their comparison with observational data. Magnetohydrodynamic simulations in a realistic Galactic potential show that the response to a two-armed spiral perturbation in the stars can yield additional, slightly tighter, arms of compressed gas between the stellar arms (M. A. Martos & G. Gómez). The Galactic bar may drive the spiral pattern and induce additional gaseous arms, which will look like a four-armed pattern (O. Gerhard). New analytic models of the Milky Way were presented and used to analyse the importance of ordered and chaotic stellar orbits (B. Pichardo & S. Villegas). The velocity ellipsoid can be used to test different potential models with spirals and bars (D. Chakrabarty & B. Famaey). Although it is non-trivial to define a best fit to such distributions, they indicate that the spiral has a significantly lower pattern speed than that of the Galactic bar. Radial mixing can be estimated from pencil beam surveys and used to place constraints on possible spiral modes in the Galaxy and their lifetime (I. Minchev). Unstable spiral modes can be present in stellar discs depending on the radial distribution functions of rotational velocity,



Figure 2. The conference poster, showing the major features of the Milky Way spiral structure.

dispersion and surface density (V. Korchagin). The number of arms and the pattern speed of the growing modes depend on these functions and suggest a four-armed pattern for a standard model of the Milky Way.

Future surveys

Finally, the last half-day was dedicated to future surveys. Several new surveys are being prepared and will improve our knowledge of the stellar disc by orders of magnitude. VISTA surveys in the NIR will allow a much better view towards the centre of the Galaxy while GAIA will assemble both spatial and kinematic data for more than a billion stars (V. Ivanov, J. Alonso-Garcia & J. de Bruijne). Surveys like APOGEE using SDSS-II data are improving the kinematic data significantly (S. Majewski).

Discussions

During the last two days of the workshop, more than three hours were devoted to intense discussions of observations and models. The two main topics were the topology of the arms and the possi-

ble angular speed of the pattern. There was wide agreement that gas and young objects show a four-armed structure with pitch angles in the range of 12–14 degrees. The major issue is whether the older stellar component has only a two-armed structure (Perseus and Scutum–Centaurus) or also four arms. In the former case, the two minor gas arms (Sagittarius and Norma) would either be generated by secondary compressions or driven by the bar. It would be possible to distinguish these options by more accurate mapping of the arms (e.g., by VLBI parallaxes of masers) and detailed analysis of the stellar density–velocity field in a region of a few kiloparsecs around the Sun. Whereas new surveys (e.g., VISTA and GAIA) will provide accurate mapping of the stellar component, radial velocities may still be an issue.

The current data are consistent with the observed spiral pattern being associated with a density wave. The life span of such waves in the Galaxy is not easy to evaluate, as only very indirect means can be used, such as radial mixing and changes of velocity dispersion with the mean age of the stellar populations. Most estimates of the pattern speed of the spiral arms show values significantly lower than that of the bar, suggesting that the disc of our Galaxy has at least two components with different pattern speeds. While star formation and shocks in the gas of the Perseus arm second GQ indicate co-rotation for the spiral to be outside this radius, the kinematics of local young clusters place it much closer to the Solar radius.

Acknowledgements

We express our deep gratitude to Paulina Jirón, Hernan Fernandez, Mariña Eugenia Gómez and the entire Local Organising Committee for a very successful meeting.

Links

¹ Conference web page: <http://www.eso.org/sci/meetings/MW2010/index.html>

The First Year of Science with X-shooter

held at the Palace Hotel and Centro Congressi, Como, Italy, 19–22 October 2010

Sofia Randich¹
Stefano Covino²
Stefano Cristiani³

¹ INAF–Osservatorio Astrofisico di Arcetri, Italy

² INAF–Osservatorio Astronomico di Brera, Italy

³ INAF–Osservatorio Astronomico di Trieste, Italy

The workshop was held with the aim of bringing together X-shooter users to discuss scientific results, performance and technical aspects, after the first year of successful operations of the instrument. The workshop was also organised to commemorate Roberto Pallavicini, whose scientific and human contribution to the development of X-shooter was invaluable and a source of continuous inspiration for all of us. A touching presentation focusing on the scientific personality of Roberto was given by Luca Pasquini on the second day of the workshop.

About 50 people attended the workshop, including several young researchers. A variety of preliminary and more advanced results from the first year of X-shooter activities was reported. In spite of the

natural need of the community to become well acquainted with a new and sophisticated instrument and its analysis tools, the first results are, already, truly exciting, spanning a wide range of different scientific fields, covering virtually all classes of astrophysical objects, and demonstrating the high flexibility and throughput of X-shooter. The scientific programme was put together thanks to the dedicated work of the Scientific Organising Committee (S. Covino, Co-Chair; S. D’Odorico; J. Fynbo; P. Groot; F. Hammer; J. Hjorth; L. Kaper; S. Randich, Co-Chair; P. Rasmussen; and F. Zerbi).

The first session of the workshop was dedicated to talks related to the instrument itself, including a description of its history, characteristics, performance and a science overview, with particular focus on the Guaranteed Time Observer (GTO) programme (presentations by S. D’Odorico; F. Zerbi et al.; C. Martayan et al.; P. Bristow et al.; M. Andersen; P. Groot). A programme aimed at setting up an X-shooter spectral library was also presented (S. Trager). The second session was devoted to star formation, while during the third session the potential of X-shooter for studies of stars and stellar populations was discussed. The fourth and fifth sessions focused on supernovae and gamma-ray bursts (GRB); speakers in the last session

presented X-shooter results on the physics of galaxies and the intergalactic medium (IGM) in the low- and high- z Universe. The full programme of the meeting and selected presentations are available on the conference web page¹.

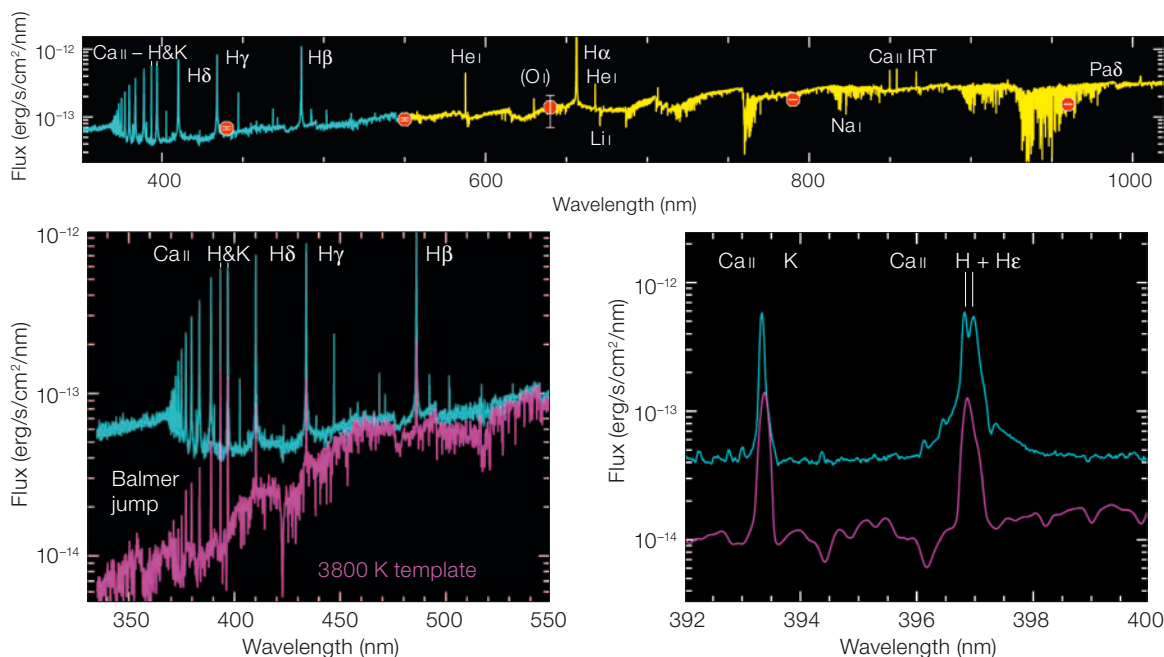
We present here a selection of the topics presented. Proceedings will be published in a dedicated volume of *Astronomische Nachrichten* and most of the quoted contributions will soon be available there.

Stellar spectroscopy

X-shooter offers a unique instrument combination for studies of star formation, from the lowest mass brown dwarfs (BDs), to the most massive young stellar objects (YSOs).

A set of spectra of very low-mass members of nearby star-forming regions (SFRs), shown in Figure 1, represents a spectacular example of the capabilities of X-shooter in this field. The large and simultaneous spectral coverage, from the U - to the K -band, allows the characteristics of these objects, such as their spectral types, lithium abundances, the accretion and wind properties and the physical conditions of the gas accreting from the circumstellar disc onto the star (J. Alcalà et al.; E. Rigliaco et al.), to

Figure 1. Example of the flux-calibrated UVB (blue) and VIS (red) X-shooter spectrum of the young, low-mass ($M = 0.6 M_{\odot}$) star Sz130 in the Lupus-3 cloud. The good match between the flux of the UVB and VIS spectra is noticeable. The emission lines of the Balmer series (up to $\sim H_{24}$), as well as the He I and Ca II (H&K and the infrared triplet), are evidence of strong accretion. There is also a very good agreement between the flux derived from the B , V , R , I , Z photometry (red dots) and the continuum flux of the spectrum. Adapted from Alcalà et al. (2011).



be studied with unprecedented reliability. A large survey of low-mass stars in different SFRs is being carried out as part of the Italian GTO and the first results were presented at the workshop. A survey of older BDs outside star-forming regions is also being carried out (B. Goldmann), which will, for the first time, allow a complete characterisation of these objects and constraints to be put on model atmospheres.

Both for low-mass pre-main sequence (PMS) stars, or T Tauri stars, and for Herbig Ae/Be stars, which are intermediate mass stars still in the PMS phase, X-shooter makes it possible to cover several accretion diagnostics. In this upper mass range, the active star-forming mechanism switches from magnetically controlled accretion to an, as yet, unknown mechanism, but which is likely to be direct disc accretion onto the star. An X-shooter study of a large sample of Herbig Ae/Be stars has started, with the main aim of mapping the differences between the accretion characteristics of low- and higher-mass stars and eventually to put constraints on the formation mechanism of the latter (R. Oudmaijer et al.).

At the highest mass end, X-shooter has the unique potential to probe the spectra of rare massive YSOs in the optical wavelength range. This, in turn, is critical to better determine their photospheric properties, to study the onset of the stellar wind, and to characterise the physical structure of the circumstellar disc. Very interesting and promising results were also obtained thanks to X-shooter observations of two massive YSO candidates. Both spectra are characterised by several emission lines, including the CO first overtone emission, H α and Ca II IR triplet; these features are indeed consistent with the presence of infall and outflow and are similar to those observed in lower-mass stars (L. Kaper et al.).

Moving to older stars, X-shooter has, in spite of the modest resolution, but thanks to the wide spectral coverage and high efficiency, allowed the determination of abundances of extremely metal-poor stars in the outer Galactic Halo — revealing, in all likelihood, the most distant dwarf stars studied in detail to date — and of two turn-off stars in the globular cluster

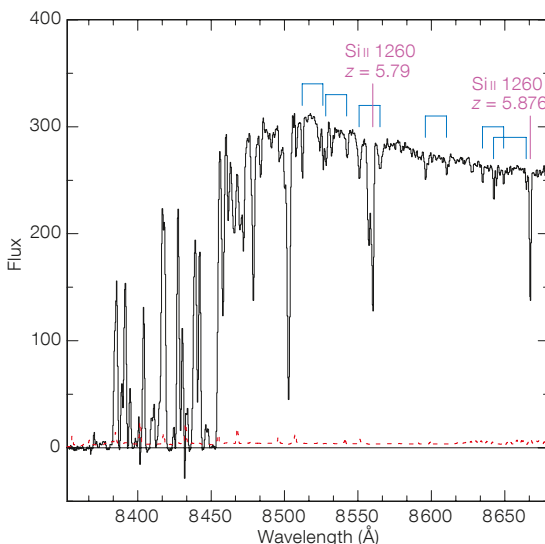


Figure 2. The region of the Ly α emission in the X-shooter spectrum of the QSO SDSS J0818+1722 ($z_{em} = 6.00$). The detected weak CIV doublets are marked in blue and the two prominent Si II 1260 Å absorption features of the systems at $z = 5.79$ and $z = 5.876$ in magenta (for details see V. D’Odorico et al., 2011).

NGC 2808 (P. Bonifacio et al.; A. Bragaglia et al.). The chemical composition of the two halo stars has been derived, showing that they are less metal-poor than expected from the initial selection, and presenting evidence of an anomalous composition (namely an underabundance of α -elements) for one of the two objects. As for the two stars belonging to NGC 2808, they are characterised by significant differences in their abundance patterns, confirming that they likely are representative of two different generations of stars. Remarkably, these results would have not been possible with other spectrographs, except with an unrealistically huge investment of observing time.

X-shooter is also proving to be a very efficient instrument for carrying out intermediate resolution studies of Solar System objects (e.g., asteroids; A. Alvarez-Candal) and for mysterious interacting binary stars. Indeed observations of one of the most well-known recurrent novae and of a candidate black hole have revealed totally unexpected results and spectral features (E. Mason & P. Gandhi).

Extragalactic spectroscopy

The efficiency of X-shooter has allowed D. Bettoni et al. to study the faintest galaxies in nearby clusters and to explore the galaxy scaling relations of early-type galaxies over a broad mass range. The star formation in galaxies at low and high redshifts has been investigated (by L.

Christensen), providing a wealth of new data. Results on the gravitationally lensed galaxy “the 8 o’clock arc” have also been reported (by M. Dessauges-Zavadsky et al.) making it possible to dissect the physical properties of a $z \sim 3$ galaxy.

Studies of the intergalactic medium at high redshift are a *pièce de résistance* for X-shooter and quasars have always been a preferential target (G. Cupani; P. Petitjean). Spectacular results have been obtained for the QSO J0818+1722, as shown in Figure 2, where a tiny subset of the wavelengths covered by X-shooter gives a flavour of the richness of information that can be derived about the processes leading to the cosmological re-ionisation and the IGM metal pollution (V. D’Odorico et al.).

Gamma-ray bursts and supernovae

Cosmological objects, in particular if rapidly varying, such as GRBs, are definitely a natural core target for X-shooter, and indeed during the first year of X-shooter observations, GRB afterglows (PI J. Fynbo) and GRB host galaxies were frequently targeted. The management of the X-shooter GTO programme has also been an opportunity for research fields with a traditionally high level of international competition to define and establish multinational collaborations, which, in turn, have also allowed young people to immediately begin their research work within this most stimulating environment.

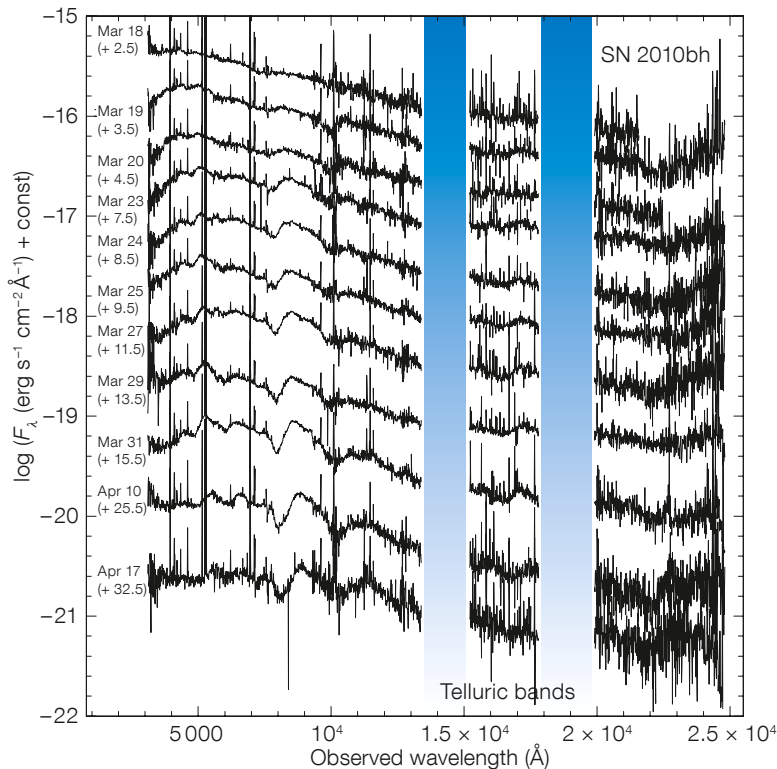


Figure 3. Spectral evolution of SN 2010bh over a period of about two months obtained with VLT + X-shooter. Phases are reported in the observed frame from the Swift/BAT trigger (2010 Mar 16.53). Spectra have been vertically displaced by an arbitrary quantity for clarity of the plot (see Bufano et al., 2011).

X-shooter pipeline is, of course, still under intense development; nevertheless, it is already mature enough to allow routine reduction and analysis of X-shooter data (P. Goldoni). During the conference a very profitable open session led by A. Modigliani, on behalf of the software development team, was devoted to feedback from the users in order to better drive the future development of the reduction package.

From extended discussions, a number of proposals for further improving the impressive capabilities of X-shooter emerged: the introduction of a cold filter in the infrared to reduce the background; upgrade of the acquisition CCD in order to provide *BVRz* photometry as a scientific and calibration added value, the possibility of infrared-only nodding; the suggestion to move X-shooter to another VLT Unit Telescope with lower time over-subscription. The action of studying an IR sensitive acquisition camera, important for high redshift work and IR flux calibration, was also taken.

Summing up, within the limits of just one year of observations with a young instrument, the wealth of data is impressive and researchers have learnt how to deal with information which, in the recent past, was (occasionally) available only through time-consuming, multi-instrument observational campaigns. X-shooter now defines the state of the art for this category of spectrographs. Not by chance it has been among the most requested instruments at ESO since the very first observational period that it was offered to the community.

References

Proceedings will be published in *Astronomische Nachrichten* in 2011.

Links

¹ Conference web page:
<http://www.brera.inaf.it/xshooter2010/>

The large X-shooter wavelength coverage allows quick and unprecedentedly reliable derivations of redshifts for GRBs crossing the so-called redshift desert ($1.4 < z < 3$). Moreover, the availability of large sets of emission and absorption lines opens up the possibility of substantially improving the knowledge of the chemical features of the environment of these remote objects (V. D’Elia; P. Jakobsson et al.; S. Piranomonte et al.; C. Thöne et al.; S. Vergani et al.) and, when possible, to perform time-resolved analyses (A. de Ugarte Postigo et al.). Integral field unit observations with X-shooter (H. Flores et al.) allowed spatially resolved chemical and dynamical information to be derived, while the extinction properties of high-redshift galaxies are explored with emission line diagnostics provided by the large wavelength range (K. Wieserma).

The supernovae and GRB communities had the opportunity to join efforts, when, in March 2010, one of the still rare SNIb/c objects associated to a GRB (SN2010bh/GRB100316D) occurred. Spectra were taken immediately and the evolution of this event was followed for months (F. Bufano et al., see Figure 3).

M. Stritzinger reviewed the state of the art of observations of type I SNe, putting X-shooter in context, while A. Pastorello et al. presented preliminary results about the impressive efficiency of X-shooter in delivering information about the interaction of SNe with their circumstellar media.

Future prospects

X-shooter is definitely not an instrument designed for high-resolution studies. Nevertheless, with good signal-to-noise, it is possible to derive reliable information about line profiles as carried out by several studies, where, for instance, the profile of Lyman- α was successfully modelled. In this case the large wavelength range of X-shooter makes it easier to find lines to study without being limited to a specific spectral range, and the high efficiency of the spectrograph allows one to deal with fainter objects not reachable at intermediate resolution in previous studies.

It is clear that, in order to cope with the impressive data flow provided by the three X-shooter arms, it is mandatory to employ reliable software tools. The

The Impact of Herschel Surveys on ALMA Early Science

held at ESO Headquarters, Garching, Germany, 16–19 November 2010

Leonardo Testi¹
Goeran Pilbratt²
Paola Andreani¹

¹ ESO

² ESA Research and Scientific Support Department, ESTEC, Noordwijk, the Netherlands

The ESA Herschel Space Observatory is currently producing new and exciting results, thanks to its unprecedented sensitivity, spectral resolution and wide-area surveying capabilities at far-infrared and submillimetre wavelengths. Many of the new discoveries by Herschel will require high angular resolution follow-up observations with ALMA. The goal of the workshop was to discuss the priorities for ALMA Early Science follow-up of the Herschel photometric and spectroscopic surveys. The possibility, or need for, simultaneous observing programmes with ALMA and Herschel was also discussed.

The ESA Herschel Space Observatory is currently in operation, covering the spectral range from the far infrared to the submillimetre, and will complete most of the key programme observations by early 2011. The exciting first results from Herschel on galaxy formation and evolution, on galactic star formation, stars and circumstellar discs, the interstellar medium, and on our own Solar System, are highly complementary to the science that the Atacama Large Millimeter/submillimetre Array (ALMA) will soon deliver. ALMA will allow a great leap forward at high angular and spectral resolution in the exploration of the cool Universe — the earliest evolutionary stages of galaxies, stars and planets. ALMA is currently in its scientific commissioning and science verification phase. The current expectation is that Early Science observations will start in the second half 2011.

Herschel and ALMA make an excellent complementary pair, not only in wavelength regime, providing rich molecular spectra and well-sampled spectral energy distributions, but also in angular resolution. The high angular resolution that ALMA will provide makes it the



Figure 1. The workshop participants collected in the entrance hall at ESO Headquarters.

perfect resource to follow up the science targets observed and identified in the wide-area multi-band photometric and spectroscopic surveys performed by Herschel.

The workshop had the goal of discussing the science rationale for possible early ALMA follow-up observations based on the first exciting Herschel results. Another topic raised in the meeting was whether there are observations where simultaneous Herschel–ALMA observations would be desirable: given Herschel's limited lifetime they would have to be identified on a short timescale. The sessions were broadcast with a live video connection to a Joint ALMA Observatory meeting room in Santiago. Figure 1 shows a photograph of the workshop attendees.

Cosmological surveys, active and nearby galaxies

The first results of the Herschel deep field and wide-area surveys were reviewed by G. de Zotti, S. Eales and E. Le Floch. These surveys allow the evolution of far-infrared luminosity functions to be measured as a function of redshift on

statistically significant samples of objects, thus mapping the evolution of star formation in the Universe. In addition, the wide-area surveys have allowed significant numbers of rare objects to be revealed. The sources found by these surveys are ideal targets for ALMA to measure the molecular gas content, dynamical masses and morphology at high angular resolution. Initial follow-ups of the gravitationally lensed candidates have shown the potential of high angular resolution millimetre observations (see Figure 2). Detailed studies of relatively small samples of luminous submillimetre galaxies with current millimetre-wave interferometers are already showing the role played by merging, gas accretion and secular evolution. As presented by L. Tacconi, ALMA will allow these studies to be significantly extended and a coherent picture of galaxy formation and evolution to be built.

In this context, observations of atomic gas in high redshift galaxies in the submillimetre are flourishing with the current generation of single dish telescopes and interferometers. The enormous step forward expected in this area with ALMA was discussed by F. Walter, R. Maiolino and K. Knudsen. Indeed preliminary test data from ALMA appear to confirm the prospects in this field (see Figure 3). The

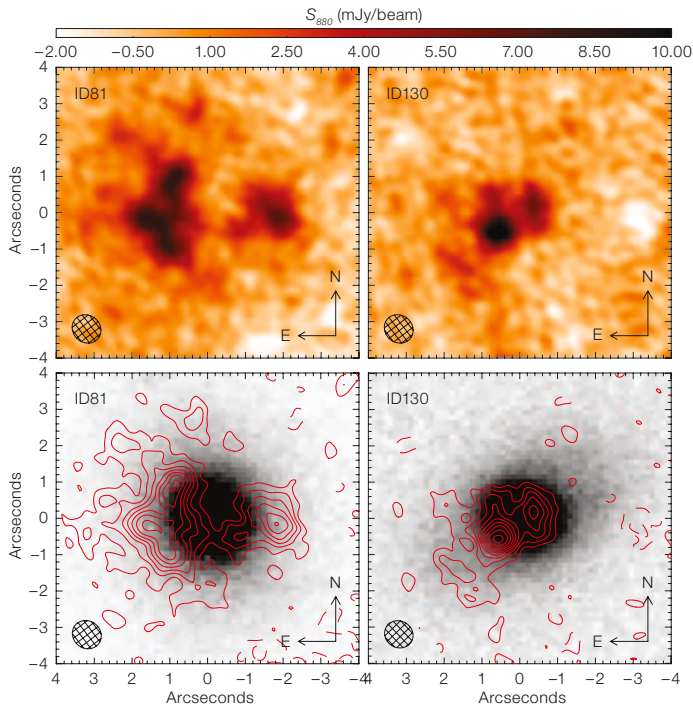


Figure 2. Submillimetre continuum images (upper) of the lens systems ID81 and ID130 from the SMA. The same continuum maps are shown (lower) as contour maps superimposed on Keck *i*-band images. (H-ATLAS team; Negrello et al., 2010).

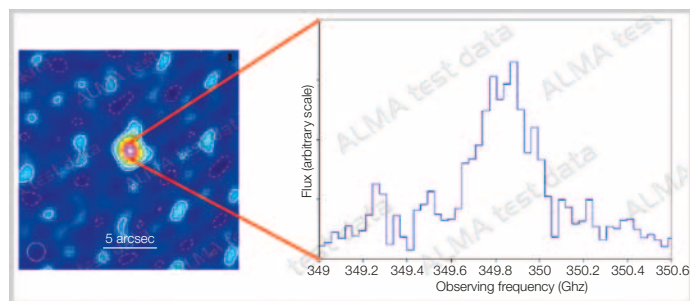


Figure 3. ALMA test data on the [C II] line from BRI 0952 at $z = 4.4$ (ALMA CSV team; the original APEX detection is from Maiolino et al., 2009).

need for a full complement of ALMA Band 5 receivers to explore the key redshift range between eight and ten was especially emphasised.

The wealth of new insights on nearby galaxies that is being gained with Herschel was reviewed at the conference by F. Combes and C. Wilson. Herschel photometry and spectroscopy are starting to allow us to probe the star formation and interstellar medium of nearby galaxies with unprecedented detail. These observations are a necessary milestone on the road to understanding the cosmological evolution of the interstellar medium in its proper context. The synergy with ALMA in this respect would be enhanced by comprehensive measurements of the fine structure far-infrared atomic lines in the nearby Universe to be compared

with future submillimetre studies at high redshift. ALMA high angular resolution observations of these galaxies will allow us to place what we understand of the interstellar medium (ISM) and star formation in our own Galaxy in context. The ALMA test data on NGC 253 have already started to show the great potential in this field (see Figure 1 of Testi et al., 2010).

Star and planet formation in our own Galaxy

Herschel is investing a large amount of time as part of the guaranteed and open time key programmes to investigate the process of star formation by surveying nearby molecular clouds and the Galactic Plane. Ph. Andre, J. di Francesco and S. Molinari reviewed the progress of the

wide-area photometric surveys and illustrated the initial results on the core mass function, the filamentary structure of molecular clouds and the ISM (see Figure 4). The thresholds for the formation of clouds and cores in filaments in the Galactic Plane and in the nearby star-forming regions were discussed, as well as the possible role of magnetic fields and instabilities in the evolution of the filaments. This topic was clearly identified as an area requiring high angular resolution molecular line and polarisation follow-up with ALMA. P. Caselli and C. Ceccarelli reviewed the Herschel results and the ALMA prospects for the study of the chemistry of the molecular gas in the earliest phases of star formation. The choice of the correct tracer to study the earliest phases of star formation was discussed; thanks to the expected sensitivity of ALMA, rare isotopes will be the prime targets when studying the cold and dense inner regions of molecular clouds and prestellar cores.

The formation of massive stars, clusters and their effect on the global evolution of galaxies were discussed in several sessions. The models and observational constraints were reviewed by J. Bally, J. Tan and A. Zavagno. S. Bontemps, M. Pestalozzi and S. Ragan discussed the main results in this field from the Herschel imaging survey of young stellar objects (HOBYS), the Galactic Plane survey (HIGAL) and the earliest phases of star formation (EPOS) projects, highlighting the prospects for early ALMA follow-up at high angular resolution.

The formation of low-mass stars and the role and properties of discs at the earliest stages of collapse were discussed in the context of the initial conditions for the formation of planetary systems (M. Walmsley, A. Maury, A. Stutz). The field of protoplanetary discs, which is being explored with Herschel, will fully benefit from ALMA's sensitivity and high angular resolution. K. Dullemond and S. Guilloteau illustrated our current understanding of the theoretical framework and observational constraints of grain growth in discs and discussed how ALMA will allow the study of the evolution of solids and the formation of planetesimals in discs. ALMA will also study in detail the chemistry of the molecular gas in discs and the

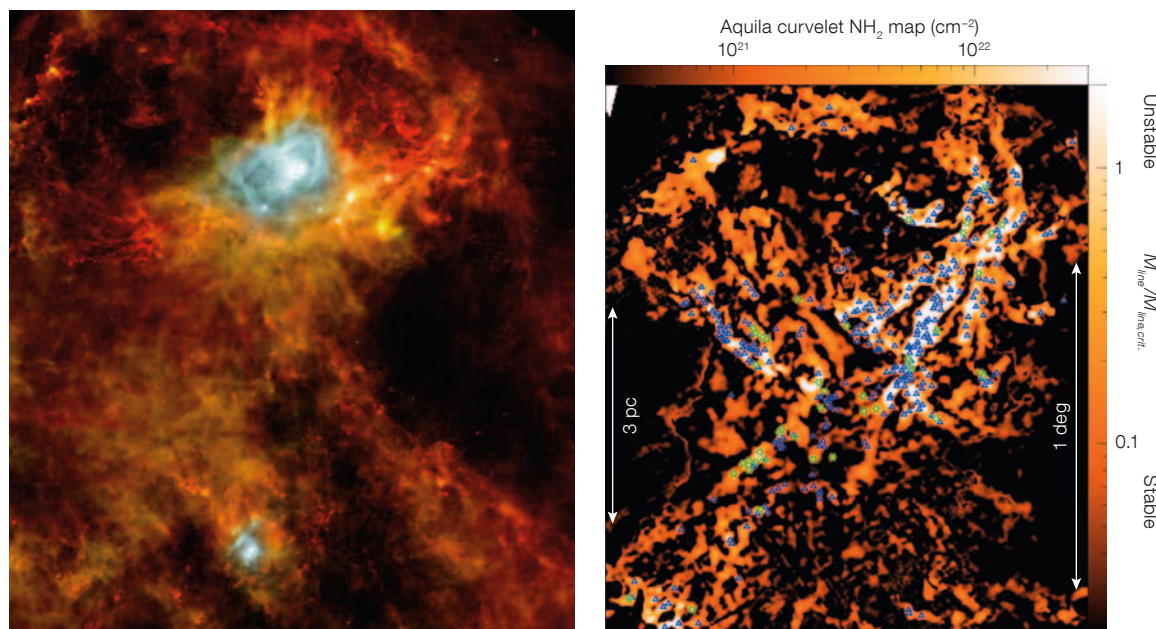


Figure 4. The Aquila molecular cloud complex as observed with Herschel: PACS-SPIRE colour composite on the left, filamentary structure and cores on the right (adapted from André et al., 2010).

formation of complex, possibly pre-biotic molecules, a field that is just starting to be explored with Herschel. Of particular relevance is the study of the gas-to-dust mass ratio and its possible variation across the disc, as well as the chemistry of water (O. Panić, I. Kamp and M. Hogerheide). The scientific opportunities offered by ALMA when fully equipped with Band 5 receivers for the study of water and its isotopes in discs and star-forming regions were emphasised.

Evolved stars

The main Herschel results obtained so far on evolved stars were reviewed by Ch. Waelkens and J. Cernicharo. Spectra of these objects from the Herschel heterodyne instrument HIFI, Photodetector Array Camera and Spectrometer (PACS) and the Spectral and Photometric Imaging REceiver (SPIRE) are revealing a new wealth of information on the chemistry in the envelopes and the yields to the interstellar medium (see Figure 5). The full ALMA array will allow the molecular atmospheres of these stars to be studied at the angular resolution required to spatially resolve the formation of complex molecules as a function of the height above the radio photosphere.

Solar System objects

Most (sub-)millimetre astronomers are very familiar with Solar System bodies, which are normally observed as primary calibrators at these wavelengths. While much is known about these objects, and, in spite of the fact that many have been studied in detail *in situ* by astronomical spacecraft, much is still to be learned. Two main areas were discussed at the meeting: the study of planetary atmospheres and comets in molecular lines; and the study of the continuum emission from minor rocky bodies. R. Moreno, P. Hartog and M. Rengel highlighted the importance of spatially resolved studies of the chemistry in the atmospheres. Water was a recurrent theme in this scientific area and the synergy between Herschel and ALMA was highlighted by all the speakers.

T. Müller and P. Hartogh showed the latest results of the observations of minor bodies of the Solar System with Herschel. Several Trans-Neptunian Objects (TNOs) have been detected at far-infrared and submillimetre wavelengths allowing the development of detailed models of their structure and composition, which require ALMA follow-up. A small set of Main Belt asteroids are being monitored by Herschel and APEX to evaluate them as secondary flux calibrators at far-infrared

and submillimetre wavelengths. The initial results of this programme were also reported at the meeting in a poster by C. Goddi and collaborators (see Figure 6). A common, well-understood and accurately modelled set of calibrators for Herschel and ALMA are needed to meet the stringent ALMA calibration goals and will provide a consistent calibration between the two observatories, a prerequisite for combining data. The primary HIFI and SPIRE calibrators, Neptune and Uranus, will be too large for ALMA at high frequencies and for extended array configurations, thus establishing a good network of common secondary calibrators is very important.

The bright future of far-infrared and submillimetre astrophysics

The highlights of the meeting were the numerous and exciting scientific results that Herschel is providing. There is a strong and very active community working on trying to extract the best possible science from the unique opportunity that Herschel represents. Nevertheless, it was also obvious that this community has ALMA on their radar and several groups had already been preparing preliminary ideas and follow-up observations for ALMA Early Science and beyond. While the time overlap when

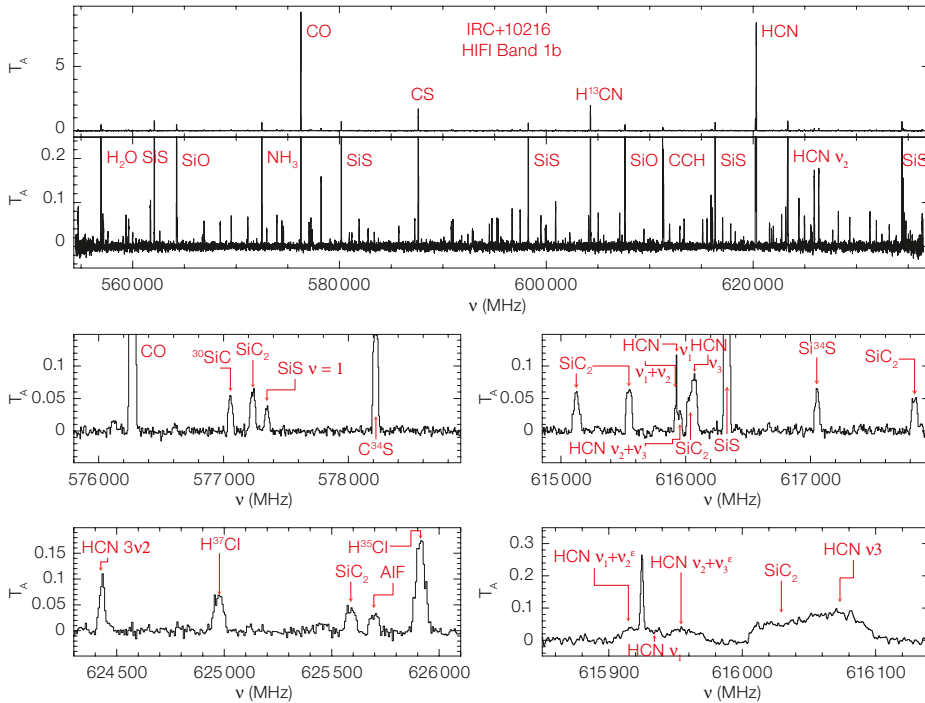


Figure 5. Herschel/HIFI spectrum of IRC+10216 showing the rich chemistry of the wind from this prototypical carbon-rich AGB star (Cernicharo et al., 2010).

scientific results that will come from the combination of the unique capabilities of both ALMA and Herschel.

The organisation of this workshop would have not been possible without the help of the ESO Fellows L. Cortese, A. Maury and O. Panić; in addition E. Bressert, S. Longmore, L. Ricci, F. Trotta and the Garching IT helpdesk supported the sessions and the necessary microphone operations. Special thanks go as usual to C. Stoffer who always steered the practical organisation back to the right path. The workshop was sponsored by ESO and Radionet, which provided travel support to a number of participants.

The presentations and most of the posters are available in electronic form on the conference website¹.

References

André, P. et al. 2010, A&A, 518, L102
 Cernicharo, J. et al. 2010, A&A, 518, L136
 Maiolino, R. et al. 2009, A&A, 500, L1
 Negrello, M. et al. 2010, Science, 330, 800
 Testi, L. et al. 2010, The Messenger, 142, 17

Links

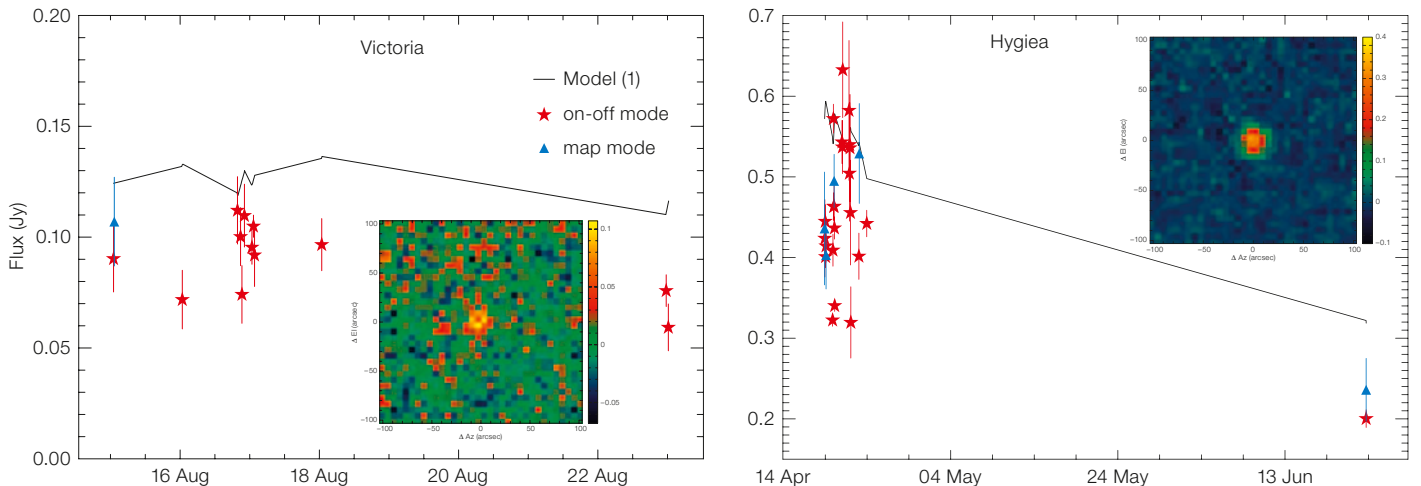
¹ Conference web page: <http://www.eso.org/sci/meetings/2010/almaherschel2010/program.html>

both Herschel and ALMA are operational will be much shorter than originally hoped, it is expected that there will be a period of at least one year in which the two observatories will potentially be available for simultaneous observations. It was emphasised that science cases for potential simultaneous observations should be identified soon, and proposals should be ready for submission by the

coming deadlines in summer 2011. The possibility of disseminating advanced data products in the community was seen as an opportunity for a long-lasting legacy for the Herschel, especially in view of long-term follow-up observations with the full ALMA array and its future upgrades.

The lively discussion at the meeting convinced us that the future of far-infrared and submillimetre astrophysics looks bright and we look forward to the flood of

Figure 6. APEX/LABOCA 870 μ m measurements of the Hygiea and Victoria asteroids with time (Goddì et al., 2011).



Site Surveys for the Extremely Large Telescopes and More: Sharing the Experience and the Data

Marc Sarazin¹

¹ ESO

As the site surveys for the Extremely Large Telescopes are nearing completion, two workshops gathered site testing specialists and atmospheric physicists to discuss the instrumental and data analysis issues. The two workshops are briefly reported.

Comprehensive Characterisation of Astronomical Sites

held at Kislovodsk, Russia,
4–9 October 2010

The meeting¹ was organised by the Sternberg Astronomical Institute (SAI) of Moscow University and the IAU Working Group Site Testing Instruments.

This workshop was the opportunity for all teams currently involved in astronomical site testing to gather and share ideas and experience. The meeting place (see Figure 1), chosen by the Sternberg group, is close to Mt. Shatdzhatmaz, chosen after a three-year site survey to host a 2.5-metre telescope currently being built in Europe. The National Astronomical Observatories of China and the Chinese Center for Antarctic Astronomy are investigating the potential of Antarctica (Dome A) and West China (Tibet) for ground-based national projects. The Indian Institute of Astrophysics is investigating high altitude sites (> 4000 metres) in Ladakh for a national project (NLOT). The site survey for the future Iranian National Observatory's 3.4-metre telescope is coming close to completion with the detailed study of the surface layer turbulence at the two shortlisted summits (Qom and Kashan areas) to determine the optimal height above ground of the telescope.

Discussions on the instrumentation illustrated the impressive evolution that has occurred over the past decade. Precipitable water vapour (PWV) monitoring is now a mature technique with a wide suite of instruments (radiosondes, radio, infrared and GPS ground-based



Figure 1. The participants of the site characterisation workshop in Kislovodsk, Russia grouped in the mountains.

monitors). Monitors of the optical turbulence (measured by the structure constant of the atmospheric refractive index C_n^2) have evolved over the last decade: the differential image motion monitor (DIMM) technique has become a standard worldwide and a number of complementary instruments (Multi Aperture Scintillation Sensor [MASS], SLOpe Detection And Ranging [SLODAR], SCIntillation Detection And Ranging [SCIDAR], SLOpe and scIntillation Detection And Ranging [SLIDAR], LUAr SCIntillometer [LuSCI]) are now available to analyse in detail the turbulence profiles along various sections of the line of sight. More effort is needed however for robotic sky monitoring of cloudiness: currently mostly performed using 1D sensors (visual light meters or infrared sky temperature sensors), while 2D all-sky cameras still rely on visual analysis.

Atmospheric Data from Astronomical Site Testing in Chile

held at Valparaíso, Chile,
1–3 December 2010

The workshop was hosted by Universidad de Valparaíso and jointly sponsored by the TMT Observatory Corporation and ESO².

The Astro-meteorology Group of the Physics Department of the University of Valparaíso has accumulated much technical know-how in the use of global and meso-scale meteorological models. As was demonstrated at a previous workshop (Masciadri, 2008) such tools

can provide accurate forecasts of observing conditions at ground-based observatories, e.g., as a support to queue scheduling in service observing mode. These models need, however, to be checked, calibrated or tuned against real site data before becoming operational. One of the main drivers for this workshop (the participants are seen in Figure 2) was to present and discuss the data collected by the observatories in Chile.

In the domain of site surveys, the US Thirty Meter Telescope (TMT) project has set the standard with the release of its site testing database to the public shortly after the site decision was taken. Obviously other institutions will follow. However data can be shared and sites can be compared worldwide only when much care has been taken to maintain a high quality standard all through the data collection process. A prerequisite is obviously that different instruments measuring the same parameters should agree. Several cross-comparison issues were discussed in detail, including the measurement of the turbulence in the surface layer, of the wavefront coherence time and of the precipitable water vapour.

Among the positive results of the meetings in Russia and Chile, was the decision to re-assert interest and support in the IAU Site Testing Instruments Working Group activity initiated by A. Tokovinin (CTIO)³, in particular adding a special section for listing the available database worldwide, which A. Otárola (TMT) has kindly agreed to organise⁴.

References

Masciadri, E. 2008, *The Messenger*, 134, 53

Links

¹ Workshop web page: <http://site2010.sai.msu.ru/>

² Workshop web page:
<http://www.dfa.uv.cl/sitetestingdata/>

³ IAU Site Testing Instruments Working Group:
<http://www.ctio.noao.edu/science/iauSite/>

⁴ Sharing of site testing data:
<http://project.tmt.org/~aotarola/ST>



Figure 2. The participants at the workshop on site testing atmospheric data in Valparaíso, Chile arrayed by the harbour.

ESO's Hidden Treasures Competition

Olivier Hainaut¹
Oana Sandu¹
Lars Lindberg Christensen¹

¹ ESO

ESO's Hidden Treasures astrophotography competition gave amateur astronomers the opportunity to search ESO's Science Archive for a well-hidden cosmic gem. The competition attracted nearly one hundred entries and the winners were announced in January 2011. Astronomy enthusiast Igor Chekalin from Russia won the first prize — a trip to the Very Large Telescope at Paranal — in this difficult but rewarding challenge.

Pictures can be powerful; and astronomical images even more so: these views of distant cosmic worlds can inspire and help to connect us with the Universe. The images could almost be works of art when particularly intriguing shapes and phenomena are captured and presented in an appropriate way. Astronomical pictures are also an efficient way to pique people's interest in astronomy and science.

Over the past two and a half years ESO has boosted its production of outreach images, both in terms of quantity and quality, so as to become one of the best sources of astronomical images. In achieving this goal, the whole work flow from the initial production process, through to publication and promotion has been optimised and strengthened. The final outputs have been made easier to re-use in other products or channels by our partners.

While the pictures of the Universe that can be seen in ESO's releases are impressive, many hours of skilful work are required to first find datasets that can become useful "public" representations of the Universe, and then to process these into colour images. Along the way significant work goes into the astronomical processing — to assemble the raw greyscale data captured by the telescopes, to correct for the instrument signature, and to process the graphics — and in compressing the image's dynamic range to fit within the limited gamut of today's monitors and printers, enhancing them so as to bring out the details contained in the astronomical data¹.

The ESO Science Archive stores all the data acquired on Paranal, and most of the data obtained on La Silla since the late 1990s. This archive constitutes a goldmine commonly used for science projects (e.g., Haines et al., 2006), and for technical studies (e.g., Patat et al., 2011). But besides their scientific value, the imaging datasets in the archive also have great outreach potential.

ESO has a small team of professional image processors, but for ESO's Hidden Treasures competition, the experts decided to give astronomy and photography enthusiasts the opportunity to show the world what they could do with the data contained in the archive. A simplified interface to the ESO Science Archive was prepared by the Archive Group for this purpose and the goal of the competition seemed at first glance simple: to produce a good outreach image with a dataset from the ESO Science Archive that had not yet been published.

The enthusiasts who responded to the call submitted nearly 100 entries in total — far exceeding initial expectations, given the difficult nature of the challenge. Navigating the Science Archive has a steep learning curve for a new user due to the

inherent complexity of the data. In addition, over the past few years we have systematically scoured the archives for valuable datasets that would allow us to release inspiring images of the Universe and thereby already found most of the available appropriate datasets. This competition was not a challenge for the faint-hearted, requiring both an advanced knowledge of data processing and an artistic eye. Digging through many terabytes of astronomical data, the entrants had to identify a series of frames that would reveal the hidden beauty of a celestial object.

The chance of a great reward for the talented winner was enough to spur on the competitors: the first prize being a trip to the Very Large Telescope, with guided tours and the opportunity to participate in a night's observations. Runners-up prizes included an iPod, books and DVDs. Furthermore, the highest ranked images were to be released for the world to see on www.eso.org as Photo Releases or Pictures of the Week, co-crediting the winners and promoted on ESO's Facebook page, Twitter feed, uploaded on Wikipedia and on ESO's Flickr account².

The jury, composed of outreach and image processing experts and astronomers, evaluated the entries based on the quality of the data processing, the originality of the image and the overall aesthetic feel. As several of the highest ranked images were submitted by the



Figure 1. Astronomy enthusiast Igor Chekalin from Russia, who participated in ESO's Hidden Treasures 2010 astrophotography competition and won the first prize: a trip to the VLT.

same people, the jury decided to make awards to the ten most talented participants, so as to give more people the opportunity to win a prize and to reward their hard work and talent.

The prize winners were:

- First prize, a trip to Paranal and other ESO outreach products: Igor Chekalin (Russia).
- Second prize, an iPod Touch and other ESO outreach products: Sergey Stepanenko (Ukraine).

- Third prize, VLT laser cube model and other ESO outreach products: Andy Strappazzon (Belgium).
- Fourth to tenth prizes, *Eyes on the Skies* book and DVD, and other ESO outreach products: Joseph (Joe) DePasquale (USA); Manuel (Manu) Mejias (Argentina); Alberto Milani (Italy); Joshua (Josh) Barrington (USA); Oleg Maliy (Ukraine); Adam Kiil (United Kingdom); Javier Fuentes (Chile).

The overall winner, Igor Chekalin (seen in Figure 1) from Russia, who won the trip to Paranal says, "It was a great experience and pleasure to work with such amazing data. As an amateur astrophotographer, this was the most difficult processing and post-processing job I have ever done. My participation in the Hidden Treasures competition gave me a range of challenges, from installing new software to studying techniques and even operating systems that I did not know before."

Some of the images submitted by the ten winners are shown. The image of the reflection nebula Messier 78 selected by Igor Chekalin is shown in the *Astronomical News* section, page (p. 46); he also produced the image of the pair of galaxies NGC 3169 and NGC 3166 shown in Figure 2. Figure 3 shows a colour image of the low-mass star-forming region NGC 6729 by Sergey Stepanenko. The winning images can be viewed from the web page announcing the winners³.



Figure 2. (Left) The colour image of the pair of galaxies NGC 3169 and NGC 3166, a field also containing the recent supernova SN 2003cg, obtained with the Wide Field Imager on the MPG/ESO 2.2-metre telescope and processed by Igor Chekalin.

Figure 3. (Right) The low-mass star-forming region NGC 6729 is shown in a VLT FORS1 colour composite of H α and S II exposures, processed by the second-prize winner Sergey Stepanenko.



Reflecting on the usefulness of the Hidden Treasures competition, we can say that it undoubtedly has served to further increase the visibility of ESO and its data. Almost thirty of the submitted images have some potential to be released publicly, and half a dozen were so impressive that they will become ESO Photo Releases over the next few months. It is also interesting that four of the best

of the datasets had already been identified by our team prior to the competition, and were at some stage of processing, showing that the ESO Science Archive has few hidden gems remaining.

References

Haines, C. P. et al. 2006, MNRAS, 371, 55
Patat, F. et al. 2010, A&A, in press, arXiv:1011.6156

Links

¹ This work is carried out using the purpose-built software developed in-house called the ESO/ESA/NASA FITS Liberator, available at: http://www.spacetelescope.org/projects/fits_liberator/.

² To follow ESO's social media accounts access: <http://www.facebook.com/ESO Astronomy> or http://twitter.com/ESO_Observatory

³ The web page of the competition is at: <http://www.eso.org/public/outreach/hidden treasures>

Fellows at ESO

Andrea Ahumada

I have always been fascinated by astronomy. As a young girl, when I watched the first episode of *Cosmos* (by Carl Sagan), I had a dream: to become an astronomer. Now, after almost 30 years, I am writing these lines as an ESO fellow. This achievement was possible because my parents and my oldest sister were pivotal in my career: they believed in me and supported my dreams.

Cordoba (Argentina), where I was born, has a long and proud history in astronomy, so, I had the opportunity to study astronomy at the FaMAF (Facultad de Matematica, Astronomia y Fisica), and finally, under the supervision of Professor J. J. Claria, I obtained my PhD at the National University of Cordoba (Argentina) in 2004. Since then, my main topics of research have been Galactic open clusters and star clusters of the Magellanic Clouds. During my career, as an observational astronomer, I have been able to observe with many different telescopes, and fortunate to go from small (at the Bosque Alegre Observatory, Argentina) to big ones (at Paranal Observatory). I remember the first time that I visited those telescopes, I was fascinated!

I joined ESO in April 2008, and as an Argentinian, I only had to cross the Andes to come to Chile. With functional duties



Andrea Ahumada

at Paranal Observatory, where I work with the world's most powerful telescopes and instruments, I have learnt new technical skills, with the opportunity to observe, in the same night, with different techniques, a large spectrum of astronomical objects, from comets to very distant objects, such as gamma-ray bursts. During the night shifts, I am the support astronomer for Antu's (UT1) instruments. After all this time in Paranal, I still continue to be amazed at how unique it is to spend a night there.

Working at ESO has been very beneficial for my development as a scientist, providing me with important opportunities to advance in my research and to expand my network of scientific collaborations, while continuing with the old ones. ESO

has also given me the opportunity to do outreach. I feel that I am lucky to do what I do for living, so outreach is very important to me, because in this way I can give something back to people.

In two months I will move to Bologna Observatory (Italy) for my fourth year as an ESO fellow. This is a wonderful scientific opportunity for me because I have started working on the BOCCE (Bologna Open Clusters Chemical Evolution) Project. In Bologna there will be new challenges, and I am very happy about having the chance to live in Italy, where my great-grandparents came from.

While I am writing this, my last *turno* at Paranal is coming up soon. I feel strange and a little sad to be leaving. Most of those whom I have met in Santiago and Paranal are really nice people; working here I had the opportunity to make new friends, and also I had the chance to meet Juan Manuel. Memories of the three years that I have spent in this beautiful country will stay for ever in my heart.

Bram Venemans

When I was around 12 years old, I became interested in astronomy for the first time. Amateur astronomers had organised a public viewing of a lunar eclipse, which made a big impression

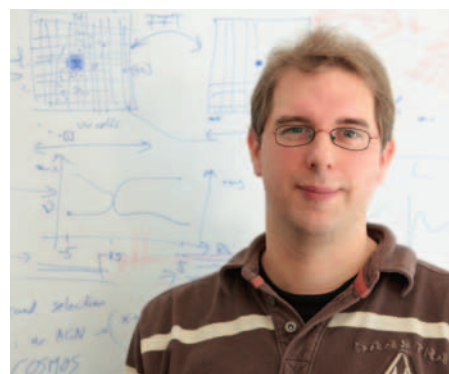
on me. Unfortunately, growing up in the light-polluted city of Amsterdam, often the Moon was the only object visible in the sky at night. I kept my interest in astronomy alive by reading lots of books, with topics ranging from a detailed description of the Solar System to the theory of the Big Bang. When I went to university, I had no doubt what I wanted to study, and in 1995 I started my undergraduate studies in astronomy at the University of Leiden. During the first few years of study I somehow was very certain I would finish my degree and start a career outside the academic world. This assumption turned out to be completely wrong ...

My ideas for the future radically changed when I was doing my Master's project at the Leiden Observatory. The research consisted of reducing multicolour imaging data. Shortly after choosing my project, my supervisor asked me whether I wanted to go for an observing run with the NTT on La Silla. Although scientifically the observing run was not a huge success (lots of clouds!), I thoroughly enjoyed the experience. Exploring various ways to get the best results and to make new discoveries fascinated me and by the time I finished my Master's thesis, I was determined to pursue a career in astronomy.

After finishing my degree in 1999 at the Leiden Observatory, I went to the University of Cambridge for a one-year Master's in astronomy working at a more numerical project. In 2000 I returned to Leiden to start my PhD project. The aim was to study the environment of powerful radio galaxies at redshifts between two and five by searching for overdensities of Lyman- α emission-line galaxies. My project got off to a flying start, as three months into my PhD our group received confirmation that our VLT large programme had been accepted. This meant that I had the opportunity to visit Paranal several times to obtain all the data I needed for my thesis. The observations went really well, giving me more than enough results to write several papers and to fill my thesis. After defending my PhD thesis in 2005, I went back to Cambridge, this time to work as a research associate at the Institute of Astronomy. My work there focused on studying galaxies and quasars at the highest redshifts ($z > 6$), using, amongst others, data from large public surveys like SDSS and UKIDSS.

As nearly all my research made use of large amounts of ESO data, applying for an ESO Fellowship was the obvious next step for me. Currently, I am in my third year as an ESO Fellow working in

Garching. One of the great things about being at ESO is the possibility of attending many of the large number of interesting workshops and talks that are organised in the area each year. Besides continuing to study very high redshift objects, working at ESO also gives me the opportunity to be involved in the E-ELT project. I find it very exciting to be able to contribute to a project with such importance for the future of European astronomy. As an undergraduate student on my first observing trip I was thoroughly impressed by the size of the mirror of the NTT, so I can hardly imagine how it will be to stand next to a 42-metre telescope in (hopefully) a few years from now!



Bram Venemans

Personnel Movements

Arrivals (1 January–31 March 2011)

Europe	
Drouart, Guillaume (F)	Student
Lakicevic, Masa (SRB)	Student
Riesel, Jürgen (D)	Administrative Clerk
Sartoris, Barbara (I)	Student
Schmid, Erich (D)	Software Engineer
Westmoquette, Mark (GB)	Fellow
Chile	
Barria, Daniela (RCH)	Student
Gorgeot, Florian (F)	Student
Jager, Henderikus (NL)	System Engineer
Jones, David (GB)	Fellow
Lieder, Stefan (D)	Student
Pozzobon, Matteo (I)	Senior Mechanical Engineer
Rioseco, Diego (RCH)	Legal Advisor

Departures (1 January–31 March 2011)

Europe	
Dremel, Günther (D)	Administrative Clerk
Feng, Lu (VR)	Student
Jalali, Behrang (IR)	Student
Müller, André (D)	Student
Nilsson, Kim (S)	Astronomer
Völk, Elisabeth (D)	Secretary/Assistant
Chile	
Andreoni, Gaetano (I)	IT Quality Assurance Manager
Emmerich, Alejandra (RCH)	Secretary/Assistant
Gallegos, Leonardo (RCH)	Telescope Instruments Operator
Gutierrez, Flavio (RCH)	System Administrator
Lassalle, Jacques (F)	Safety Engineer
Lira, Luis Felipe (RCH)	Legal Advisor
Planesas, Pere (E)	Test Scientist



ESO

European Organisation
for Astronomical
Research in the
Southern Hemisphere



ESO Studentship Programme

The European Southern Observatory research student programme aims to provide opportunities to enhance the PhD programmes of ESO member-state universities. Its goal is to bring young scientists into close contact with the activities and people at one of the world's foremost observatories. For more information about ESO's astronomical research activities please consult <http://www.eso.org/science/>.

The ESO studentship programme is shared between the ESO Headquarters in Garching (Germany) and the ESO offices in Santiago (Chile). These positions are open to students enrolled in a PhD programme in astronomy or related fields. In addition, ESO will provide up to two studentship positions per year in Santiago for students enrolled in South American universities.

Students in the programme work on their doctoral project under the formal supervision of their home university. They come to either Garching or Santiago for a stay of normally between one and two years to conduct part of their studies under the co-supervision of an ESO staff astronomer. Candidates and their home institute supervisors should agree on a research project together with the ESO local supervisor. A list of potential ESO supervisors and their research interests can be found at <http://www.eso.org/sci/activities/personnel.html>. A list of current PhD projects offered by ESO staff is available at <http://www.eso.org/sci/activities/thesis-topics/>. It is highly recommended that the applicants start their PhD studies at their home institute before continuing their PhD work and developing their research projects at ESO.

ESO Chile students will have an opportunity to visit the observatories and to get involved in small projects aimed at giving insights into the observatory operations.

In Garching students may attend, if desired, and benefit from the series of lectures given to the PhD students enrolled in the IMPRS (International Max-Planck Research School on Astrophysics) PhD programme. Students who are already enrolled in a PhD programme in the Munich area (e.g., the IMPRS or at a Munich University) and wish to apply for an ESO studentship in Garching, should provide compelling justification for their application.

The Outline of the Terms of Service for Students (<http://www.eso.org/public/employment/student.html>) provides some more details on employment conditions and benefits.

Please attach to your application the following documents:

- a Curriculum Vitae (including a list of publications, if any), with a copy of the transcript of university certificate(s)/diploma(s);
- a summary of the Masters thesis project (if applicable) and ongoing projects, indicating the title and the supervisor (maximum half a page), as well as an outline of the PhD project, highlighting the advantages of coming to ESO (recommended 1 page, max. 2);
- two letters of reference, one from the home institute supervisor/advisor and one from the ESO local supervisor;
- a letter from the home institution that: i) guarantees the financial support for the remaining PhD period after the termination of the ESO studentship; and ii) indicates whether the requirements to obtain the PhD degree at the home institute are already fulfilled.

All documents should be submitted in English (but no translation is required for the certificates and diplomas).

Review of the received material, including the recommendation letters, will start on 15 June 2011. Applications arriving after this deadline will be considered until all the positions are filled. Incomplete applications will not be considered. All reference letters must be sent electronically to vacancy@eso.org.

Candidates will be notified of the results of the selection process in July 2011. Studentships typically begin between August and December of the year in which they are awarded. In well-justified cases, starting dates in the year following the application can be negotiated.

For further information please contact Christina Stoffer (cstoffer@eso.org).

Although recruitment preference will be given to nationals of ESO Member States (Austria, Belgium, Brazil, the Czech Republic, Denmark, Finland, France, Germany, Italy, the Netherlands, Portugal, Spain, Sweden, Switzerland and United Kingdom) no nationality is in principle excluded.

The post is open equally to suitably qualified male and female applicants.



Announcement of the ESO Workshop

Multiwavelength Views of the ISM in High-redshift Galaxies

27–30 June 2011, ESO Vitacura, Santiago, Chile



The study of the interstellar matter (ISM) is no longer limited to the nearby Universe. Major progress in observational capabilities from the optical to the radio have allowed the first studies out to the highest redshift galaxies known, while theoretical modelling has proved essential to interpret the different environments in the early Universe. The imminent availability of the Atacama Large Millimeter/submillimeter Array (ALMA) will revolutionise this field, thanks to its exquisite sensitivity and spatial resolution. At the same time, the Herschel Space

Observatory is observing nearby galaxies in atomic and molecular lines, which will be redshifted down to ALMA frequencies at high redshift. This workshop aims to provide an overview of this field at this crucial moment, and foster collaboration between scientists working at low and high redshifts and in different wavelength regimes.

Topics to be covered include:

- Theoretical predictions of the physical properties of gas in high- z galaxies;
- Outflows and inflows at high redshifts;
- Effects of star formation and active galactic nuclei activity;
- Census of molecular gas masses and excitation at high- z ;
- Interplay between mass, metallicity and star formation rate in galaxies;
- ALMA and far-infrared line emission in high- z studies;
- Synergy between ALMA, the Expanded Very Large Array (EVLA) and the future Extremely Large Telescopes (ELTs).

The meeting will be held at the ESO and Joint ALMA Office (JAO) campus

in Santiago, and will be limited to 100 participants. At the end of the workshop, interested participants will be given the opportunity to fly to San Pedro de Atacama and enjoy a guided tour of the ALMA and APEX Chajnantor site.

The Scientific Organising Committee consists of: Andrew Baker (Rutgers University), Chris Carilli (NRAO), Carlos De Breuck (ESO, co-chair), Leopoldo Infante (PUC), Rob Ivison (UK ATC and IfA, Edinburgh), Roberto Maiolino (INAF, Roma), Alison Peck (JAO), Dominik Riechers (Caltech), Linda Tacconi (MPE), Jeff Wagg (ESO, co-chair), Fabian Walter (MPIA), Tommy Wiklind (JAO) and Min Yun (University of Massachusetts).

The deadline for registration is 8 April 2011.

Further information can be found at <http://www.eso.org/sci/meetings/2011/gas2011.html>.

Announcement of the ESO/MPE/MPA/Excellence Cluster/USM Joint Astronomy Workshop

Formation and Early Evolution of Very Low Mass Stars and Brown Dwarfs

11–14 October 2011, Garching, Germany



The wide-area surveys in nearby molecular clouds that are currently being conducted with Herschel in the far-infrared and APEX in the submillimetre will soon be complemented and extended with observations by SCUBA2 at the James Clerk Maxwell Telescope. Together they will add to the enormous amount of data that will be collected by ground-based wide-area surveys with telescopes like VISTA and the VST, and those already available, most notably those carried out with the Spitzer Space Telescope. These surveys will offer complete samples of objects in nearby star-forming regions, from cores to protostars and young stars, with unprecedented sensitivity. The surveys will probe the physical conditions at

the sites where the lowest mass isolated objects form.

Together, these facilities will provide a multiwavelength view of the origin of the full stellar and sub-stellar mass function. In parallel, detailed studies of individual objects and small samples are already underway with new and existing VLT/I instruments and with current millimetre interferometers, and will shortly begin with ALMA. At the same time, increasingly realistic computations of the collapse and fragmentation processes, the early evolution of the resulting objects, their inner structure, and the dynamics and chemistry of their atmospheres and surrounding medium are

producing a sound framework for the interpretation of observations.

This workshop will review the current progress in our understanding of low-mass star and brown dwarf (BD) formation in nearby molecular clouds, and will bring together observers and theoreticians to promote stimulating discussion.

The main science topics include:

- Properties of nearby molecular clouds and cores forming stars and BDs;
- Theory and observations of collapse of protostars and protobinaries;
- Early evolutionary stages of very low mass stars and BDs: disc-mediated accretion and ejection;

- The initial mass functions of stars and BDs and their possible relation with the molecular cloud clump mass function;
- The processes that regulate star formation in giant molecular clouds from theoretical and observational aspects;
- Surveys for young, very low mass stars and BDs.

The workshop is jointly organised by ESO, the Max-Planck Institute for Extraterrestrial Physics, the Excellence Cluster Origin and Structure of the Universe and the University Observatory Munich. The meeting will take place at ESO Garching. There will be five main sessions, each introduced by an invited observational review and a theoretical

review. The sessions will be further complemented by contributed talks and open discussions. Ample space will be provided for posters. Proposals for both contributed talks and posters are invited. Owing to the capacity of the local facilities, the number of participants will be limited to around 120. Financial support will be available for a small number of participants, mainly for students and young researchers.

The registration deadline is 30 June 2011.

Further details are available at <http://www.eso.org/sci/meetings/2011/vlms2011.html>.

Announcement of the Workshop

Feeding the Giants: ELTs in the Era of Surveys

29 August–2 September 2011, Hotel Continental Terme, Ischia, Italy

Over the next decade, by the time of first light of the Extremely Large Telescopes (ELTs), an incredible wealth of data will have become available through many new survey facilities. Astronomy will enter an era of surveys. At the same time, the ELTs will open up a new parameter space of unprecedented sensitivity and spatial resolution. This workshop is aimed at exploring the synergies between these two approaches. It will review ongoing and forthcoming survey projects and explore the developments that these will bring to a wide range of science areas, including exoplanets, star formation, stellar populations, galaxy formation/evolution and cosmology.

The workshop will address two broad questions:

- Along with surveys conducted by current and forthcoming observatories, how will the upcoming dedicated survey facilities (such as, to name just a few, Kepler, Gaia, the Large Synoptic Survey Telescope [LSST], the Dark Energy Survey [DES], the VLT Survey Telescope [VST] and the VLT Infrared

Survey Telescope for Astronomy [VISTA], the Panoramic Survey Telescope & Rapid Response System [Pan-STARRS], the Wide-Field Infrared Survey Telescope [WFIRST], SCUBA-2, WISE, Euclid, Plato, the Square Kilometer Array [SKA] and its pathfinders, etc.) profit from follow-up by the ELTs?

- To what extent do the three ELT projects (Giant Magellan Telescope [GMT], Thirty Meter Telescope [TMT] and European Extremely Large Telescope [E-ELT]) require surveys to prepare scientific breakthroughs?

The goal is to bring together the survey and ELT communities and to define first strategies to maximise the success of both aspects.

The workshop is organised jointly by ESO (Markus Kissler-Patig and Jochen Liske), OPTICON and the INAF–Observatory of Rome (Annalisa Calamida and Isobel Hook) and the University of Oxford (Aprajita Verma). The other members of the Scientific Organising Committee are: Daniel Eisenstein (University of Arizona),

Josh Frieman (Fermilab), Gerry Gilmore (University of Cambridge), Anne-Marie Lagrange (Grenoble Observatory), Pat McCarthy (GMT Observatory), Timo Prusti (ESA), Hans-Walter Rix (MPIA), Elaine Sadler (University of Sydney), David Silva (NOAO/GSMT), Luc Simard (CNRC/TMT) and Will Sutherland (University of London). The Local Organising Committee is composed of Annalisa Calamida, Vanessa Ferraro-Wood, Giuliana Giobbi and Aprajita Verma.

The workshop will be held at the Hotel Continental Terme, on the Island of Ischia near Naples. Further details can be found at <http://www.eso.org/sci/meetings/2011/feedgiant.html>.

Registration will open at the end of March 2011.



Annual Index 2010 (Nos. 139–142)

Subject Index

The Organisation

Enabling Virtual Access to Latin-American Southern Observatories; Filippi, G.; 142, 2

Telescopes and Instrumentation

The Visible and Infrared Survey Telescope for Astronomy (VISTA): Looking Back at Commissioning; Emerson, J.; Sutherland, W.; 139, 2
VISTA Science Verification — The Galactic and Extragalactic Mini-surveys; Arnaboldi, M.; Petr-Gotzens, M.; Rejkuba, M.; Neeser, M.; Szeifert, T.; Ivanov, V. D.; Hummel, W.; Hilker, M.; Neumayer, N.; Möller, P.; Nilsson, K.; Venemans, B.; Hatziminaoglou, E.; Hussain, G.; Stanke, T.; Teixeira, P.; Ramsay, S.; Retzlaff, J.; Slijkhuis, R.; Comerón, F.; Melnick, J.; Romaniello, M.; Emerson, J.; Sutherland, W.; Irwin, M.; Lewis, J.; Hodgkin, S.; Gonzales-Solares, E.; 139, 6

Laser Development for Sodium Laser Guide Stars at ESO; Bonaccini Calia, D.; Feng, Y.; Hackenberg, W.; Holzjöhner, R.; Taylor, L.; Lewis, S.; 139, 12

A New Facility Receiver on APEX: The Submillimetre APEX Bolometer Camera, SABOCA; Siringo, G.; Kreysa, E.; De Breuck, C.; Kovacs, A.; Lundgren, A.; Schuller, F.; Stanke, T.; Weiss, A.; Guesten, R.; Jethava, N.; May, T.; Menten, K. M.; Meyer, H.-G.; Starkloff, M.; Zakosarenko, V.; 139, 20

Recent Progress on the KMOS Multi-object Integral Field Spectrometer; Sharples, R.; Bender, R.; Agudo Berbel, A.; Bennett, R.; Bezawada, N.; Bouché, N.; Bramall, D.; Casali, M.; Cirasuolo, M.; Clark, P.; Cliffe, M.; Davies, R.; Davies, R.; Drory, N.; Dubbeldam, M.; Fairley, A.; Finger, G.; Genzel, R.; Haefner, R.; Hess, A.; Jeffers, P.; Lewis, I.; Montgomery, D.; Murray, J.; Muschelk, B.; Förster Schreiber, N.; Pirard, J.; Ramsey-Howat, S.; Rees, P.; Richter, J.; Robertson, D.; Robson, I.; Rolt, S.; Saglia, R.; Schlichter, J.; Tecza, M.; Todd, S.; Wegner, M.; Wierorrek, E.; 139, 24

Twenty Years of FORS Science Operations on the VLT; Rupprecht, G.; Böhnhardt, H.; Moehler, S.; Möller, P.; Saviane, I.; Ziegler, B.; 140, 2

A New Lenslet Array for the NAOCO Laser Guide Star Wavefront Sensor; Kasper, M.; Zins, G.; Feautrier, P.; O'Neal, J.; Michaud, L.; Rabou, P.; Stadler, E.; Charton, J.; Cumani, C.; Delboulbe, A.; Geimer, C.; Gillet, G.; Girard, J.; Huerta, N.; Kern, P.; Lizon, J.-L.; Lucuix, C.; Mouillet, D.; Moulin, T.; Rochat, S.; Sönke, C.; 140, 8

The High Order Test Bench: Evaluating High Contrast Imaging Concepts for SPHERE and EPICS; Martinez, P.; Aller-Carpentier, E.; Kasper, M.; 140, 10

A New Coronagraph for NAOS–CONICA — the Apodising Phase Plate; Kenworthy, M.; Quanz, S.; Meyer, M.; Kasper, M.; Girard, J.; Lenzen, R.; Codona, J.; Hinz, P.; 141, 2

On the Difference between Seeing and Image Quality: When the Turbulence Outer Scale Enters the Game; Martinez, P.; Kolb, J.; Sarazin, M.; Tokovinin, A.; 141, 5

Balloons over the La Silla Paranal Observatory; Kerber, F.; Querel, R.; Hanuschik, R.; Chacón, A.; Sarazin, M.; on behalf of the project team; 141, 9

On the Instrumental Polarisation of NAOS–CONICA; Witzel, G.; Eckart, A.; Lenzen, R.; Straubmeier, C.; 142, 5

Upgrading VIMOS; Hammersley, P.; Christensen, L.; Dekker, H.; Izzo, C.; Selman, F.; Bristow, P.; Bourget, P.; Castillo, R.; Downing, M.; Haddad, N.; Hilker, M.; Lizon, J.-L.; Lucuix, C.; Mainieri, V.; Mieske, S.; Reiner, C.; Rejkuba, M.; Rojas, C.; Smette, A.; Urrutia del Rio, J.; Valenzuela, J.; Wolff, B.; 142, 8

Progress on the VLT Adaptive Optics Facility; Arsenaault, R.; Madec, P.-Y.; Paufigue, J.; Ströbele, S.; Pirard, J.-F.; Vernet, É.; Hackenberg, W.; Hubin, N.; Jochum, L.; Kuntschner, H.; Glindemann, A.; Amico, P.; Lelouarn, M.; Kolb, J.; Tordo, S.; Donaldson, R.; Sönke, C.; Bonaccini Calia, D.; Conzelmann, R.; Delabre, B.; Kiekbusch, M.; Duhoux, P.; Guidolin, I.; Quattri, M.; Guzman, R.; Buzzoni, B.; Comin, M.; Dupuy, C.; Quentin, J.; Lizon, J.-L.; Silber, A.; Jolly, P.; Manescau, A.; Hammersley, P.; Reyes, J.; Jost, A.; Duchateau, M.; Heinz, V.; Bechet, C.; Stuik, R.; 142, 12

ALMA Status and Progress towards Early Science; Testi, L.; Hills, R.; Laing, R.; Stanghellini, S.; Wild, W.; 142, 17

Synopses of E-ELT Phase A and Instrument Concept Studies

An Introduction to the E-ELT Instrumentation and Post-focal Adaptive Optics Module Studies; D'Odorico, S.; Ramsay, S.; Hubin, N.; Gonzalez, J. C.; Zerbi, F. M.; 140, 17

ATLAS: An Advanced Tomographic Laser-assisted Adaptive Optics System; Fusco, T.; 140, 18

CODEX: An Ultra-stable High Resolution Spectrograph for the E-ELT; Pasquini, L.; Cristiani, S.; Garcia-Lopez, R.; Haehnelt, M.; Mayor, M.; 140, 20

EAGLE: An Adaptive Optics Fed, Multiple Integral Field Unit, Near-infrared Spectrograph; Morris, S.; Cuby, J.-G.; 140, 22

EPICS: An Exoplanet Imaging Camera and Spectrograph for the E-ELT; Kasper, M.; Beuzit, J.-L.; 140, 24

HARMONI: A Single Field, Visible and Near-infrared Integral Field Spectrograph for the E-ELT; Thatte, N.; 140, 26

MAORY: A Multi-conjugate Adaptive Optics Relay for the E-ELT; Diolaiti, E.; 140, 28

METIS: A Mid-infrared E-ELT Imager and Spectrograph; Brandl, B.; Blommaert, J.; Glasse, A.; Lenzen, R.; Pantin, E.; 140, 30

MICADO: The Multi-adaptive Optics Imaging Camera for Deep Observations; Davies, R.; Genzel, R.; 140, 32

OPTIMOS–DIORAMAS: A Wide-field Imaging and Multi-slit Spectrograph for the E-ELT; Le Fèvre, O.; Hill, L.; Le Mignant, D.; Maccagni, D.; Tresse, L.; Paltani, S.; 140, 34

OPTIMOS–EVE: A Fibre-fed Optical–Near-infrared Multi-object Spectrograph for the E-ELT; Hammer, F.; Kaper, L.; Dalton, G.; 140, 36

SIMPLE: A High Resolution Near-infrared Spectrograph for the E-ELT; Origlia, L.; Oliva, E.; Maiolino, R.; 140, 38

Astronomical Science

A Slitless Spectroscopic Survey for H α -emitting Stars in the Magellanic Clouds; Martayan, C.; Baade, D.; Fabregat, J.; 139, 29

CRIFES–POP — A Library of High Resolution Spectra in the Near-infrared; Lebzelter, T.; Seifahrt, A.; Ramsay, S.; Almeida, P.; Bagnulo, S.; Dall, T.; Hartman, H.; Hussain, G.; Käufel, H.U.; Nieva, M.-F.; Przybilla, N.; Seemann, U.; Smette, A.; Uttenthaler, S.; Wahlgren, G.; Wolff, B.; 139, 33

SINFONI on the Nucleus of Centaurus A; Neumayer, N.; Cappellari, M.; van der Werf, P.; Reunanen, J.; Rix, H.-W.; de Zeeuw, T.; Davies, R.; 139, 36

The Properties of Star-forming Regions within a Galaxy at Redshift 2; Swinbank, M.; Edge, A.; Richard, J.; Smail, I.; De Breuck, C.; Lundgren, A.; Siringo, G.; Weiss, A.; Harris, A.; Baker, A.; Longmore, S.; Ivison, R.; 139, 42

The CRIFES Search for Planets at the Bottom of the Main Sequence; Bean, J.; Seifahrt, A.; Hartman, H.; Nilsson, H.; Wiedemann, G.; Reiners, A.; Dreizler, S.; Henry, T.; 140, 41

Spectropolarimetry of Wolf–Rayet Stars in the Magellanic Clouds: Constraining the Progenitors of Gamma-ray Bursts; Vink, J.; 140, 46

ESO–GOODS: Closing the Book, Opening New Chapters; Rosati, P.; The ESO–GOODS Team; 140, 50

The Outer Frontiers of the Solar System: Trans-Neptunian Objects and Centaurs; Barucci, M. A.; Alvarez-Candal, A.; Belskaya, I.; de Bergh, C.; DeMeo, F.; Dotto, E.; Fornasier, S.; Merlin, F.; Perna, D.; 141, 15

The APEX Telescope Large Area Survey of the Galaxy (ATLASGAL); Schuller, F.; Beuther, H.; Bontemps, S.; Bronfman, L.; Carlhoff, P.; Cesaroni, R.; Contreras, Y.; Csengeri, T.; Deharveng, L.; Garay, G.; Henning, T.; Herpin, F.; Immer, K.; Lefloch, B.; Linz, H.; Mardones, D.; Menten, K.; Minier, V.; Molinari, S.; Motte, F.; Nguyen Luong, Q.; Nyman, L.-Å.; Rathborne, J.; Reveret, V.; Risacher, C.; Russeil, D.; Schilke, P.; Schneider, N.; Tackenberg, J.; Testi, L.; Troost, T.; Vasyunina, T.; Walmsley, M.; Wienen, M.; Wyrowski, F.; Zavagno, A.; 141, 20

VISTA Variables in the Via Láctea (VVV): Current Status and First Results; Saito, R.; Hempel, M.; Alonso-García, J.; Toledo, I.; Borissova, J.; González, O.; Beamin, J. C.; Minniti, D.; Lucas, P.; Emerson, J.; Ahumada, A.; Aigrain, S.; Alonso, M. V.; Amôres, E.; Angeloni, R.; Arias, J.; Bandyopadhyay, R.; Barbá, R.; Barbay, B.; Baume, G.; Bedin, L.; Bica, E.; Bronfman, L.; Carraro, G.; Catelan, M.; Clariá, J.; Contreras, C.; Cross, N.; Davis, C.; de Grijs, R.; Dékány, I.; Drew, J.; Fariña, C.; Feinstein, C.; Fernández Lajús, E.; Folkes, S.; Gamen, R.; Geisler, D.; Gieren, W.; Goldman, B.; Gosling, A.; Gunthardt, G.; Gurovich, S.; Hambly, N.; Hanson, M.; Hoare, M.; Irwin, M.; Ivanov, V.; Jordán, A.; Kerins, E.; Kinemuchi, K.; Kurtev, R.; Longmore, A.; López-Corredoira, M.; Maccarone, T.; Martín, E.; Masetti, N.; Mennickent, R.; Merlo, D.; Messineo, M.; Mirabel, F.; Monaco, L.; Moni Bidin, C.; Morelli, L.; Padilla, N.; Palma, T.; Parisi, M. C.; Parker, Q.; Pavani, D.; Pietrukowicz, P.; Pietrzynski, G.; Pignata, G.; Rejkuba, M.; Rojas, A.; Roman-Lopes, A.; Ruiz, M. T.; Sale, S.; Saviane, I.; Schreiber, M.; Schröder, A.; Sharma, S.; Smith, M.; Sodrú Jr., L.; Soto, M.; Stephens, A.; Tamura, M.; Tappert, C.; Thompson, M.; Valenti, E.; Vanzi, L.; Weidmann, W.; Zoccali, M.; 141, 24

- A Wide-angle VIMOS Survey of the Sagittarius Dwarf Spheroidal Galaxy; Giuffrida, G.; Sbordone, L.; Zaggia, S.; Marconi, G.; Bonifacio, P.; Izzo, C.; Szeifert, T.; Buonanno, R.; 141, 29
- Studying the Properties of Early Galaxies with the ESO Remote Galaxy Survey; Bremer, M.; Lehnert, M.; Douglas, L.; Stanway, E.; Davies, L.; Clowe, D.; Milvang-Jensen, B.; Birkinshaw, M.; 141, 32
- Precise Modelling of Telluric Features in Astronomical Spectra; Seifahrt, A.; Käufel, H. U.; Zängl, G.; Bean, J.; Richter, M.; Siebenmorgen, R.; 142, 21
- Astronomy Meets Biology: EFOSC2 and the Chirality of Life; Sterzik, M.; Bagnulo, S.; Azua, A.; Salinas, F.; Alfaro, J.; Vicuna, R.; 142, 25
- Observations of Multiple Stellar Populations in Globular Clusters with FLAMES at the VLT; Gratton, R.; Carretta, E.; Bragaglia, A.; Lucatello, S.; D'Orazi, V.; 142, 28
- Dissecting the Galactic Super Star Cluster Westerlund 1 — A Laboratory for Stellar Evolution; Clark, S.; Negueruela, I.; Ritchie, B.; Crowther, P.; Dougherty, S.; 142, 31
- AMAZE and LSD: Metallicity and Dynamical Evolution of Galaxies in the Early Universe; Maiolino, R.; Mannucci, F.; Cresci, G.; Gnerucci, A.; Troncoso, P.; Marconi, A.; Calura, F.; Cimatti, A.; Cocchia, F.; Fontana, A.; Granato, G.; Grazian, A.; Matteucci, F.; Nagao, T.; Pentericci, L.; Pipino, A.; Pozzetti, L.; Risaliti, G.; Silva, L.; 142, 36
- Astronomical News**
- Report on the Joint ESO/MPE/MPA/LMU Workshop "From Circumstellar Disks to Planetary Systems"; Testi, L.; van Dishoeck, E.; 139, 47
- Report on the CAUP and ESO Workshop "Towards other Earths: Perspectives and Limitations in the ELT Era"; Santos, N.; Melo, C.; Pasquini, L.; Glindeman, A.; 139, 49
- Report on the ESO Workshop "Galaxy Clusters in the Early Universe"; Lidman, C.; West, M.; 139, 51
- ALMA Achieves Closure Phase with Three Antennas on Chajnantor; Testi, L.; 139, 52
- Report on the Workshop "Data Needs for ALMA, From Data Cubes to Science: Ancillary Data and Advanced Tools for ALMA"; Testi, L.; Schilke, P.; Brogan, C.; 139, 53
- The Messenger* on the Web; Erdmann, C.; 139, 55
- New Staff at ESO: Daniel Bramich, Elizabeth Humphreys; 139, 56
- Fellows at ESO: Thomas Bensby, Paula Stella Teixeira; 139, 58
- Announcement of the ESO Workshop "Spiral Structure in the Milky Way: Confronting Observations and Theory"; 139, 59
- ESO Studentship Programme; 139, 60
- Announcement of the Workshop "Science with ALMA Band 5 (163–211 GHz)"; 139, 61
- Announcement of the Workshop "HTRA-IV: Era of Extremely Large Telescopes"; 139, 62
- Beyond 2009: ESO at the Closing Ceremony of the International Year of Astronomy; Mignone, C.; Russo, P.; Christensen, L. L.; 139, 62
- In Memoriam Karin Horn-Hansen; de Zeeuw, T.; 139, 64
- In Memoriam Nelson Montano; Tamai, R.; 139, 65
- Personnel Movements; 139, 65
- Report on the ESO Workshop "The Origin and Fate of the Sun: Evolution of Solar-mass Stars Observed with High Angular Resolution"; Wittkowski, M.; Testi, L.; 140, 53
- Report on the ESO/ESA Workshop "JWST and the ELTs: An Ideal Combination"; Kissler-Patig, M.; McCaughrean, M.; 140, 56
- The ESO Solidarity Group in Support of the Earthquake Victims; The ESO Solidarity Group; 140, 60
- ESO Participates in Germany's Girls' Day Activities; Pierce-Price, D.; 140, 60
- New Staff at ESO: Julien Girard, Willem-Jan de Wit; 140, 61
- Fellows at ESO: Nadine Neumayer, Irina Yegorova; 140, 63
- ESO Fellowship Programme 2010/2011; 140, 65
- Announcement of the ESO Workshop on "The Impact of Herschel Surveys on ALMA Early Science"; 140, 66
- Personnel Movements; 140, 66
- Report on the ESO Workshop "Central Massive Objects: The Stellar Nuclei – Black Hole Connection"; Neumayer, N.; Emsellem, E.; 141, 37
- The 2010 SPIE Symposium on Astronomical Telescopes and Instrumentation; Casali, M.; 141, 40
- Report on the ESO Workshop "Science with ALMA Band 5"; Laing, R.; Maiolino, R.; Rykaczewski, H.; Testi, L.; 141, 41
- Solargraphs of ESO; Fosbury, R.; Trygg, T.; 141, 43
- The Experience of Two High School Students Doing Astronomical Research at ESO; Sartori, L.; Pelloni, C.; 141, 46
- ESO Astronomers Emeriti — Sandro D'Odorico and Alan Moorwood; Primas, F.; Casali, M.; Walsh, J.; 141, 50
- New Staff at ESO: Adrian Russell, Elena Valenti; 141, 51
- Fellows at ESO: Pamela Klaassen, Rodolfo Smiljanic; 141, 53
- Announcement of the ESO Workshop "Dynamics of Low-Mass Stellar Systems: From Star Clusters to Dwarf Galaxies"; 141, 54
- Announcement of the ESO/Universidad de Valparaíso Workshop "Evolution of Compact Binaries"; 141, 55
- Personnel Movements; 141, 55
- Raymond Wilson Honoured with Two Prestigious Prizes; Walsh, J.; 142, 41
- Availability of Reduction Software for HARPS Data at ESO Headquarters in Garching; Lo Curto, G.; Beniflah, T.; Burrows, A.; Emsellem, E.; Maguire, K.; Pasquini, L.; Pritchard, J.; Romaniello, M.; 142, 42
- ESO Participation at the Joint European and National Astronomy Meeting in Lisbon, Portugal; Sandu, O.; Christensen, L. L.; 142, 42
- Visiting ESO's Office in Santiago; West, M.; 142, 44
- Café & Kosmos Events in Munich; Boffin, H.; Hämmerle, H.; Wankerl, B.; Zollinger, S.; 142, 44
- New Staff at ESO: Jean-Philippe Berger; 142, 45
- Fellows at ESO: Margaret Moerchen, Davor Krajnović; 142, 47
- In Memoriam Christine Nieuwenkamp; de Zeeuw, T.; 142, 48
- Announcement of the "ALMA Community Days: Towards Early Science"; 142, 49
- Announcement of the ESO Workshop "Fornax, Virgo, Coma et al: Stellar Systems in Nearby High Density Environments"; ESO; 142, 49
- Personnel Movements; 142, 50
- In Memoriam Adriaan Blaauw; 142, 51

Author Index

A

- Arnaboldi, M.; Petr-Gotzens, M.; Rejkuba, M.; Neeser, M.; Szeifert, T.; Ivanov, V. D.; Hummel, W.; Hilker, M.; Neumayer, N.; Moller, P.; Nilsson, K.; Venemans, B.; Hatziminaoglou, E.; Hussain, G.; Stanke, T.; Teixeira, P.; Ramsay, S.; Retzlaff, J.; Slijkhuis, R.; Comerón, F.; Melnick, J.; Romaniello, M.; Emerson, J.; Sutherland, W.; Irwin, M.; Lewis, J.; Hodgkin, S.; Gonzales-Solares, E.; VISTA Science Verification — The Galactic and Extragalactic Mini-surveys; 139, 6
- Arsenault, R.; Madec, P.-Y.; Pauflique, J.; Ströbele, S.; Pirard, J.-F.; Vernet, É.; Hackenberg, W.; Hubin, N.; Jochum, L.; Kuntschner, H.; Glindemann, A.; Amico, P.; Lelouarn, M.; Kolb, J.; Tordo, S.; Donaldson, R.; Sönke, C.; Bonaccini Calia, D.; Conzelmann, R.; Delabre, B.; Kiekebusch, M.; Duhoux, P.; Guidolin, I.; Quattri, M.; Guzman, R.; Buzzoni, B.; Comin, M.; Dupuy, C.; Quentin, J.; Lizon, J.-L.; Silber, A.; Jolly, P.; Manescau, A.; Hammersley, P.; Reyes, J.; Jost, A.; Duchateau, M.; Heinz, V.; Bechet, C.; Stuik, R.; Progress on the VLT Adaptive Optics Facility; 142, 12

B

- Barucci, M.A.; Alvarez-Candal, A.; Belskaya, I.; de Bergh, C.; DeMeo, F.; Dotto, E.; Fornasier, S.; Merlin, F.; Perna, D.; The Outer Frontiers of the Solar System: Trans-Neptunian Objects and Centaurs; 141, 15
- Bean, J.; Seifahrt, A.; Hartman, H.; Nilsson, H.; Wiedemann, G.; Reiners, A.; Dreizler, S.; Henry, T.; The CRIRES Search for Planets at the Bottom of the Main Sequence; 140, 41
- Boffin, H.; Hämmerle, H.; Wankerl, B.; Zollinger, S.; Café & Kosmos Events in Munich; 142, 44
- Bonaccini Calia, D.; Feng, Y.; Hackenberg, W.; Holzlohner, R.; Taylor, L.; Lewis, S.; Laser Development for Sodium Laser Guide Stars at ESO; 139, 12
- Brandl, B.; Blommaert, J.; Glasse, A.; Lenzen, R.; Pantin, E.; METIS: A Mid-infrared E-ELT Imager and Spectrograph; 140, 30
- Bremer, M.; Lehnert, M.; Douglas, L.; Stanway, E.; Davies, L.; Clowe, D.; Milvang-Jensen, B.; Birkinshaw, M.; Studying the Properties of Early Galaxies with the ESO Remote Galaxy Survey; 141, 32

C

- Casali, M.; The 2010 SPIE Symposium on Astronomical Telescopes and Instrumentation; 141, 40
- Clark, S.; Negueruela, I.; Ritchie, B.; Crowther, P.; Dougherty, S.; Dissecting the Galactic Super Star Cluster Westerlund 1 — A Laboratory for Stellar Evolution; 142, 31

D

- D’Odorico, S.; Ramsay, S.; Hubin, N.; Gonzalez, J. C.; Zerbi, F. M.; An Introduction to the E-ELT Instrumentation and Post-focal Adaptive Optics Module Studies; 140, 17
- Davies, R.; Genzel, R.; MICADO: The Multi-adaptive Optics Imaging Camera for Deep Observations; 140, 32
- de Zeeuw, T.; In Memoriam Karin Horn-Hansen; 139, 64
- de Zeeuw, T.; In Memoriam Christine Nieuwenkamp; 142, 48
- Diolaiti, E.; MAORY: A Multi-conjugate Adaptive Optics Relay for the E-ELT; 140, 28

E

- Emerson, J.; Sutherland, W.; The Visible and Infrared Survey Telescope for Astronomy (VISTA): Looking Back at Commissioning; 139, 2
- Erdmann, C.; *The Messenger* on the Web; 139, 55

F

- Filippi, G.; Enabling Virtual Access to Latin-American Southern Observatories; 142, 2
- Fosbury, R.; Trygg, T.; Solargraphs of ESO; 141, 43
- Fusco, T.; ATLAS: An Advanced Tomographic Laser-assisted Adaptive Optics System; 140, 18

G

- Giuffrida, G.; Sbordonè, L.; Zaggia, S.; Marconi, G.; Bonifacio, P.; Izzo, C.; Szeifert, T.; Buonanno, R.; A Wide-angle VIMOS Survey of the Sagittarius Dwarf Spheroidal Galaxy; 141, 29
- Gratton, R.; Carretta, E.; Bragaglia, A.; Lucatello, S.; D’Orazi, V.; Observations of Multiple Stellar Populations in Globular Clusters with FLAMES at the VLT; 142, 28

H

- Hammer, F.; Kaper, L.; Dalton, G.; OPTIMOS-EVE: A Fibre-fed Optical-Near-infrared Multi-object Spectrograph for the E-ELT; 140, 36
- Hammersley, P.; Christensen, L.; Dekker, H.; Izzo, C.; Selman, F.; Bristow, P.; Bourget, P.; Castillo, R.; Downing, M.; Haddad, N.; Hilker, M.; Lizon, J.-L.; Lucuix, C.; Mainieri, V.; Mieske, S.; Reiner, C.; Rejkuba, M.; Rojas, C.; Smette, A.; Urrutia del Rio, J.; Valenzuela, J.; Wolff, B.; Upgrading VIMOS; 142, 8

K

- Kasper, M.; Zins, G.; Feautrier, P.; O’Neal, J.; Michaud, L.; Rabou, P.; Stadler, E.; Charton, J.; Cumani, C.; Delboulbe, A.; Geimer, C.; Gillet, G.; Girard, J.; Huerta, N.; Kern, P.; Lizon, J.-L.; Lucuix, C.; Mouillet, D.; Moulin, T.; Rochat, S.; Sönke, C.; A New Lenslet Array for the NACO Laser Guide Star Wavefront Sensor; 140, 8
- Kasper, M.; Beuzit, J.-L.; EPICS: An Exoplanet Imaging Camera and Spectrograph for the E-ELT; 140, 24
- Kenworthy, M.; Quanz, S.; Meyer, M.; Kasper, M.; Girard, J.; Lenzen, R.; Codona, J.; Hinz, P.; A New Coronagraph for NAOS-CONICA — the Apodising Phase Plate; 141, 2
- Kerber, F.; Querel, R.; Hanuschik, R.; Chacón, A.; Sarazin, M.; on behalf of the project team; Balloons over the La Silla Paranal Observatory; 141, 9
- Kissler-Patig, M.; McCaughrean, M.; Report on the ESO/ESA Workshop “JWST and the ELTs: An Ideal Combination”; 140, 56

L

- Laing, R.; Maiolino, R.; Rykaczewski, H.; Testi, L.; Report on the ESO Workshop “Science with ALMA Band 5”; 141, 41
- Le Fèvre, O.; Hill, L.; Le Mignant, D.; Maccagni, D.; Tresse, L.; Paltani, S.; OPTIMOS-DIORAMAS: A Wide-field Imaging and Multi-slit Spectrograph for the E-ELT; 140, 34
- Lebzelter, T.; Seifahrt, A.; Ramsay, S.; Almeida, P.; Bagnulo, S.; Dall, T.; Hartman, H.; Hussain, G.; Käufli, H.U.; Nieva, M.-F.; Przybilla, N.; Seemann, U.; Smette, A.; Uttenthaler, S.; Wahlgren, G.; Wolff, B.; CRIRES-POP — A Library of High Resolution Spectra in the Near-infrared; 139, 33
- Lidman, C.; West, M.; Report on the ESO Workshop “Galaxy Clusters in the Early Universe”; 139, 51
- Lo Curto, G.; Beniflah, T.; Burrows, A.; Emsellem, E.; Maguire, K.; Pasquini, L.; Pritchard, J.; Romaniello, M.; Availability of Reduction Software for HARPS Data at ESO Headquarters in Garching; 142, 42

M

- Maiolino, R.; Mannucci, F.; Cresci, G.; Gnerucci, A.; Troncoso, P.; Marconi, A.; Calura, F.; Cimatti, A.; Cocchia, F.; Fontana, A.; Granato, G.; Grazian, A.; Matteucci, F.; Nagao, T.; Pentericci, L.; Pipino, A.; Pozzetti, L.; Risaliti, G.; Silva, L.; AMAZE and LSD: Metallicity and Dynamical Evolution of Galaxies in the Early Universe; 142, 36
- Martayan, C.; Baade, D.; Fabregat, J.; A Slitless Spectroscopic Survey for H α -emitting Stars in the Magellanic Clouds; 139, 29
- Martinez, P.; Aller-Carpentier, E.; Kasper, M.; The High Order Test Bench: Evaluating High Contrast Imaging Concepts for SPHERE and EPICS; 140, 10
- Martinez, P.; Kolb, J.; Sarazin, M.; Tokovinin, A.; On the Difference between Seeing and Image Quality: When the Turbulence Outer Scale Enters the Game; 141, 5
- Mignone, C.; Russo, P.; Christensen, L. L.; Beyond 2009: ESO at the Closing Ceremony of the International Year of Astronomy; 139, 62
- Morris, S.; Cuby, J.-G.; EAGLE: An Adaptive Optics Fed, Multiple Integral Field Unit, Near-infrared Spectrograph; 140, 22

N

- Neumayer, N.; Cappellari, M.; van der Werf, P.; Reunanen, J.; Rix, H.-W.; de Zeeuw, T.; Davies, R.; SINFONI on the Nucleus of Centaurus A; 139, 36
- Neumayer, N.; Emsellem, E.; Report on the ESO Workshop "Central Massive Objects: The Stellar Nuclei – Black Hole Connection"; 141, 37

O

- Origlia, L.; Oliva, E.; Maiolino, R.; SIMPLE: A High Resolution Near-infrared Spectrograph for the E-ELT; 140, 38

P

- Pasquini, L.; Cristiani, S.; Garcia-Lopez, R.; Haehnelt, M.; Mayor, M.; CODEX: An Ultra-stable High Resolution Spectrograph for the E-ELT; 140, 20
- Pierce-Price, D.; ESO Participates in Germany's Girls' Day Activities; 140, 60
- Primas, F.; Casali, M.; Walsh, J.; ESO Astronomers Emeriti — Sandro D'Odorico and Alan Moorwood; 141, 50

R

- Rosati, P.; The ESO-GOODS Team; ESO-GOODS: Closing the Book, Opening New Chapters; 140, 50
- Rupperecht, G.; Böhnhardt, H.; Moehler, S.; Möller, P.; Saviane, I.; Ziegler, B.; Twenty Years of FORS Science Operations on the VLT; 140, 2

S

- Saito, R.; Hempel, M.; Alonso-García, J.; Toledo, I.; Borissova, J.; González, O.; Beamin, J.C.; Minniti, D.; Lucas, P.; Emerson, J.; Ahumada, A.; Aigrain, S.; Alonso, M.V.; Amôres, E.; Angeloni, R.; Arias, J.; Bandyopadhyay, R.; Barbá, R.; Barbuy, B.; Baume, G.; Bedin, L.; Bica, E.; Bronfman, L.; Carraro, G.; Catelan, M.; Clariá, J.; Contreras, C.; Cross, N.; Davis, C.; de Grijs, R.; Dékány, I.; Drew, J.; Fariña, C.; Feinstein, C.; Fernández Lajús, E.; Folkes, S.; Gamen, R.; Geisler, D.; Gieren, W.; Goldman, B.; Gosling, A.; Gunthardt, G.; Gurovich, S.; Hambly, N.; Hanson, M.; Hoare, M.; Irwin, M.; Ivanov, V.; Jordán, A.; Kerins, E.; Kinemuchi, K.; Kurtev, R.; Longmore, A.; López-Corredoira, M.; Maccarone, T.; Martín, E.; Masetti, N.; Mennickent, R.; Merlo, D.; Messineo, M.; Mirabel, F.; Monaco, L.; Moni Bidin, C.; Morelli, L.; Padilla, N.; Palma, T.; Parisi, M.C.; Parker, Q.; Pavani, D.; Pietrukowicz, P.; Pietrzynski, G.; Pignata, G.; Rejkuba, M.; Rojas, A.; Roman-Lopes, A.; Ruiz, M.T.; Sale, S.; Saviane, I.; Schreiber, M.; Schröder, A.; Sharma, S.; Smith, M.; Sodrê Jr., L.; Soto, M.; Stephens, A.; Tamura, M.; Tappert, C.; Thompson, M.; Valenti, E.; Vanzì, L.; Weidmann, W.; Zoccali, M.; VISTA Variables in the Vía Láctea (VVV): Current Status and First Results; 141, 24
- Sandu, O.; Christensen, L. L.; ESO Participation at the Joint European and National Astronomy Meeting in Lisbon, Portugal; 142, 42
- Santos, N.; Melo, C.; Pasquini, L.; Glindeman, A.; Report on the CAUP and ESO Workshop "Towards other Earths: Perspectives and Limitations in the ELT Era"; 139, 49
- Sartori, L.; Pelloni, C.; The Experience of Two High School Students Doing Astronomical Research at ESO; 141, 46
- Schuller, F.; Beuther, H.; Bontemps, S.; Bronfman, L.; Carlhoff, P.; Cesaroni, R.; Contreras, Y.; Csengari, T.; Deharveng, L.; Garay, G.; Henning, T.; Herpin, F.; Immer, K.; Lefloch, B.; Linz, H.; Mardones, D.; Menten, K.; Minier, V.; Molinari, S.; Motte, F.; Nguyen Luong, Q.; Nyman, L.-Å.; Rathborne, J.; Reveret, V.; Risacher, C.; Russeil, D.; Schilke, P.; Schneider, N.; Tackenberg, J.; Testi, L.; Troost, T.; Vasyunina, T.; Walmsley, M.; Wienen, M.; Wyrowski, F.; Zavagno, A.; The APEX Telescope Large Area Survey of the Galaxy (ATLASGAL); 141, 20
- Seifahrt, A.; Käufel, H. U.; Zängl, G.; Bean, J.; Richter, M.; Siebenmorgen, R.; Precise Modelling of Telluric Features in Astronomical Spectra; 142, 21
- Sharples, R.; Bender, R.; Agudo Berbel, A.; Bennett, R.; Bezawada, N.; Bouché, N.; Bramall, D.; Casali, M.; Cirasuolo, M.; Clark, P.; Cliffe, M.; Davies, R.; Davies, R.; Drory, N.; Dubeldam, M.; Fairley, A.; Finger, G.; Genzel, R.; Haefner, R.; Hess, A.; Jeffers, P.; Lewis, I.; Montgomery, D.; Murray, J.; Muschielok, B.; Förster Schreiber, N.; Pirard, J.; Ramsey-Howat, S.; Rees, P.; Richter, J.; Robertson, D.; Robson, I.; Rolt, S.; Saglia, R.; Schlichter, J.; Tecza, M.; Todd, S.; Wegner, M.; Wierorrek, E.; Recent Progress on the KMOS Multi-object Integral Field Spectrometer; 139, 24
- Siringo, G.; Kreysa, E.; De Breuck, C.; Kovacs, A.; Lundgren, A.; Schuller, F.; Stanke, T.; Weiss, A.; Guesten, R.; Jethava, N.; May, T.; Menten, K. M.; Meyer, H.-G.; Starkloff, M.; Zakosarenko, V.; A New Facility Receiver on APEX: The Submillimetre APEX Bolometer Camera, SABOCA; 139, 20

- Sterzik, M.; Bagnulo, S.; Azua, A.; Salinas, F.; Alfaro, J.; Vicuna, R.; Astronomy Meets Biology: EFOSC2 and the Chirality of Life; 142, 25
- Swinbank, M.; Edge, A.; Richard, J.; Smail, I.; De Breuck, C.; Lundgren, A.; Siringo, G.; Weiss, A.; Harris, A.; Baker, A.; Longmore, S.; Ivison, R.; The Properties of Star-forming Regions within a Galaxy at Redshift 2; 139, 42

T

- Tamai, R.; In Memoriam Nelson Montano; 139, 65
- Testi, L.; van Dishoeck, E.; Report on the Joint ESO/MPE/MPA/LMU Workshop "From Circumstellar Disks to Planetary Systems"; 139, 47
- Testi, L.; ALMA Achieves Closure Phase with Three Antennas on Chajnantor; 139, 52
- Testi, L.; Schilke, P.; Brogan, C.; Report on the Workshop "Data Needs for ALMA From Data Cubes to Science: Ancillary Data and Advanced Tools for ALMA"; 139, 53
- Testi, L.; Hills, R.; Laing, R.; Stanghellini, S.; Wild, W.; ALMA Status and Progress towards Early Science; 142, 17
- Thatte, N.; HARMONI: A Single Field, Visible and Near-infrared Integral Field Spectrograph for the E-ELT; 140, 26
- The ESO Solidarity Group; The ESO Solidarity Group in Support of the Earthquake Victims; 140, 60

V

- Vink, J.; Spectropolarimetry of Wolf-Rayet Stars in the Magellanic Clouds: Constraining the Progenitors of Gamma-ray Bursts; 140, 46

W

- Walsh, J.; Raymond Wilson Honoured with Two Prestigious Prizes; 142, 41
- West, M.; Visiting ESO's Office in Santiago; 142, 44
- Wittkowski, M.; Testi, L.; Report on the ESO Workshop "The Origin and Fate of the Sun: Evolution of Solar-mass Stars Observed with High Angular Resolution"; 140, 53
- Witzel, G.; Eckart, A.; Lenzen, R.; Straubmeier, C.; On the Instrumental Polarisation of NAOS-CONICA; 142, 5

ESO, the European Southern Observatory, is the foremost intergovernmental astronomy organisation in Europe. It is supported by 15 countries: Austria, Belgium, Brazil, the Czech Republic, Denmark, France, Finland, Germany, Italy, the Netherlands, Portugal, Spain, Sweden, Switzerland and the United Kingdom. ESO's programme is focused on the design, construction and operation of powerful ground-based observing facilities. ESO operates three observatories in Chile: at La Silla, at Paranal, site of the Very Large Telescope, and at Llano de Chajnantor. ESO is the European partner in the Atacama Large Millimeter/submillimeter Array (ALMA) under construction at Chajnantor. Currently ESO is engaged in the design of the 42-metre European Extremely Large Telescope.

The Messenger is published, in hard-copy and electronic form, four times a year: in March, June, September and December. ESO produces and distributes a wide variety of media connected to its activities. For further information, including postal subscription to The Messenger, contact the ESO education and Public Outreach Department at the following address:

ESO Headquarters
Karl-Schwarzschild-Straße 2
85748 Garching bei München
Germany
Phone +49 89 320 06-0
information@eso.org

The Messenger:
Editor: Jeremy R. Walsh; Design:
Jutta Boxheimer; Layout, Typesetting:
Mafalda Martins and Jutta Boxheimer;
Graphics: Roberto Duque
www.eso.org/messenger/

Printed by Mediengruppe UNIVERSAL
Grafische Betriebe München GmbH
Kirschstraße 16, 80999 München
Germany

Unless otherwise indicated, all images in The Messenger are courtesy of ESO, except authored contributions which are courtesy of the respective authors.

© ESO 2011
ISSN 0722-6691

Contents

The Organisation

T. de Zeeuw, S. Pottasch, R. Wilson – Adriaan Blaauw, 1914–2010	2
T. de Zeeuw – Brazil to Join ESO	5

Telescopes and Instrumentation

N. Piskunov et al. – HARPSpol – The New Polarimetric Mode for HARPS	7
B. Nikolic et al. – Tests of Radiometric Phase Correction with ALMA	11
F. Eisenhauer et al. – GRAVITY: Observing the Universe in Motion	16
R. Gilmozzi, M. Kissler-Patig – The E-ELT has Successfully Passed the Phase B Final Design Review	25

Astronomical Science

R. Fosbury et al. – Ozone: Twilit Skies, and (Exo-)planet Transits	27
K. M. Pontoppidan et al. – Planet-forming Regions at the Highest Spectral and Spatial Resolution with VLT-CRIRES	32
C. Péroux et al. – The SINFONI Integral Field Spectroscopy Survey for Galaxy Counterparts to Damped Lyman- α Systems	37
T. Shanks et al. – The VLT VIMOS Lyman-break Galaxy Redshift Survey – First Results	42

Astronomical News

P. Grosbøl et al. – Report on the ESO Workshop “Spiral Structure in the Milky Way: Confronting Observations and Theory”	47
S. Randich et al. – Report on the Workshop “The First Year of Science with X-shooter”	49
L. Testi et al. – Report on the ESO Workshop “The Impact of Herschel Surveys on ALMA Early Science”	52
M. Sarazin – Site Surveys for the Extremely Large Telescopes and More: Sharing the Experience and the Data	56
O. Hainaut et al. – ESO's Hidden Treasures Competition	57
Fellows at ESO – A. Ahumada, B. Venemans	59
Personnel Movements	60
ESO Studentship Programme	61
Announcement of the ESO Workshop “Multiwavelength Views of the ISM in High-redshift Galaxies”	62
Announcement of the ESO/MPE/MPA/ExcellenceCluster/USM Joint Astronomy Workshop “Formation and Early Evolution of Very Low Mass Stars and Brown Dwarfs”	62
Announcement of the Workshop “Feeding the Giants: ELTs in the Era of Surveys”	63
Annual Index 2010 (Nos. 139–142)	64

Front cover: The nearby (1.9 Mpc) spiral galaxy NGC 300 (type SAd), part of the Sculptor group, is shown in a colour image taken with the MPG/ESO 2.2-metre Wide Field Imager by combining broad *B*-, *V*- and *I*-band images with narrow-band [O III] and H α images. Further details of the image can be found in release eso1037. NGC 300 hosted a recently detected luminous optical transient (an unusual stellar explosion intermediate between a classical nova and a supernova) located to the northwest (lower right in this view) of the galaxy centre.